Characterizing the roles of gut microbiota, probiotic Lactobacilli and CX_3CR1 in the development of autoimmunity in MRL/*lpr* mice.

Xavier Cabana-Puig

Dissertation submitted to the faculty of the Virginia Polytechnic Institute and State University in partial fulfillment of the requirements for the degree of

Doctor of Philosophy

In

Biomedical and Veterinary Sciences

Xin M. Luo

Christopher M. Reilly

Irving C. Allen

Clayton C. Caswell

July 26, 2022

Blacksburg, VA

Keywords: Systemic lupus erythematosus, gut microbiota, microbial metabolites, *Lactobacillus*, lymphocytes T cells, CX_3CR1, glomerulonephritis

Characterizing the roles of gut microbiota, probiotic Lactobacilli and CX_3CR1 in the development of autoimmunity in MRL/*lpr* mice.

Xavier Cabana-Puig

ABSTRACT

Systemic lupus erythematosus (SLE) is a multi-system autoimmune disease with no known cure. The crosstalk between the gut microbiota and the immune system plays an important role in the tolerance induction to self-antigens both in the intestinal mucosa and at the systemic level.

The MRL/*lpr* mouse model exhibits lupus-like symptoms early in life due to multiple SLE susceptible loci of the MRL background, plus the Fas^{lpr} mutation that offers an accelerated model. Recently, we experienced a loss of disease phenotype in our in-house colony compared to the previous published phenotype of MRL/*lpr* mice. We thus compared mice newly obtained from The Jackson Laboratory (JAX) with our in-house MRL/*lpr* mice and found that the phenotypic drift, most significantly the attenuation of glomerulonephritis, was present in both colonies. In addition, while JAX mice and mice in our colony are genetically identical, there were minor differences in disease that might be due to differences in splenic microRNAs and the gut microbiota.

Once confirming that our MRL/*lpr* mouse model was as good as that from JAX, we continued our investigation of the role of Lactobacilli in the pathogenesis of lupus-like disease in MRL/*lpr* mice. We previously published that the mixture of *Lactobacillus reuteri (L. reuteri), L. oris, L. johnsonii, L. gasseri, and L. rhamnosus* significantly attenuated disease in MRL/*lpr* mice by restoring the imbalance between regulatory T

cells and T helper-17 cells. To further understand the role of *Lactobacillus spp.*, we treated MRL/*lpr* mice with the combined culture supernatant of the 5 strains containing secreted metabolites, given that the metabolites may induce an immunosuppressive response. The results showed significant attenuation of the inflammation of the spleen and renal lymph nodes similar to the effect of the bacteria themselves. There was also a trending decrease of double-stranded DNA autoantibodies with the combined supernatant. We thus tested the strains individually but none was able to recapitulate the effect of the bacterial mixture. This suggests cell-to-cell contact among different strains of lactobacilli may be required in ameliorating the disease. With these results, we now have a better understanding of the role of probiotic *Lactobacillus spp.* against SLE. Future investigations will focus on the potential therapeutic effect of *Lactobacillus spp*. as a combination.

Additionally, our group generated a *Cx3cr1*-deficient MRL/*lpr* mouse which exhibits a distinct phenotype of exacerbated glomerulonephritis with concurrent change of the gut microbiota composition compared to *Cx3cr1*$^{+/+}$ MRL/*lpr* littermates. Interestingly, upon correction of the gut microbiota with *Lactobacillus* administration, the phenotype of exacerbated glomerulonephritis was reversed, suggesting that CX_3CR1 controls glomerulonephritis in MRL/*lpr* mice through a gut microbiota-dependent mechanism. In addition, a collaborative project revealed that *Cx3cr1* deficiency-mediated pathogenic mechanisms also contributed to SLE-associated cardiovascular disease in MRL/*lpr* mice. The results of these studies will lead to the identification of new therapeutic targets for the treatment of two severe manifestations, glomerulonephritis and

cardiovascular disease, that together account for most of the morbidity and mortality in SLE.

Characterizing the roles of gut microbiota, probiotic Lactobacilli and CX_3CR1 in the development of autoimmunity in MRL/*lpr* mice.

Xavier Cabana-Puig

GENERAL AUDIENCE ABSTRACT

Systemic lupus erythematosus (SLE) is an autoimmune disease with no known cure. Commensal microbiota, mostly bacteria living in our gut, and the immune system have a strong relationship in maintaining a healthy state of the gut as well as the whole body. Alterations in the gut microbiota, known as dysbiosis, can facilitate SLE in human and animal models. Current treatments for SLE are primarily focused on using immunosuppressants, but the side effects are still a concern. The use of long-term nonselective immunosuppressant conducts a higher incidence of severe infections in SLE patients. It is thus necessary to develop new approaches and treatments against SLE. My dissertation research is focused on understanding how commensal bacteria influence in the pathogenesis of SLE. My studies have shown that environmental factors can manipulate the gut microbiota leading to different disease outcomes. In addition, following upon previously published studies from our laboratory, I have delineated the mechanism how a mixture of probiotic Lactobacilli can exert a beneficial effect against lupus. Finally, I have revealed a new, CX_3CR1-mediated mechanism through which the gut microbiota controls kidney disease in the MRL/*lpr* lupus-prone mouse model.

DEDICATION

This dissertation is dedicated to my family; my parents, Josep Cabana Armengol and Dolors Puig Espelt; my brother, Albert Cabana Puig; my sister, Marta Cabana Puig; my sister-in-law, Ariadna Roqué Riba; and my nephew, Pau Cabana Roqué, for their unconditional love and support.

In particular, my mom, Dolors, for being my role model and for always believing in me. I couldn't have done this if it wasn't for her.

ACKNOWLEDGEMENTS

First of all, I would like to express my sincere gratitude to my advisor, Dr. Xin M. Luo, for believing in me, for her invaluable dedication and support during my PhD, and for her patience during our endless meetings where her mentorship guided me in both my career and personal life. I feel honored, and proud to have worked with her. I'll never have enough words to express my gratitude, and it wouldn't have been possible to finish my PhD without her. I also owe my sincere gratefulness to Dr. Christopher M. Reilly, for his stories and laughs; and to the rest of the members of my doctoral advisory committee, Dr. Irving C. Allen and Dr. Clay C. Caswell, for all the help, guidance, feedbacks and also, good times, that they offered throughout my graduate school.

I'm grateful to the Biomedical and Veterinary Sciences program, Dr. Ahmed and Ms. Andrea Green, for providing this opportunity and my assistantship.

I would like to thank all people who helped me in the lab all these years: Dr. Qinghui Mu, Dr. Brianna Swartwout, Dr. Leila Abdelhamid, Dr. Xiaofeng Liao, Dr. Jingjing Ren, Dr. Michael Edwards, Dr. Jing Zhu, Dr. Ran Lu, Dr. Michael Appiah, Razan Alajoleen, Caitlin Armstrong, and Noah Oakland.

Finally, I would like to express my deep gratitude to my family, my friends, and especially my two roommates, Eric Brooks and Phil Miskovic, and Kathy Barron, who are my American family, for bearing with me throughout the ups and downs of my PhD life, for all the fun during this 5-year journey, and for making me feel I was always home. Thank you!

TABLE OF CONTENTS

ABSTRACT ii
GENERAL AUDIENCE ABSTRACT v
DEDICATION vi
ACKNOWLEDGEMENTS vii
LIST OF TABLES x
LIST OF FIGURES xi
CHAPTER 1 1
Gut microbiota- and host-derived metabolites in systemic lupus erythematosus 1
Abstract 2
Introduction 3
Role of gut microbiota in SLE 4
Gut microbiota- and host-derived metabolites in SLE 7
Microbiota-related management of SLE 13
Conclusions 14
Author Contributions 15
Funding 15
References 16
CHAPTER 2 24
Phenotypic drift in lupus-prone MRL/*lpr* mice: Potential roles of microRNAs and gut microbiota 24
Abstract 25
Introduction 26
Materials and Methods 27
Results 32
Discussion 39
Acknowledgments 42
Competing interests 42
Contributorship 42
Funding information 43
Ethical approval information 43
Data sharing information 43
References 44
CHAPTER 3 57
Lactobacillus spp. act in synergy to attenuate splenomegaly and lymphadenopathy in lupus-prone MRL/*lpr* mice 57
Abstract 58
Introduction 60
Material and Methods 61
Results 65
Discussion 71
Ethics 78
Data Availability Statement 78
Conflict of Interest 79
Author Contributions 79

Funding 79
Acknowledgments 79
Supplementary Material 79
References 80
CHAPTER 4 98
CX_3CR1 modulates SLE-associated glomerulonephritis and cardiovascular disease in MRL/*lpr* mice 98
Abstract 99
Introduction 100
Materials and Methods 103
Results 110
Discussion 118
Acknowledgements 122
Conflicts of Interest 123
Availability of Data and Materials 123
References 124
CHAPTER 5 145
Discussion and Future Directions 145

LIST OF TABLES

CHAPTER 3
Table S1 97

LIST OF FIGURES

CHAPTER 2
Figure 1. Phenotypic drift in MRL/*lpr* mice 47
Figure 2. Splenic differences between in-house and new JAX mice as assessed with flow cytometry 48
Figure 3. Splenic differences between in-house and new JAX mice as assessed with immunohistochemistry 49
Figure 4. Renal differences between in-house and new JAX mice 50
Figure 5. Analysis of lupus-associated microRNAs 51
Figure 6. Analysis of gut microbiota composition 52
Figure 7. Analysis of gut microbiota with a focus on *Lactobacillaceae* and *Lachnospiraceae* 54
Figure S1 55
Figure S2 56
CHAPTER 3
Figure 1. Five *Lactobacillus* species act synergistically to attenuate splenomegaly and lymphadenopathy 86
Figure 2. Gut microbiota at early stage is associated with the decrease of gut-draining lymph node size 88
Figure 3. *Lactobacillus* spp. attenuate splenomegaly and renal lymphadenopathy through secreted factors and a CX_3CR1-dependent mechanism 89
Figure 4: *Lactobacillus* spp. control inflammation through regulating splenic and MLN immune cell populations 90
Figure S1 92
Figure S2 93
Figure S3 94
Figure S4 95
CHAPTER 4
Figure 1. *Cx3cr1* deficiency exacerbates lymphoproliferation and glomerulonephritis in female MRL/*lpr* mice 130
Figure 2. Exacerbation of glomerulonephritis with *Cx3cr1* deficiency is gut microbiota-dependent, but exacerbation of lymphoproliferation is not 132
Figure 3. Significant differences in several splenic populations between *Cx3cr1*$^{+/+}$ and *Cx3cr1*$^{-/-}$ MRL/*lpr* mice are equalized by Lactobacillus treatment 134
Figure 4. A high-fat diet exacerbates cardiovascular inflammation in *Cx3cr1*$^{-/-}$ MRL/*lpr* mice 135
Figure 5. ICOS-L expressing $Ly6C^+$ monocytes promote germinal center reaction in *Cx3cr1*$^{-/-}$ MRL/*lpr* mice fed a high-fat diet 136
Figure 6. The high-fat diet induces anti-dsDNA IgG in *Cx3cr1*$^{-/-}$ MRL/*lpr* mice that in turn promotes monocyte expression of ICOS-L 137
Figure S1 139
Figure S2 140
Figure S3 141
Figure S4 142

Figure S5 143
Figure S6 144

CHAPTER 1

Gut microbiota- and host-derived metabolites in systemic lupus erythematosus

Literature Review

Xavier Cabana-Puig[1], Christopher M. Reilly[2], and Xin M. Luo[1]

1. Department of Biomedical Sciences & Pathobiology, Virginia-Maryland College of Veterinary Medicine, Virginia Polytechnic Institute and State University, 205 Duck Pond Drive, Blacksburg, VA 24061, USA.
2. Edwards Via College of Osteopathic Medicine, Blacksburg, VA 24060, USA.

Under Review in Nutrients, July 2022

Abstract

Systemic lupus erythematosus (SLE) is an autoimmune disease where multiple organs of the body are targets of persistent inflammation leading to deposition of immune complexes that damage the organs. The disease is not fully understood; however, it is known that both genetic and environmental factors contribute to its pathogenesis. The gut microbiota is a complex microbial ecosystem that interacts with the host via a symbiotic relationship and is essential for basic functions of the host. It has been shown that the disturbance of gut microbiota can contribute to the progression of SLE. Recently, there has been an increased interest in the metabolites produced by the gut microbiota. A broad spectrum of bioactive compounds modulating the development of autoimmunity may be the mediators of how the gut microbiota alters the pathogenesis of SLE. In this review, we summarize recent advances on the role of gut microbiota dysbiosis in SLE and how the gut microbiota works together with metabolites, their signaling pathways, and the host metabolism to modulate SLE pathogenesis. The knowledge gained may lead to therapeutic approaches based on the microbial metabolome and provide novel opportunities for exploring gut microbiota-based treatments in SLE.

Introduction

Systemic lupus erythematosus (SLE) is a prototypical autoimmune disease that englobes a wide range of different symptoms and is one of the most common autoimmune diseases. It affects diverse organs including kidney, gastrointestinal tract, skin, among others. Women of childbearing age are diagnosed more often than men (1). The different clinical symptoms presented in SLE indicate a complex disease; but a large percentage of patients presents the common feature of autoantibodies (2). The immune system is dysregulated with abnormal response to self-antigens, T and B cell super-activation, as well as an apoptotic characteristic leading to more production of self-antigens (2). Pro-inflammatory signaling pathways involving different receptors (e.g., toll-like receptors TLR7 and TLR9) and transcription factors (e.g., signal transducers and activators of transcription STAT4 and STAT5, or interferon-regulatory factors IRF5 and IRF7) trigger the production of type I interferons (IFN-I) from myeloid cells, aggravating local inflammation that recruits more autoreactive T and B cells (3, 4). SLE is thus a vicious cycle that is difficult to stop once it starts. The molecular and cellular basis for the diverse manifestations of SLE is still unclear. Environmental factors such as diet, pollution, and contaminants can play potential roles in triggering the initiation and/or promotion of the exaggerated immune response in SLE (5).

Microorganisms located in the mammalian intestinal tract, namely the gut microbiota, are acquiring more attention due to its codependent relationship with the host (6, 7). Gut microbiota is considered a dynamic organ contributing to the physiological balance that if broken, would set off the progression of inflammatory diseases. Being the most studied microorganisms in the gut microbiota, bacteria play a key role in the

homeostasis and functions of host immune cells (8, 9). There are many tools to identify microorganisms in the environment leading to studies that have established an association between the gut microbiota and SLE (10). Three major bacterial phyla represent the mammalian gut microbiota; among them, an increased ratio of Bacteroidetes and Firmicutes is an important indicator of SLE progression (10, 11). Furthermore, the gut microbiota can function via their contributions to metabolic processes, where their metabolites can educate the immune system (12, 13). In fact, metabolites produced by the gut microbiota are essential for the host immune homeostasis (14). Alterations of bacterial metabolites and their byproducts can disrupt the host immune homeostasis resulting in local inflammation that has the potential to become systemic (15). Understanding the crosstalk between the immune system and metabolites derived from the commensal bacteria is a key for mapping the molecular and cellular basis of SLE pathogenesis (16).

In this review, we will discuss recent advances on how the gut microbiota and its products affect SLE outcomes and how changing the metabolite profile can contribute to disease modulation. In addition, we will discuss future therapeutic strategies and translational applications of gut microbiota-derived metabolites for the management of SLE.

Role of gut microbiota in SLE

Many autoimmune diseases, including SLE, exhibit gut dysbiosis, or an altered gut microbiota (17, 18). The dysbiosis profile is usually characterized by higher proportions of different taxa of pathogenic bacteria compared to healthy bacteria (19). Patients with

SLE tend to have a lower Firmicutes/Bacteroidetes ratio compared to healthy individuals (10). Our research team was the first to describe changes of gut microbiota in lupus mice *vs*. healthy controls, with lupus mice having a decrease of *Lactobacillaceae* and an increase of *Lachnospiraceae* (20). Interestingly, female lupus-prone mice have a more dramatic loss of lactobacilli compared to males and as a consequence they tend to have more severe clinical signs (20). In line with this finding, there is an increase of *Lachnospiraceae* abundance in female lupus mice associated with an earlier onset of and/or more severe lupus disease, suggesting that the disturbed gut microbiota can contribute to lupus disease progression in a sex-dependent manner (20). Based on these observations, we administered a mixture of 5 strains of *Lactobacillus* spp. into lupus mice via oral gavage, which restored the leaky gut, promoted anti-inflammatory IL-10 production, and led to improved renal function and better survival (21). This follow-up study, which was done using lupus-prone MRL/*lpr* mice, along with two recent studies using additional models of murine lupus (22, 23), established gut microbiota as a cause, instead of effect, of lupus pathogenesis. In SLE patients, one cross-sectional study showed a strong association between SLE disease activity and expansion of *Ruminococcus (Blautia) gnavus* in the gut microbiota (24). While the classification of *Ruminococcus (Blautia) gnavus* is still being determined, the abundance of *Ruminococcus* genus has been shown to be correlated with the absolute count of regulatory T (Treg) lymphocytes, suggesting that circulatory immune cells may be directly affected by bacterial dynamics in the gut (25).

Notably, *Lactobacillus* spp. are one of the most used probiotics for their anti-inflammatory and regulatory functions. They have been shown to have a beneficial effect

by downregulating the expression of miR-155 and miR-181a in the PBMCs of SLE patients, two microRNAs positively correlated with the SLE disease activity index (SLEDAI) and SLE-associated kidney disease (26, 27). However, *Lactobacillus reuteri* has been shown to stimulate IFN-I production and worsen lupus progression in lupus mouse models (28). As the IFN-I signaling pathway drives the pathogenesis of SLE (29), gut microbiota-mediated promotion of IFN-I can exacerbate the disease (28). The role of gut microbiota in SLE is thus quite complex, with bacteria from the same genus exerting opposite effects. Future studies should employ metagenomic analysis rather than just 16S ribosomal RNA sequencing, and focus on species- or even strain-specific differences regarding the roles of gut microbes on the pathogenesis of SLE.

The gut microbiota also uses molecular mimicry to impact SLE pathogenesis. For example, autoantibodies against Ro60/SSA/TROVE2 are generated in SLE that target RNA-binding proteins (30). Interestingly, intestinal bacteria can also produce these compounds that are used by the microbes for environmental stress mitigation (31). As the epitopes on RNA-binding proteins are highly conserved, cross-reactivity can occur after infections (i.e., environmental stress to intestinal bacteria leading to generation of such epitopes). The antibodies generated against gut microbiota products mimic autoantibodies thus exacerbating lupus (32, 33).

Microbial dysbiosis in the gut of SLE patients is characterized by reduced bacterial diversity and decreased proportions of healthy commensal species. It is possible that gut dysbiosis can break immunological tolerance leading to autoreactive T cell and/or B cell generation in SLE. The fact that the frequencies of autoreactive immune cells and their products (e.g., autoantibodies) are correlated with gut dysbiosis in SLE

supports this hypothesis (34). However, some specific bacteria are implicated in stimulating immunological tolerance to self-antigens suggesting a complex relationship between microbiota and the immune system (35). Moreover, it remains unclear how bacteria or their products translocate from the gut lumen to distal organs such as the kidney in human SLE. Future research of novel gut microbiota-mediated mechanisms leading to the onset and/or progression of SLE will significantly enhance our understanding of disease pathogenesis and impact clinical practice.

Gut microbiota- and host-derived metabolites in SLE

Bacterial metabolites are important particularly in food digestion, as the human body cannot synthetize all the enzymes necessary for the catabolism of dietary carbohydrates, proteins, fat, as well as micronutrients such as vitamins (36). In addition, gut microbiota can modulate the production of host metabolites (37). Here, we discuss both bacterial and host metabolite changes observed in SLE that may impact disease pathogenesis.

Short-chain fatty acids (SCFAs)

SCFAs are between 2 to 5 carbon weak acids and include acetate (C2), propionate (C3), and butyrate (C4). They are generated from the fermentation of dietary fibers by gut microbiota and play an important immune modulatory role (38). Two of their properties are to provide energy to colonocytes and to promote a healthier gut barrier by secreting cytokines such as IL-22 (39). Moreover, SCFAs play important roles as modulators of the immune system. They function as ligands for G-protein coupled receptors (GPCRs),

including GPR41, GPR43 and GPR109A, through which to promote immune regulatory effects and maintain the integrity of the intestinal barrier (40, 41).

One of the most important SCFAs is butyrate, which is involved in the maintenance of colonic health, such as stimulating the mucous layer, inducing production of antimicrobial peptides (AMP), and/or functioning as an anti-inflammatory agent due to its regulatory effects on gene expression (42). Colonic acidity helps gram-positive anaerobic bacteria (e.g., Clostridia spp.), mainly producers of butyrate, to compete against gram-negative bacteria (e.g., Bacteroides spp.) (43). Although butyrate is mainly produced in the colon, the ileum and cecum (terminal part of the small intestine) also participate in exerting and extending the beneficial effects of butyrate based on their proximity (44). Butyrate activity includes inhibiting histone deacetylases (HDACs) as well as signaling through several GPCRs. HDACs promote a condensed chromatin structure and HDAC inhibitors have shown promise as treatments for SLE at least in mice (45). Beside its role as an HDAC inhibitor, butyrate can also activate GPR43 and GPR109a signaling (46, 47). GPR43 and GPR109a play important roles in the gut by promoting an anti-inflammatory and anti-cancer environment. Colonic type 3 innate lymphoid cells (ILC3s) express GPR43 and are able to sense SCFAs such as butyrate. GPR43 signaling activates AKT-STAT3 and/or ERK-STAT3 signaling pathways, and deficiency of *Ffar2* (gene name of GPR43) in ILC3s decreases their proliferation and IL-22 production, thereby altering the mucus and AMP production and increasing susceptibility to infection (48). Importantly, butyrate, through recognition by GPR43, is able to stimulate the proliferation and functions of ILC3s. Furthermore, butyrate can inhibit nuclear factor kappa-light-chain-enhancer of activated B cells (NF-κB). NF-κB is

involved in inflammatory responses mediated by pro-inflammatory cytokines such as IL-1β, IL-17, TNFα, and IL-6. Dysregulated activity of NF-κB is frequently observed in colon cancer and IBD (49, 50) as well as autoimmune diseases such as multiple sclerosis (51). The inhibition of NF-κB by butyrate is thus beneficial.

In lupus-prone mice, one study has reported that supplementation with a high fiber diet improves lupus-related disease symptoms in a TLR7-dependent mouse model (52). Notably, gut commensal *Lactobacillus reuteri* was found to be enriched in these mice, triggering plasmacytoid dendritic cells (pDCs) to produce IFN-I, thus worsening autoimmune response and exacerbating lupus disease (52). Resistant starch as a dietary intervention can promote the fermentation of intestinal microbiota to produce SCFAs, which in turn control *L. reuteri* growth and ameliorate lupus-like disease by downregulating the IFN-I pathway. However, in MRL/*lpr* and NZB/W F1 mice, we have shown that a high-fiber diet (unpublished data) or oral administration of SCFAs (53) does not have an effect on disease initiation or progression, raising the possibility that the benefits of SCFAs are mouse model-specific.

Lipid metabolism

The gut microbiota modulates the formation of lipids, as well as lipid digestion and absorption from the diet (54). It has been suggested that SLE patients are more susceptible to having a dysregulated lipid profile in both serum and feces (55). In addition, farnesoid X receptor (FXR), which helps to regulate bile acid synthesis and transport, in the liver is negatively correlated with immune dysfunction in SLE patients and lupus-prone mouse models (56). Administration of FXR agonists such as

chenodeoxycholic acid (CDCA) can suppress inflammatory cytokines TNFα, IFNγ, and IL-6 in lupus-prone MRL/*lpr* mice (56). In fact, bile acids have modulatory effects on gut immunity (57). For example, bile acid metabolites such as lithocholic acid (LCA) and isoalloLCA can inhibit the differentiation of Th17 cells by downregulating the transcription factor retinoid-related orphan receptor-γt (RORγt) (57, 58). Moreover, bile acid metabolites can increase FOXP3 expression by promoting the production of reactive oxygen species in the mitochondria leading to the expansion of Treg cells (59). Furthermore, microbial fermentation leading to lipid metabolites such as low-density lipoproteins (LDLs) and oxidized LDL (oxLDL) can confer a regulatory profile in dendritic cells to maintain intestinal homeostasis (60, 61). Notably, while it is known that lipid profiles differ between SLE patients and healthy individuals, there is a lack of mechanistic pathways on how a dysregulated lipid profile can trigger SLE development (62). More studies are needed to provide a direct elucidation of how gut microbiota and their products affect lipid metabolism, and whether lipid metabolism is a cause or consequence of SLE development.

Tryptophan metabolism

Tryptophan is an essential amino acid that cannot be synthesized by humans (63). A healthy gut microbiota is important for maintaining the necessary concentrations of tryptophan (64). SLE patients have been found to have a higher level of the tryptophan metabolite kynurenin (65). In triple congenic (TC) lupus-prone mice (B6.*Sle1*.*Sle2*.*Sle3*) fed with low- or high-tryptophan diets, reduced dietary tryptophan was shown to be protective, which was correlated with lower anti-dsDNA IgG and kynurenine levels in

the serum (23). Interestingly, high tryptophan metabolism is associated with the expansion of *Lactobacillus* spp. that can promote gut epithelial integrity (23, 66). The TC mice thus do not possess a leaky gut.

Besides kynurenine, some tryptophan metabolites, including indole-3-aldehyde (IAld) and indole-3-acetic acid (I3AA), are aryl hydrocarbon receptor (AhR) ligands (67). AhR is a cytosolic ligand-inducible transcription factor activated by small molecules provided by microorganisms, diet or others; and is expressed by immune cells as well as epithelial cells (68). Specific gut microbiota-derived indole metabolites of dietary components, as mentioned above, can bind to AhR (69). Ligation of AhR activates genes encoding cytokines such as IL-10, which is important for immunoregulation (70). AhR can also regulate mucosal immune responses (71). AhR activation is a requirement for the expansion of intestinal lymphoid follicles and specific ILC populations, particularly IL-22-producing RORγt^{+} ILC3s (72). Deficiency of *Ahr* or lack of AhR ligands in mice results in gut microbiota disruption, increasing the number of certain detrimental bacteria such as *Bacteroides* spp., decreasing AMP production, and reducing the number of specialized intraepithelial lymphocytes (IELs) (73). Restoring wild-type IELs to *Ahr*$^{-/-}$ mice can enhance normal functions of the intestinal epithelial barrier and normalize the bacterial load (74). Importantly, diet and gut microbiota can regulate AhR activation. Specific gut bacteria, particularly *Lactobacillus* spp., can metabolize dietary tryptophan to generate AhR ligands that in turn stimulate ILC3s (75). Thus, gut microbiota-mediated tryptophan metabolism, especially the generation of AhR ligands, plays a key role in maintaining gut barrier function and inducing tolerance in

mucosal tissues (76), thus being a potential control of autoimmune disorders such as SLE.

Polyamines

Polyamines are small polycationic molecules ubiquitously present in all tissues and all cell types (77). The polyamines spermine, spermidine, and putrescine are part of many biological processes, such as cell proliferation, gene transcription and translation, as well as the recovery of injured mucosa (78). A major source of polyamines is the gut microbiota, and the small intestine is the primary site for the absorption of the majority of the polyamines for cell growth used throughout the body (79). However, the gut microbiota is also considered a key source of polyamines in the large intestine (80). Evidences suggest that both the host and microbiota require polyamines (81). Production of polyamines stimulates intercellular junction proteins, including occludin, ZO-1 and E-cadherin, *in vitro*, which are important for the control of cellular permeability and maintenance of epithelial barrier function (82). Polyamines also restore gut barrier integrity through cell-cell adhesion proteins such as E-cadherin (83). Depletion of polyamines in intestinal epithelial cells (IECs) leads to increased permeability and consequently bacterial translocation due to decreased expression of E-cadherin (84). Bacteria, on the other hand, constantly use polyamines for cell-cell communications, signaling, and cell differentiation (85). Many pathogenic bacteria need polyamines for survival within the host or expression of virulence genes (78). The polyamines concentration is regulated by the abundance of producing bacteria that can synthesize polyamines, and the presence of absorbing bacteria, which lack the synthetic pathways to

produce polyamines, suggesting the existence of metabolic interactions between these two types of bacteria (86). Probiotics, such as *Bifidobacterium animalis* subsp., can exponentially increase the concentration of polyamides in the gut lumen (87). The consumption of *B. animalis* subsp. contained in yogurt helps to increase the polyamine concentration in the gut, thus improving intestinal health, with IECs having a longer lifespan especially in the colon (88). In addition, the use of probiotic *Lactobacillus rhamnosus* can increase the synthesis of polyamines in the gut, downregulate carcinogenesis in gastric cells (89), and promote a beneficial health effect in colonic mucosa (89, 90). As both human and murine SLE have a leaky gut component (91), the fact that polyamines can restore intestinal barrier functions suggests an important role of these metabolites in controlling disease progression in SLE.

Microbiota-related management of SLE

SLE has no known cure, and traditional therapeutic strategies aim to manage the disease using glucocorticoids or other immunosuppressants (92, 93). The downside of these strategies is that life-long treatments are required to fight flares and remain in remission and as a consequence, severe side effects can occur that are associated with a high chance of infections during treatments. Therefore, it is imperative to find new and more effective ways to specifically target lupus symptoms and avoid adverse reactions.

Microbiota interventions have been considered as a treatment strategy against SLE for a long time. They usually work through personalized diet changes or probiotics, are cost-effective, and can have a huge impact on disease outcomes. Encouraging results have been obtained from combining the use of probiotics or diet intervention with

traditional SLE medications. The use of less invasive therapies such as prebiotics or probiotics, through correcting the disrupted gut microbiota, would be a plausible preventive and/or therapeutic strategy for individuals susceptible to SLE. For example, it has been shown that long term use of probiotics or prebiotics can reduce autoantibody production and improve SLE symptoms (94). In addition, intraperitoneal injection of *Lactobacillus casei* has been shown to inhibit the expansion of pathogenic $B220^+$ T cells in the spleen and mesenteric lymph nodes of MRL/*lpr* mice, thereby attenuating lupus-like disease (95). Therefore, pre- and probiotics, together with the newly tested microbiota transplantation strategy that has been recently reported (96), can be viable methods for the management of SLE.

Conclusions

In this review we discussed how the interaction between gut microbiota and the immune system modulates autoimmune diseases, such as SLE, with a focus on the functions of host and microbial metabolites. The gut microbiota is essential for the production of SCFAs and tryptophan metabolites, both of which have anti-inflammatory properties in multiple immune cell populations. In addition, commensal bacteria can regulate systemic lipid homeostasis and alter polyamine levels, thereby restoring the impaired intestinal epithelium and correcting the imbalanced immune response. It has become apparent that the gut microbiota and its metabolites have a big impact on our body, not only in a food/diet context but also to our immune system. Notably, the more tools that we have to analyze the microbiome, the more we can see how closely related and dependable it is to systemic autoimmunity. However, mechanistic pathways remain unclear regarding how

microbiota-derived metabolites educate the host immune system. Advancing our understanding of the mechanisms through which the intestinal microbiota and its metabolites participate in the etiology of SLE will likely benefit a lot of patients. Future research should include deciphering the pathways by which nutrients and metabolites derived from commensal bacteria educate the immune system and understanding the functional link between host/microbial metabolites and autoimmune disease.

Author Contributions

Conceptualization, X.C.P. and X.M.L.; software, X.C.P. and X.M.L.; investigation, X.C.P.; resources, X.C.P.; writing—original draft preparation, X.C.P.; writing—review and editing, X.C.P, C.M.R. and X.M.L.; visualization, X.C.P. and X.M.L.; supervision, X.M.L.; funding acquisition, X.M.L. All authors have read and agreed to the published version of the manuscript.

Funding

This research was funded by NIH, grant number R01AR073240.

References

1. Tsokos GC. Systemic lupus erythematosus. The New England journal of medicine. 2011;365(22):2110-21.

2. Han S, Zhuang H, Shumyak S, Yang L, Reeves WH. Mechanisms of autoantibody production in systemic lupus erythematosus. Frontiers in immunology. 2015;6:228.

3. Yaniv G, Twig G, Shor DB-A, Furer A, Sherer Y, Mozes O, et al. A volcanic explosion of autoantibodies in systemic lupus erythematosus: A diversity of 180 different antibodies found in SLE patients. Autoimmunity Reviews. 2015;14(1):75-9.

4. Baquero F, Nombela C. The microbiome as a human organ. Clinical Microbiology and Infection. 2012;18:2-4.

5. Flint HJ, Scott KP, Louis P, Duncan SH. The role of the gut microbiota in nutrition and health. Nature reviews Gastroenterology & hepatology. 2012;9(10):577-89.

6. Arumugam M, Raes J, Pelletier E, Le Paslier D, Yamada T, Mende DR, et al. Enterotypes of the human gut microbiome. Nature. 2011;473(7346):174-80.

7. Xu C, Zhu H, Qiu P. Aging progression of human gut microbiota. BMC Microbiology. 2019;19(1):236.

8. Vamanu E, Rai SN. The Link between Obesity, Microbiota Dysbiosis, and Neurodegenerative Pathogenesis. Diseases. 2021;9(3):45.

9. Choi J, Kim ST, Craft J. The pathogenesis of systemic lupus erythematosus-an update. Current opinion in immunology. 2012;24(6):651-7.

10. Hevia A, Milani C, López P, Cuervo A, Arboleya S, Duranti S, et al. Intestinal dysbiosis associated with systemic lupus erythematosus. mBio. 2014;5(5):e01548-14.

11. Mu Q, Zhang H, Luo XM. SLE: Another Autoimmune Disorder Influenced by Microbes and Diet? Frontiers in immunology. 2015;6.

12. Marcobal A, Kashyap PC, Nelson TA, Aronov PA, Donia MS, Spormann A, et al. A metabolomic view of how the human gut microbiota impacts the host metabolome using humanized and gnotobiotic mice. ISME J. 2013;7(10):1933-43.

13. Levy M, Thaiss CA, Elinav E. Metabolites: messengers between the microbiota and the immune system. Genes & development. 2016;30(14):1589-97.

14. Tong Y, Marion T, Schett G, Luo Y, Liu Y. Microbiota and metabolites in rheumatic diseases. Autoimmun Rev. 2020;19(8):102530.

15. Maldonado MA, Kakkanaiah V, MacDonald GC, Chen F, Reap EA, Balish E, et al. The role of environmental antigens in the spontaneous development of autoimmunity in MRL-lpr mice. Journal of immunology (Baltimore, Md : 1950). 1999;162(11):6322-30.

16. Man SM, Kaakoush NO, Mitchell HM. The role of bacteria and pattern-recognition receptors in Crohn's disease. Nature reviews Gastroenterology & hepatology. 2011;8(3):152-68.

17. Caruso R, Lo BC, Núñez G. Host-microbiota interactions in inflammatory bowel disease. Nature reviews Immunology. 2020;20(7):411-26.

18. Knip M, Siljander H. The role of the intestinal microbiota in type 1 diabetes mellitus. Nature reviews Endocrinology. 2016;12(3):154-67.

19. Scher JU, Abramson SB. The microbiome and rheumatoid arthritis. Nature reviews Rheumatology. 2011;7(10):569-78.

20. Zhang H, Liao X, Sparks JB, Luo XM. Dynamics of gut microbiota in autoimmune lupus. Applied and environmental microbiology. 2014;80(24):7551-60.

21. Mu Q, Zhang H, Liao X, Lin K, Liu H, Edwards MR, et al. Control of lupus nephritis by changes of gut microbiota. Microbiome. 2017;5(1):73.

22. Manfredo Vieira S, Hiltensperger M, Kumar V, Zegarra-Ruiz D, Dehner C, Khan N, et al. Translocation of a gut pathobiont drives autoimmunity in mice and humans. Science (New York, NY). 2018;359(6380):1156-61.

23. Choi SC, Brown J, Gong M, Ge Y, Zadeh M, Li W, et al. Gut microbiota dysbiosis and altered tryptophan catabolism contribute to autoimmunity in lupus-susceptible mice. Science translational medicine. 2020;12(551).

24. Azzouz D, Omarbekova A, Heguy A, Schwudke D, Gisch N, Rovin BH, et al. Lupus nephritis is linked to disease-activity associated expansions and immunity to a gut commensal. Annals of the rheumatic diseases. 2019;78(7):947-56.

25. Zhang SX, Wang J, Chen JW, Zhang MX, Zhang YF, Hu FY, et al. The level of peripheral regulatory T cells is linked to changes in gut commensal microflora in patients with systemic lupus erythematosus. Annals of the rheumatic diseases. 2021;80(11):e177.

26. Vahidi Z, Samadi M, Mahmoudi M, RezaieYazdi Z, Sahebari M, Tabasi N, et al. Lactobacillus rhamnosus and Lactobacillus delbrueckii ameliorate the expression of miR-155 and miR-181a in SLE patients. Journal of Functional Foods. 2018;48:228-33.

27. Toral M, Robles-Vera I, Romero M, de la Visitación N, Sánchez M, O'Valle F, et al. Lactobacillus fermentum CECT5716: a novel alternative for the prevention of vascular disorders in a mouse model of systemic lupus erythematosus. FASEB journal :

official publication of the Federation of American Societies for Experimental Biology. 2019;33(9):10005-18.

28. Zegarra-Ruiz DF, El Beidaq A, Iñiguez AJ, Lubrano Di Ricco M, Manfredo Vieira S, Ruff WE, et al. A Diet-Sensitive Commensal Lactobacillus Strain Mediates TLR7-Dependent Systemic Autoimmunity. Cell host & microbe. 2019;25(1):113-27.e6.

29. Crow MK. Type I interferon in the pathogenesis of lupus. Journal of immunology (Baltimore, Md : 1950). 2014;192(12):5459-68.

30. Hung T, Pratt GA, Sundararaman B, Townsend MJ, Chaivorapol C, Bhangale T, et al. The Ro60 autoantigen binds endogenous retroelements and regulates inflammatory gene expression. Science (New York, NY). 2015;350(6259):455-9.

31. Szymula A, Rosenthal J, Szczerba BM, Bagavant H, Fu SM, Deshmukh US. T cell epitope mimicry between Sjögren's syndrome Antigen A (SSA)/Ro60 and oral, gut, skin and vaginal bacteria. Clinical immunology (Orlando, Fla). 2014;152(1-2):1-9.

32. Sim S, Wolin SL. Emerging roles for the Ro 60-kDa autoantigen in noncoding RNA metabolism. Wiley interdisciplinary reviews RNA. 2011;2(5):686-99.

33. Rowland I, Gibson G, Heinken A, Scott K, Swann J, Thiele I, et al. Gut microbiota functions: metabolism of nutrients and other food components. European journal of nutrition. 2018;57(1):1-24.

34. Dema B, Charles N. Autoantibodies in SLE: Specificities, Isotypes and Receptors. Antibodies (Basel, Switzerland). 2016;5(1).

35. Esmaeili S-A, Mahmoudi M, Momtazi AA, Sahebkar A, Doulabi H, Rastin M. Tolerogenic probiotics: potential immunoregulators in Systemic Lupus Erythematosus. Journal of cellular physiology. 2017;232(8):1994-2007.

36. Brestoff JR, Artis D. Commensal bacteria at the interface of host metabolism and the immune system. Nature immunology. 2013;14(7):676-84.

37. Tremaroli V, Bäckhed F. Functional interactions between the gut microbiota and host metabolism. Nature. 2012;489(7415):242-9.

38. Smith PM, Howitt MR, Panikov N, Michaud M, Gallini CA, Bohlooly-Y M, et al. The microbial metabolites, short-chain fatty acids, regulate colonic Treg cell homeostasis. Science (New York, NY). 2013;341(6145):569-73.

39. Vinolo MA, Rodrigues HG, Hatanaka E, Sato FT, Sampaio SC, Curi R. Suppressive effect of short-chain fatty acids on production of proinflammatory mediators by neutrophils. The Journal of nutritional biochemistry. 2011;22(9):849-55.

40. Zhao Y, Chen F, Wu W, Sun M, Bilotta AJ, Yao S, et al. GPR43 mediates microbiota metabolite SCFA regulation of antimicrobial peptide expression in intestinal

epithelial cells via activation of mTOR and STAT3. Mucosal immunology. 2018;11(3):752-62.

41. Li M, van Esch B, Henricks PAJ, Folkerts G, Garssen J. The Anti-inflammatory Effects of Short Chain Fatty Acids on Lipopolysaccharide- or Tumor Necrosis Factor α-Stimulated Endothelial Cells via Activation of GPR41/43 and Inhibition of HDACs. Frontiers in pharmacology. 2018;9:533.

42. Seo G-Y, Giles DA, Kronenberg M. The role of innate lymphoid cells in response to microbes at mucosal surfaces. Mucosal immunology. 2020;13(3):399-412.

43. Guilloteau P, Martin L, Eeckhaut V, Ducatelle R, Zabielski R, Van Immerseel F. From the gut to the peripheral tissues: the multiple effects of butyrate. Nutrition research reviews. 2010;23(2):366-84.

44. Maggi E, Veneziani I, Moretta L, Cosmi L, Annunziato F. Group 2 Innate Lymphoid Cells: A Double-Edged Sword in Cancer? Cancers. 2020;12(11).

45. Reilly CM, Regna N, Mishra N. HDAC inhibition in lupus models. Molecular medicine (Cambridge, Mass). 2011;17(5-6):417-25.

46. Litvak Y, Byndloss MX, Bäumler AJ. Colonocyte metabolism shapes the gut microbiota. Science (New York, NY). 2018;362(6418).

47. Priyadarshini M, Kotlo KU, Dudeja PK, Layden BT. Role of Short Chain Fatty Acid Receptors in Intestinal Physiology and Pathophysiology. Comprehensive Physiology. 2018;8(3):1091-115.

48. Chun E, Lavoie S, Fonseca-Pereira D, Bae S, Michaud M, Hoveyda HR, et al. Metabolite-Sensing Receptor Ffar2 Regulates Colonic Group 3 Innate Lymphoid Cells and Gut Immunity. Immunity. 2019;51(5):871-84.e6.

49. Schreiber S, Nikolaus S, Hampe J. Activation of nuclear factor kappa B inflammatory bowel disease. Gut. 1998;42(4):477-84.

50. Segain JP, Raingeard de la Blétière D, Bourreille A, Leray V, Gervois N, Rosales C, et al. Butyrate inhibits inflammatory responses through NFkappaB inhibition: implications for Crohn's disease. Gut. 2000;47(3):397-403.

51. Zhou Y, Cui C, Ma X, Luo W, Zheng SG, Qiu W. Nuclear Factor κB (NF-κB)-Mediated Inflammation in Multiple Sclerosis. Frontiers in immunology. 2020;11:391.

52. Zegarra-Ruiz DF, El Beidaq A, Iñiguez AJ, Lubrano Di Ricco M, Manfredo Vieira S, Ruff WE, et al. A Diet-Sensitive Commensal Lactobacillus Strain Mediates TLR7-Dependent Systemic Autoimmunity. Cell host & microbe. 2019;25(1):113-27.e6.

53. Mu Q, Edwards MR, Swartwout BK, Cabana Puig X, Mao J, Zhu J, et al. Gut Microbiota and Bacterial DNA Suppress Autoimmunity by Stimulating Regulatory B Cells in a Murine Model of Lupus. Frontiers in immunology. 2020;11.

54. Greer RL, Morgun A, Shulzhenko N. Bridging immunity and lipid metabolism by gut microbiota. The Journal of allergy and clinical immunology. 2013;132(2):253-62; quiz 63.

55. Leong KH, Koh ET, Feng PH, Boey ML. Lipid profiles in patients with systemic lupus erythematosus. The Journal of rheumatology. 1994;21(7):1264-7.

56. Lian F, Wang Y, Chen J, Xu H, Yang X, Liang L, et al. Activation of farnesoid X receptor attenuates liver injury in systemic lupus erythematosus. Rheumatology international. 2012;32(6):1705-10.

57. Sun R, Xu C, Feng B, Gao X, Liu Z. Critical roles of bile acids in regulating intestinal mucosal immune responses. Therapeutic advances in gastroenterology. 2021;14:17562848211018098.

58. Hang S, Paik D, Yao L, Kim E, Trinath J, Lu J, et al. Bile acid metabolites control T(H)17 and T(reg) cell differentiation. Nature. 2019;576(7785):143-8.

59. He J, Chan T, Hong X, Zheng F, Zhu C, Yin L, et al. Microbiome and Metabolome Analyses Reveal the Disruption of Lipid Metabolism in Systemic Lupus Erythematosus. Frontiers in immunology. 2020;11:1703.

60. Ryu H, Kim J, Kim D, Lee JE, Chung Y. Cellular and Molecular Links between Autoimmunity and Lipid Metabolism. Molecules and cells. 2019;42(11):747-54.

61. Dai X, Hou H, Zhang W, Liu T, Li Y, Wang S, et al. Microbial Metabolites: Critical Regulators in NAFLD. Frontiers in Microbiology. 2020;11.

62. Mihara K, Isoda M. Immunohistochemical study of lysozyme in lupus miliaris disseminatus faciei. The British journal of dermatology. 1986;115(2):187-92.

63. Wyatt M, Greathouse KL. Targeting Dietary and Microbial Tryptophan-Indole Metabolism as Therapeutic Approaches to Colon Cancer. Nutrients. 2021;13(4).

64. Silvano A, Seravalli V, Strambi N, Cecchi M, Tartarotti E, Parenti A, et al. Tryptophan metabolism and immune regulation in the human placenta. Journal of reproductive immunology. 2021;147:103361.

65. Åkesson K, Pettersson S, Ståhl S, Surowiec I, Hedenström M, Eketjäll S, et al. Kynurenine pathway is altered in patients with SLE and associated with severe fatigue. Lupus Science & Medicine. 2018;5(1):e000254.

66. Brown J, Robusto B, Morel L. Intestinal Dysbiosis and Tryptophan Metabolism in Autoimmunity. Frontiers in immunology. 2020;11.

67. Boule LA, Burke CG, Jin GB, Lawrence BP. Aryl hydrocarbon receptor signaling modulates antiviral immune responses: ligand metabolism rather than chemical source is the stronger predictor of outcome. Scientific reports. 2018;8(1):1826.

68. Schiering C, Wincent E, Metidji A, Iseppon A, Li Y, Potocnik AJ, et al. Feedback control of AHR signalling regulates intestinal immunity. Nature. 2017;542(7640):242-5.

69. Murray IA, Patterson AD, Perdew GH. Aryl hydrocarbon receptor ligands in cancer: friend and foe. Nature reviews Cancer. 2014;14(12):801-14.

70. Shinde R, Hezaveh K, Halaby MJ, Kloetgen A, Chakravarthy A, da Silva Medina T, et al. Apoptotic cell–induced AhR activity is required for immunological tolerance and suppression of systemic lupus erythematosus in mice and humans. Nature immunology. 2018;19(6):571-82.

71. Cervantes-Barragan L, Chai JN, Tianero MD, Di Luccia B, Ahern PP, Merriman J, et al. Lactobacillus reuteri induces gut intraepithelial CD4(+)CD8αα(+) T cells. Science (New York, NY). 2017;357(6353):806-10.

72. Kiss EA, Vonarbourg C, Kopfmann S, Hobeika E, Finke D, Esser C, et al. Natural aryl hydrocarbon receptor ligands control organogenesis of intestinal lymphoid follicles. Science (New York, NY). 2011;334(6062):1561-5.

73. Li Y, Innocentin S, Withers David R, Roberts Natalie A, Gallagher Alec R, Grigorieva Elena F, et al. Exogenous Stimuli Maintain Intraepithelial Lymphocytes via Aryl Hydrocarbon Receptor Activation. Cell. 2011;147(3):629-40.

74. Li Y, Innocentin S, Withers DR, Roberts NA, Gallagher AR, Grigorieva EF, et al. Exogenous stimuli maintain intraepithelial lymphocytes via aryl hydrocarbon receptor activation. Cell. 2011;147(3):629-40.

75. Zelante T, Iannitti RG, Cunha C, De Luca A, Giovannini G, Pieraccini G, et al. Tryptophan catabolites from microbiota engage aryl hydrocarbon receptor and balance mucosal reactivity via interleukin-22. Immunity. 2013;39(2):372-85.

76. Hubbard TD, Murray IA, Bisson WH, Lahoti TS, Gowda K, Amin SG, et al. Adaptation of the human aryl hydrocarbon receptor to sense microbiota-derived indoles. Scientific reports. 2015;5:12689.

77. Chen J, Rao JN, Zou T, Liu L, Marasa BS, Xiao L, et al. Polyamines are required for expression of Toll-like receptor 2 modulating intestinal epithelial barrier integrity. American journal of physiology Gastrointestinal and liver physiology. 2007;293(3):G568-76.

78. Di Martino ML, Campilongo R, Casalino M, Micheli G, Colonna B, Prosseda G. Polyamines: emerging players in bacteria-host interactions. International journal of medical microbiology : IJMM. 2013;303(8):484-91.

79. Milovic V. Polyamines in the gut lumen: bioavailability and biodistribution. European Journal of Gastroenterology & Hepatology. 2001;13(9):1021-5.

80. Matsumoto M, Benno Y. The Relationship between Microbiota and Polyamine Concentration in the Human Intestine: A Pilot Study. Microbiology and Immunology. 2007;51(1):25-35.

81. Zhang M, Wang H, Tracey KJ. Regulation of macrophage activation and inflammation by spermine: a new chapter in an old story. Critical care medicine. 2000;28(4 Suppl):N60-6.

82. Liu L, Guo X, Rao JN, Zou T, Xiao L, Yu T, et al. Polyamines regulate E-cadherin transcription through c-Myc modulating intestinal epithelial barrier function. American journal of physiology Cell physiology. 2009;296(4):C801-10.

83. Liu L, Guo X, Rao JN, Zou T, Xiao L, Yu T, et al. Polyamines regulate E-cadherin transcription through c-Myc modulating intestinal epithelial barrier function. American Journal of Physiology-Cell Physiology. 2009;296(4):C801-C10.

84. Guo X, Rao JN, Liu L, Zou T-T, Turner DJ, Bass BL, et al. Regulation of adherens junctions and epithelial paracellular permeability: a novel function for polyamines. American Journal of Physiology-Cell Physiology. 2003;285(5):C1174-C87.

85. Nakamura A, Ooga T, Matsumoto M. Intestinal luminal putrescine is produced by collective biosynthetic pathways of the commensal microbiome. Gut microbes. 2019;10(2):159-71.

86. Tofalo R, Cocchi S, Suzzi G. Polyamines and Gut Microbiota. Frontiers in nutrition. 2019;6:16.

87. Matsumoto M, Benno Y. Consumption of Bifidobacterium lactis LKM512 yogurt reduces gut mutagenicity by increasing gut polyamine contents in healthy adult subjects. Mutation Research/Fundamental and Molecular Mechanisms of Mutagenesis. 2004;568(2):147-53.

88. Matsumoto M, Kitada Y, Shimomura Y, Naito Y. Bifidobacterium animalis subsp. lactis LKM512 reduces levels of intestinal trimethylamine produced by intestinal microbiota in healthy volunteers: A double-blind, placebo-controlled study. Journal of Functional Foods. 2017;36:94-101.

89. Linsalata M, Cavallini A, Messa C, Orlando A, Refolo MG, Russo F. Lactobacillus rhamnosus GG Influences Polyamine Metabolism in HGC-27 Gastric Cancer Cell Line: A Strategy Toward Nutritional Approach to Chemoprevention of Gastric Cancer. Current Pharmaceutical Design. 2010;16(7):847-53.

90. Orlando A, Messa C, Linsalata M, Cavallini A, Russo F. Effects of Lactobacillus rhamnosus GG on proliferation and polyamine metabolism in HGC-27 human gastric and

DLD-1 colonic cancer cell lines. Immunopharmacology and Immunotoxicology. 2009;31(1):108-16.

91. Mu Q, Kirby J, Reilly CM, Luo XM. Leaky Gut As a Danger Signal for Autoimmune Diseases. Frontiers in immunology. 2017;8:598.

92. Levy AN, Allegretti JR. Insights into the role of fecal microbiota transplantation for the treatment of inflammatory bowel disease. Therapeutic advances in gastroenterology. 2019;12:1756284819836893.

93. Kim B, Choi HN, Yim JE. Effect of Diet on the Gut Microbiota Associated with Obesity. Journal of obesity & metabolic syndrome. 2019;28(4):216-24.

94. Esmaeili SA, Mahmoudi M, Momtazi AA, Sahebkar A, Doulabi H, Rastin M. Tolerogenic probiotics: potential immunoregulators in Systemic Lupus Erythematosus. Journal of cellular physiology. 2017;232(8):1994-2007.

95. Mike A, Nagaoka N, Tagami Y, Miyashita M, Shimada S, Uchida K, et al. Prevention of B220+ T cell expansion and prolongation of lifespan induced by Lactobacillus casei in MRL/lpr mice. Clinical and experimental immunology. 1999;117(2):368-75.

96. Huang C, Yi P, Zhu M, Zhou W, Zhang B, Yi X, et al. Safety and efficacy of fecal microbiota transplantation for treatment of systemic lupus erythematosus: An EXPLORER trial. Journal of autoimmunity. 2022;130:102844.

CHAPTER 2

Phenotypic drift in lupus-prone MRL/*lpr* mice: Potential roles of microRNAs and gut microbiota

Xavier Cabana-Puig*, Jacob M. Bond†, Zhuang Wang*, Rujuan Dai*, Ran Lu*, Amy Lin*, Vanessa Oakes*, Amy Rizzo*, Brianna Swartwout†, Leila Abdelhamid*, Jiangdi Mao*, Meeta Prakash‡, Constanza Sangmeister*, Nathaniel Cheung*, Catharine Cowan*, Christopher M. Reilly§, Sha Sun¶, S. Ansar Ahmed*, Xin M. Luo*

*Department of Biomedical Sciences and Pathobiology, College of Veterinary Medicine, Virginia Tech, Blacksburg, VA, USA

†Graduate Program in Translational Biology, Medicine, and Health, Virginia Tech, Roanoke, VA, USA

‡Carilion School of Medicine, Virginia Tech, Roanoke, VA, USA

§Edward Via College of Osteopathic Medicine, Blacksburg, VA, USA

¶Department of Development and Cell Biology, University of California, Irvine, CA, USA

Published in ImmunoHorizons January 1, 2022, 6(1)36-46.

Abstract

MRL/*lpr* mice have been extensively used as a murine model of lupus. Disease progression in MRL/*lpr* mice can differ among animal facilities, suggesting a role for environmental factors. We noted a phenotypic drift of our in-house colony, which was the progeny of mice obtained from The Jackson Laboratory (JAX; Stocking Number 000485), that involved attenuated glomerulonephritis, increased splenomegaly, and reduced lymphadenopathy. To validate our in-house mice as a model of lupus, we compared these mice with those newly obtained from JAX, which were confirmed to be genetically identical to our in-house mice. Surprisingly, the new JAX mice exhibited a similar phenotypic drift, most notably the attenuation of glomerulonephritis. Interestingly, our in-house colony differed from JAX mice in body weight and kidney size (both sexes), and splenic size, germinal center formation, and level of anti-double stranded DNA auto-IgG in the circulation (male only). In addition, we noted differential expression of microRNA (miR)-21 and miR-183 that might explain the splenic differences in males. Furthermore, the composition of gut microbiota was different between in-house and new JAX mice at early time points, which might explain some of the renal differences (e.g., kidney size). However, we could not identify the reason for attenuated glomerulonephritis, a shared phenotypic drift between the two colonies. It is likely that this was due to certain changes of environmental factors present in both JAX and our facilities. Together, these results suggest a significant phenotypic drift in MRL/*lpr* mice in both colonies that may require strain recovery from cryopreservation.

Introduction

Systemic lupus erythematosus (SLE) is an autoimmune disease that affects multiple organs of the body, including lymphoid organs as well as peripheral organs such as kidney and brain. The manifestations of SLE include skin rash, blood/serum abnormalities (e.g., interferon signature, anti-nuclear antibodies), lupus nephritis, arthritis, splenomegaly, lung inflammation, and neurological damage. A large proportion of patients also exhibit lymphadenopathy as a major side effect that may not be caused by SLE. Many mouse models of SLE have been developed over the years, including both spontaneous (e.g., NZB/W F1, MRL/lpr, BXSB) and inducible models (e.g., pristane-induced lupus). Among these, the MRL/lpr model (MRL/Mp-$Fas^{lpr/lpr}$) stands out as one that exhibits all of the manifestations and side effect of SLE described above. Compared to its parent strain MRL, MRL/lpr mice develop lupus-like disease early in life due to the $Fas^{lpr/lpr}$ mutation. However, it is important to note that their clinical signs do not solely depend on this mutation; rather, the exhibition of lupus-like disease mainly comes from the MRL background, where multiple SLE susceptibility loci are present. The $Fas^{lpr/lpr}$ mutation simply accelerates the disease, thus making MRL/lpr a more efficient model than MRL.

We have studied the MRL/lpr model for the past 10 years. Female mice develop severe lupus-like disease (e.g., skin rash, glomerulonephritis, splenomegaly, lymphadenopathy, arthritis, brain inflammation, etc.) at around 16 weeks of age. In recent years, however, we noticed the attenuation of kidney disease in our in-house colony, which had originated from The Jackson Laboratory (JAX; Stock Number 000485). This was not entirely surprising, as JAX had experienced a loss of disease phenotype in their

colony about 15 years ago, when they had to recover the strain from cryopreservation in order to preserve the original phenotype. In that incident, the loss of phenotype was manifested by reduced splenomegaly and lymphadenopathy, as well as prolonged survival. Importantly, the single-nucleotide polymorphism (SNP) profile did not show any genetic drift, suggesting that the phenotypic drift may be due to environmental factors.

As we routinely use both the in-house colony and mice directly purchased from JAX for our studies, it became important to investigate whether our in-house colony had indeed lost the kidney phenotype compared to JAX mice. Here, we report a phenotypic drift of MRL/lpr mice in both our and JAX colonies. Both exhibit attenuated glomerulonephritis; however, some clinical signs are different between the two types of mice in a sex-dependent manner, even though they are genetically identical. In addition, since MRL/lpr mice manifest signature changes in splenic miRNAs and gut microbiota, these parameters are analyzed to investigate their potential contributions to the phenotypic drift.

Materials and Methods

Ethics statement

This study was carried out in strict accordance with the recommendations in the Guide for the Care and Use of Laboratory Animals of the NIH. The protocol was approved by the Institutional Animal Care and Use Committee (IACUC) of Virginia Tech College of Veterinary Medicine (Animal Welfare Assurance Number: A3208-01). All animal

experiments were conducted under IACUC protocol #18-060. Euthanasia was performed with CO_2 according to the IACUC protocol.

Mice

All MRL/lpr (MRL/Mp-*Fas*$^{lpr/lpr}$) mice originated from The Jackson Laboratory (JAX). Mice purchased in 2015 were bred and the colony was maintained in our animal facility at Virginia-Maryland College of Veterinary Medicine (VMCVM) for 3 years. Mice in the "in-house" group were descendants from this colony. As a comparison, 5-week-old female and male were introduced from JAX in 2018 right before the initiation of this study and identified as the "JAX" group. All mice were monitored for proteinuria every week, and euthanized at 15 weeks of age. Urine samples were analyzed with a Pierce Coomassie Protein Assay Kit (Thermo Scientific). Body and whole tissue weights were recorded, and the level of anti-dsDNA IgG was determined as previously described (1-7). Tail clips were sent to JAX for single-nucleotide polymorphism (SNP) analysis to determine any genetic drift from the MRL background. An additional group of mice labeled "JAX-2015" were purchased in 2015 at 3~5 weeks of age and euthanized at 15 weeks of age. For this group, historical data were used.

Flow cytometry

Spleen was collected and mashed in 70-μm cell strainers with C10 medium (RPMI-1640, 10% fetal bovine serum, 1 mM sodium pyruvate, 1% 100× MEM non-essential amino acids, 10 mM HEPES, 55 μM 2-mercaptoethanol, 2 mM L-glutamine, 100 U/ml penicillin-streptomycin, all from Life Technologies, Grand Island, NY). To isolate

splenocytes, red blood cells were lysed with RBC lysis buffer (eBioscience, San Diego, CA). For surface marker staining, cells were blocked by anti-mouse CD16/32 (eBioscience), stained with fluorochrome-conjugated antibodies, and analyzed with BD FACSAria Fusion flow cytometer (BD Biosciences, San Jose, CA). Anti-mouse antibodies used in this study include: CD38-FITC, GL7-APC, CD19-BV421, and CD138-PerCP-Cy5 (all from BioLegend, San Diego, CA). For analysis of germinal center B cells, the plots were pre-gated on $CD19^+$ cells. Flow cytometry data were analyzed with FlowJo.

Immunohistochemistry

Splenic and kidney sections were embedded in Tissue-Tek OCT Compound (Sakura Finetek) and rapidly frozen in a freezing bath of dry ice and 2-methylbutane. Frozen OCT samples were cryosectioned and unstained slides were stored at −80°C. Immunohistochemical staining procedures were performed as previously described (1, 2, 5). For detection of germinal centers in the spleen, the following monoclonal antibodies were used: GL7-AF488, IgD-PE, and CD4-APC (all from BioLegend). For detection of renal deposition, C3-FITC (Cedarlane, Burlington, NC) and IgG2a-PE (eBioscience) antibodies were used. Pictures were captured with a Zeiss LSM 880 confocal microscope (Fralin Imaging Center, Virginia Tech). Corrected total cell fluorescence (CTCF) scores were calculated with the ImageJ software (National Institutes of Health, Rockville, MD).

Histopathology

Kidneys were fixed in formalin immediately after isolation. Fixed tissues were paraffin-embedded, sectioned, and stained for Periodic Acid-Schiff (PAS) at the Histopathology Laboratory at VMCVM. Glomerular lesions were graded for increased cellularity, increased mesangial matrix, necrosis, percentage of sclerotic glomeruli, and presence of crescents (8). Similarly, tubulointerstitial lesions were graded for interstitial mononuclear infiltration, tubular damage, interstitial fibrosis, and vasculitis. Slides were scored by a board-certified veterinary pathologist (Oakes) in a blinded fashion.

Analysis of splenic miRNAs

The spleen was removed immediately after the mouse was euthanized and mashed into single-cell suspension. After flowing through a 70 μm Nylon Mesh (Fisher Scientific), the cells were treated with ACK (Ammonium-Chloride-Potassium) lysis buffer to deplete erythrocytes. The freshly-prepared splenic lymphocytes were pelleted, washed with cold PBS, and stored at −80°C. Total RNA containing small RNA was extracted from cells using the miRNeasy Mini Kit (Qiagen) following the manufacturer's protocol. On-column DNA digestion was performed to remove any residual DNA in the RNA samples during RNA extraction. Concentration and purity of RNA were determined by a Nanodrop 2000 spectrophotometer (Thermo Fisher Scientific) and samples with the OD260/280 ratio of ~2.0 were used. TaqMan microRNA assays (Applied Biosystems, Waltham, MA) were used to quantify miRNA expression levels. Briefly, the total RNAs were reverse-transcribed into cDNA with the TaqMan MicroRNA Reverse Transcription Kit, followed by quantitative real-time PCR with the TaqMan miRNA assay reagent

using the 7500 Fast Real-Time PCR system (Applied Biosystems). The relative expression level of a specific miRNA was normalized to the endogenous small nucleolar RNA 202 (sno202) and calculated using the 2-ΔΔCt method.

16S rRNA sequencing analysis of gut microbiota

Fecal samples were collected weekly directly from the anus of the mouse. To avoid cross-contamination, each microbiota sample was collected by using a new pair of sterile tweezers. Samples were stored at -80°C till being processed at the same time. Sample homogenization, cell lysis and DNA extraction were performed in-house. PCR were performed and purified amplicons (V4 region) were sequenced bidirectionally on an Illumina MiSeq at Argonne National Laboratory. Data analysis was performed as previously described (3, 4, 6, 7, 9), and 16S rRNA sequences are available in the NIH SRA database (PRJNA758126).

Statistical analysis

For the comparison of two groups, unpaired student's *t*-test was used. For the comparison of three groups, one-way ANOVA and Tukey's post-test were used. Two-way ANOVA was used to reveal time- and group-dependent effects. High-dimensional omics data was visualized by principal coordinates analysis with permutational multivariate ANOVA. Results were considered statistically significant when $p<0.05$. All analyses were performed with the GraphPad Prism software.

Results

Phenotypic drift in lupus-prone MRL/lpr mice

We routinely breed MRL/lpr mice in-house and only re-introduce the mouse strain from JAX every 2-3 years. Prior to this study, we had purchased female and male MRL/lpr mice in 2015 and started a breeding colony at VMCVM. Two years later, we noticed that the mice in our colony had delayed onset of proteinuria. By 2018, we could no longer detect a significant increase of proteinuria even at the endpoint of 15 weeks of age. As lupus-prone mice were known to exhibit different levels of disease severity in different facilities (10), we hypothesized that the animal housing conditions at VMCVM led to the gradual loss of disease phenotype and particularly attenuated glomerulonephritis. To test the hypothesis, we purchased 5-week-old female and male MRL/lpr mice from JAX that were age-matched to a group of mice in our in-house colony. Surprisingly, both groups of mice (In-house *vs*. JAX) regardless of sex exhibited low levels of proteinuria at 15 weeks of age (Fig. 1A). As a comparison we used historical data from mice purchased and analyzed in 2015, which had significantly higher levels of proteinuria at 15 weeks of age, especially for females.

Interestingly, while the level of endpoint proteinuria was similarly low, the new JAX mice (purchased and analyzed in 2018) were considerably larger than the MRL/lpr mice in our in-house colony for both females and males (Fig. 1B). Upon euthanasia at 15 weeks of age, we measured the weight of different organs including spleen, mesenteric lymph node (MLN), and kidney, and calculated the organ-to-body weight ratios. Our in-house male mice had significantly larger spleens than the new JAX mice, whereas the size of the spleen was similar between female in-house and JAX mice (Fig. 1C). Both

female groups sacrificed in 2018 had significantly larger spleens than female mice sacrificed back in 2015. This suggests that the housing conditions at VMCVM did not adversely affect splenomegaly, one of the key clinical signs of lupus-like disease in MRL/lpr mice. The weight of MLN, on the other hand, was significantly smaller in female in-house and new JAX mice than that recorded in 2015 (Fig. 1D). Both in-house and new JAX mice had similarly small MLNs, suggesting a phenotypic drift in lymphadenopathy at JAX as well. Another hallmark of lupus-like disease in MRL/lpr mice is the increase of autoantibodies, including anti-dsDNA IgG. While there was no difference in female mice, the male mice in our colony had a significantly lower level of anti-dsDNA IgG in the blood than both groups obtained from JAX (Fig. 1E), suggesting a loss of this disease parameter only in males. Moreover, we measured the weight of the kidney and observed that our in-house MRL/lpr had significantly smaller kidneys than the JAX mice (Fig. 1F).

These results indicate a significant phenotypic drift in our in-house MRL/lpr mice from mice purchased in 2015 that involves attenuated proteinuria and smaller MLNs and kidneys (both sexes), larger spleens (females), and smaller body weight and reduced circulatory autoantibodies (males). Surprisingly, female MRL/lpr mice at JAX also exhibited a phenotypic drift over 3 years that involves attenuated proteinuria, increased splenomegaly, and reduced lymphadenopathy. To exclude the contribution from genetic factors, we ordered SNP analysis that did not identify any genetic drift (100% identical between in-house and JAX mice). This suggests that the phenotypic drift in MRL/lpr mice, most notably the attenuated proteinuria, may be solely due to environmental factors present both in-house and at JAX.

Splenic differences between in-house and new JAX mice

As splenomegaly was exacerbated in in-house male mice, we asked whether there were immunological changes in the spleen. Neither the frequency of germinal center B cells ($CD19^{+}GL7^{+}CD38^{-/low}$) nor those of plasmablasts ($CD19^{+}CD138^{+}$) and plasma cells ($CD19^{-}CD138^{+}$) were different between in-house and new JAX mice, regardless of sex (Fig. 2A and 2B). However, we noted a small increase of total GL7-expressing cells (Fig. 3A), which prompted us to investigate the localization of germinal center B cells in relevance to splenic T-helper (Th) cells. Interestingly, GL7-expressing cells were scattered among Th cells in the splenic section suggesting the lack of germinal center formation in both groups of females as well as in-house male mice. However, in the new JAX male mice, these cells were significantly brighter (Fig. 3B) and clustered (Fig. 3C). While cells expressing a higher amount of GL7 have not been shown to exhibit enhanced functions, the clustering pattern suggests that the spleen of male mice newly obtained from JAX may contain more mature germinal centers even though the spleen size was smaller. This is consistent with the observation that the level of anti-dsDNA IgG was significantly higher in this group of male mice.

Renal differences between in-house and new JAX mice

We were particularly interested in glomerulonephritis that made the MRL/lpr mice a classical model of lupus nephritis, a leading cause of mortality for SLE patients (11). Using weekly collected urine samples, we observed that the time course of proteinuria was not different between our in-house mice and new JAX mice for both females and males (Fig. 4A and 4C). There was a slight increase of proteinuria in both female groups

close to the endpoint, but it was not statistically significant. Importantly, histopathological analysis (Fig. 4B and 4D) revealed no difference in glomerular and tubulointerstitial lesions as well as leukocyte infiltration between the in-house and new JAX mice. Immunohistochemical analysis also showed no difference in renal depositions of complement C3 and IgG2a, the pathogenic IgG in this mouse strain (Fig. 4E and 4F). These results suggest that the severity of renal damage is the same between in-house and new JAX mice, and that the environmental factors driving the attenuation of glomerulonephritis may be common between the two facilities.

Analysis of lupus-associated microRNAs

While the severity of glomerulonephritis was the same between the two groups, the MRL/lpr mice in our colony did have significantly smaller kidneys and body weight (both sexes), and significantly larger spleens and lower blood levels of anti-dsDNA IgG (males) than the mice newly purchased from JAX. We asked whether there were associations between the disease phenotype and differential expression of lupus-associated miRNAs in the spleen. We had previously identified several lupus-associated miRNAs that were increased in multiple murine models of SLE compared to healthy controls (12). While the levels of these miRNAs were not statistically different between JAX and in-house female mice due to large variations within groups, in-house males had significantly higher levels of miR-183, miR-21, miR-148a, miR-127 and miR-411 than males purchased from JAX in 2018 (Fig. 5). A similar trend was observed for miR-182 and miR-146a in males albeit no statistical significance. Notably, miR-146 has been

shown to limit germinal center formation (13); thus, the lower level of this miRNA in new JAX mice may be associated with more mature germinal centers in these mice. Among the noted lupus-associated miRNAs, the expression of miR-21 has been shown to be positively correlated with splenic size in lupus-prone mice (14), consistent with our observation of larger spleens in male in-house MRL/lpr mice. Interestingly, while our previous studies point to a pathogenic role for miR-183 (12, 15), a recent report showed that intraperitoneal injection of this miRNA attenuated several disease parameters in MRL/lpr mice, including the reduction of anti-dsDNA antibodies (16). It is consistent with our observation that in-house males had less anti-dsDNA IgG in the circulation while expressing more miR-183 in the spleen. Together, these results suggest that the differential expression of miR-21 and miR-183 in the spleen may explain the phenotypic differences observed for male mice in our colony *vs*. those newly purchased from JAX. In addition, the lack of miRNA expression difference in the female spleen is consistent with the lack of phenotypic difference in this tissue for females.

Analysis of gut microbiota

To establish associations between changes of disease phenotype with the composition of gut microbiota, we analyzed fecal samples collected from the two groups of mice harvested in 2018. It was evident that at the earlier time points of 5 and 7 weeks of age, the gut microbiota of our in-house mice was significantly more diverse than that of the new JAX mice as indicated by the Shannon Index (Fig. 6A). This was true for both female and male mice, suggesting that the housing conditions were indeed different between our facility and JAX. In addition, based on Principal Coordinate Analysis

(PCA), the gut microbiotas were significantly distinct comparing the two groups especially for female mice (Fig. 6B). At the phylum level (Fig. 6C), it was consistent between sexes that Proteobacteria were significantly higher in the in-house mice than the new JAX mice (Fig. S1). Increased Proteobacteria has been found to be associated with human SLE (17). Other phyla that were different included significantly increased Verrucomicrobia in the in-house male mice, and significantly increased Tenericutes (females) and Bacteroidetes (males) in the new JAX mice (Fig. S1). Verrucomicrobia, which is essentially *Akkermansia muciniphila*, is considered protective in the pathogenesis of some autoimmune diseases (18, 19). The opposite functions of pro-inflammatory Proteobacteria and anti-inflammatory Verrucomicrobia may neutralize each other leading to similar levels of severity in glomerulonephritis between our in-house mice and the new JAX mice (Fig. 4). At the order level (Fig. 6D), Lactobacillales was significantly higher in female in-house mice (Fig. S2). Erysipelotrichales, on the other hand, was significantly higher in female JAX but significantly lower in male JAX mice than our in-house mice. These two orders represented around 5-10% of the gut bacteria.

We paid special attention on the families *Lactobacillaceae* and *Lachnospiraceae*, which we had previously shown to be associated with disease outcomes in female MRL/lpr mice (20). A higher level of *Lactobacillaceae* and a lower level of *Lachnospiraceae* were associated with less severe lupus-like disease including glomerulonephritis, splenomegaly, lymphadenopathy and autoantibodies. Here, we found time-dependent differences of *Lactobacillaceae*, with an increased abundance of these bacteria in our colony than the new JAX mice only in females at the earlier time points of

5 and 7 weeks of age (Fig. 7A). However, it is difficult to establish associations with disease because the phenotypic differences in females were not obvious between the two groups except the body weight and kidney size. The levels of *Lachnospiraceae* were not different for both sexes (Fig. 7B). Therefore, the difference of the ratio of *Lactobacillaceae* to *Lachnospiraceae* resembled the difference in *Lactobacillaceae* (Fig. 7C).

Many groups of bacteria at the genus level were altered comparing in-house *vs.* JAX mice (Table S1). Consistent for both females and males, *Odoribacter* and *Parabacteroides* from the family of *Porphyromonadaceae,* as well as *Flavonifractor* in *Ruminococcaceae,* were significantly upregulated in our in-house colony. In contrast, the following genera were significantly upregulated in the new JAX mice: f_*Lachnospiraceae* g_*Eubacterium,* f_*Peptostreptococcaceae* g_*Romboutsia,* and f_*Ruminococcaceae* g_*Acutalibacter*. One genus of interest was *Enterococcus* under the order Lactobacillales, family *Enterococcaceae*. It has been recently discovered that *Enterococcus gallinarum* can translocate into the liver of lupus-prone mice to facilitate the development of autoimmunity (21). *Enterococcus* was significantly higher in female mice from JAX, which might be associated with the significant increase of kidney size comparing female JAX to female in-house mice.

Together, these results indicate that the gut microbiota is different between in-house and new JAX mice at early time points, suggesting significant housing/environmental differences in the two facilities. They also suggest that the difference in gut microbiota may explain some of the phenotypic differences (e.g., kidney size) but not the attenuated glomerulonephritis, which is a shared phenotype between in-

house and new JAX mice. The latter may be due to certain changes of environmental factors common for both our and JAX facilities.

Discussion

The MRL (Murphy Roths Large) background, which came from various mouse strains including LG/J, AKR/J, C3H/Di and C57BL/6J, distinguishes MRL/lpr mice from other mouse strains with the *Fas*^{lpr} mutation. Genomic mapping identified 4 SLE susceptibility loci in mice with MRL background that contribute to splenomegaly, lymphadenopathy, glomerulonephritis (22). The loci responsible for splenomegaly and lymphadenopathy (chromosomes 4, 5, 7) are different from those important for glomerulonephritis (chromosome 10). Notably, our in-house mice are different from the new JAX mice in the spleen (splenic size, germinal center formation, and level of anti-dsDNA autoantibodies; males only), but similar to JAX in terms of attenuated glomerulonephritis (both sexes). While we have confirmed that the in-house mice were genetically identical to the new JAX mice, it remains unclear whether there had been a genetic drift in both colonies during a period of 3 years (2015-2018), particularly within chromosome 10. Notably, female JAX mice from 2015 exhibited a significantly higher level of proteinuria than female JAX mice purchased in 2018. In addition, while both from JAX, female mice purchased in 2015 had significantly smaller spleens and significantly larger MLNs than female mice purchased in 2018. These results suggest a significant phenotypic drift in MRL/lpr mice that may require JAX to perform strain recovery from cryopreservation.

We next explored the potential associations between the phenotypic changes and splenic expression of lupus-associated microRNAs. We have previously reported a

positive correlation between miR-183-96-182 cluster miRNAs (miR-183C) and murine lupus (12, 15). Previous studies from another laboratory also showed the pathogenic role of miR-182 in lupus, as inhibition of miR-182 *in vivo* with antagomir-182 was able to attenuate lupus nephritis in MRL/lpr mice (23). In addition, our unpublished data showed that conditional deletion of the whole miR-183C cluster specifically in lymphocytes significantly reduced the serum level of anti-dsDNA as well as IgG deposition in the kidney, but not renal function in B6/lpr mice. Lymphocyte-specific deletion of miR-182 alone, on the other hand, reduced renal deposition of IgG and slightly suppressed the serum level of anti-dsDNA. Consistent with these results, positive correlations between miR-182/miR-183c have been observed in murine models of rheumatoid arthritis (24) and multiple sclerosis (25, 26). Notably, while these studies showed potential pathogenic roles of miR-182 and miR-183C in lupus nephritis and other autoimmune diseases, contradictory data exists regarding the role of miR-183 in lupus nephritis. miR-183 was found to be reduced in the renal biopsy of MRL/lpr mice and human patients with lupus nephritis (16) suggesting a potential protective role of this microRNA. In addition, intraperitoneal delivery of miR-183 mimics reduced anti-dsDNA antibodies and attenuated lupus nephritis in MRL/lpr mice (16). If this microRNA indeed plays a protective role in lupus, our results of reduced miR-183 expression in male (but not female) JAX mice may explain the increase of anti-dsDNA autoantibodies specifically in male JAX mice. Female in-house and JAX mice, on the other hand, did not differ in either the phenotype or microRNA expression in the spleen.

Recent studies have started to establish the effects of different microRNAs on gut microbiota composition. Without miR-21, for example, Proteobacteria (27) and

Lactobacillus spp. (28) flourished in the mouse gut microbiota. This is opposite to our observations for splenic expression of miR-21 and the relative abundances of Proteobacteria and *Lactobacillus* spp. in male in-house *vs*. JAX mice. However, deletion of miR-21 also led to a reduction of Verrucomicrobia (27), which is consistent with our observation that JAX mice with lower splenic expression of miR-21 had significantly lower Verrucomicrobia in the gut microbiota. This suggests a possible connection between splenic microRNA expression and the composition of gut microbiota.

It is important to note that once both types of mice were in our facility, they were housed in the same room on the same rack. Therefore, starting 5 weeks of age, the housing conditions were essentially the same including bedding, water, feed, light/dark hours, noise, and room temperature and humidity (29). However, the JAX mice had been exposed to different housing conditions as detailed in Table 1. MRL/lpr mice were housed in maximum barrier rooms at JAX with acidified water and more excluded pathogens or opportunistic agents. In addition, a quaternary ammonium compound (QAC) disinfectant was used at JAX. We have previously shown that QAC disinfectants decrease splenomegaly in female MRL/lpr mice (30). In this study, the splenic size was not different between JAX and in-house female mice, probably because our facility shared a cage washing machine with adjacent facilities that did use QAC disinfectants leading to ambient exposure of in-house mice to QACs. However, while we did not investigate male mice in the previous QAC study (30), our observation that the male splenic size was significantly larger in in-house *vs*. new JAX mice may be explained by QAC-associated decrease in splenomegaly. Furthermore, the differences in previous

housing conditions may explain why JAX mice after arriving at our facility harbored significantly different gut microbiotas from our in-house mice during the first month.

In summary, we have characterized a phenotypic drift in MRL/lpr mice housed in our facility as well as at JAX. Some phenotypic changes may be associated with differential expression of microRNAs in the spleen and/or changes of the gut microbiota composition. Future studies will involve modifications of specific microRNAs (e.g., miR-21 or miR-183) or commensal bacteria (e.g., *Enterococcus*) followed by phenotypic characterizations of MRL/lpr mice to provide more mechanistic insight.

Acknowledgments

We thank Sarah Owens for assistance on Illumina MiSeq sequencing, and Husen Zhang for bioinformatic analysis of 16S rRNA sequences. We also thank Melissa Makris for assistance on flow cytometry.

Competing interests

There are no competing interests.

Contributorship

XML and SAA designed the study. XCP, JMB, ZW, RD, RL, AL, BS, LA, JM, MP, CS, NC and CC performed the experiments. XCP, ZW, RD, RL, AL, CMR and SS analyzed the data. VO scored the histopathological slides. AR provided facility information. XML, SAA and RD wrote the manuscript.

Funding information

This work was supported by internal funding from VMCVM and NIH grants AR067418 and AR073240 (Luo).

Ethical approval information

This study was carried out in strict accordance with the recommendations in the Guide for the Care and Use of Laboratory Animals of the NIH. The protocol was approved by the Institutional Animal Care and Use Committee (IACUC) of Virginia Tech College of Veterinary Medicine (Animal Welfare Assurance Number: A3208-01). All animal experiments were conducted under IACUC protocol #18-060.

Data sharing information

The 16S rRNA sequences are available in the NIH SRA database (PRJNA758126).

References

1. Liao X, Ren J, Wei CH, Ross AC, Cecere TE, Jortner BS, et al. Paradoxical Effects of All-Trans-Retinoic Acid on Lupus-Like Disease in the MRL/lpr Mouse Model. PLoS One. 2015;10(3):e0118176.

2. Liao X, Ren J, Reihl A, Pirapakaran T, Sreekumar B, Cecere TE, et al. Renal-infiltrating CD11c+ cells are pathogenic in murine lupus nephritis through promoting CD4+ T cell responses. Clin Exp Immunol. 2017.

3. Mu Q, Tavella VJ, Kirby JL, Cecere TE, Chung M, Lee J, et al. Antibiotics ameliorate lupus-like symptoms in mice. Sci Rep. 2017;7(1):13675.

4. Mu Q, Zhang H, Liao X, Lin K, Liu H, Edwards MR, et al. Control of lupus nephritis by changes of gut microbiota. Microbiome. 2017;5(1):73.

5. Abdelhamid L, Cabana-Puig X, Swartwout B, Lee J, Li S, Sun S, et al. Retinoic Acid Exerts Disease Stage-Dependent Effects on Pristane-Induced Lupus. Front Immunol. 2020;11:408.

6. Mu Q, Edwards MR, Swartwout BK, Cabana Puig X, Mao J, Zhu J, et al. Gut Microbiota and Bacterial DNA Suppress Autoimmunity by Stimulating Regulatory B Cells in a Murine Model of Lupus. Front Immunol. 2020;11:593353.

7. Mu Q, Cabana-Puig X, Mao J, Swartwout B, Abdelhamid L, Cecere TE, et al. Pregnancy and lactation interfere with the response of autoimmunity to modulation of gut microbiota. Microbiome. 2019;7(1):105.

8. Perez de Lema G, Lucio-Cazana FJ, Molina A, Luckow B, Schmid H, de Wit C, et al. Retinoic acid treatment protects MRL/lpr lupus mice from the development of glomerular disease. Kidney Int. 2004;66(3):1018-28.

9. Mu Q, Swartwout BK, Edwards M, Zhu J, Lee G, Eden K, et al. Regulation of neonatal IgA production by the maternal microbiota. Proc Natl Acad Sci U S A. 2021;118(9).

10. Lei Y, Sehnert B, Voll RE, Jacobs-Cacha C, Soler MJ, Sanchez-Nino MD, et al. A multicenter blinded preclinical randomized controlled trial on Jak1/2 inhibition in MRL/MpJ-Fas(lpr) mice with proliferative lupus nephritis predicts low effect size. Kidney Int. 2021;99(6):1331-41.

11. Tsokos GC. Systemic lupus erythematosus. The New England journal of medicine. 2011;365(22):2110-21.

12. Dai R, Zhang Y, Khan D, Heid B, Caudell D, Crasta O, et al. Identification of a common lupus disease-associated microRNA expression pattern in three different murine models of lupus. PLoS One. 2010;5(12):e14302.

13. Pratama A, Srivastava M, Williams NJ, Papa I, Lee SK, Dinh XT, et al. MicroRNA-146a regulates ICOS-ICOSL signalling to limit accumulation of T follicular helper cells and germinal centres. Nat Commun. 2015;6:6436.

14. Garchow BG, Bartulos Encinas O, Leung YT, Tsao PY, Eisenberg RA, Caricchio R, et al. Silencing of microRNA-21 in vivo ameliorates autoimmune splenomegaly in lupus mice. EMBO Mol Med. 2011;3(10):605-15.

15. Choi EW, Lee M, Song JW, Shin IS, Kim SJ. Mesenchymal stem cell transplantation can restore lupus disease-associated miRNA expression and Th1/Th2 ratios in a murine model of SLE. Sci Rep. 2016;6:38237.

16. Li X, Luo F, Li J, Luo C. MiR-183 delivery attenuates murine lupus nephritis-related injuries via targeting mTOR. Scand J Immunol. 2019;90(5):e12810.

17. Luo XM, Edwards MR, Mu Q, Yu Y, Vieson MD, Reilly CM, et al. Gut microbiota in human SLE and a mouse model of lupus. Appl Environ Microbiol. 2017.

18. Hanninen A, Toivonen R, Poysti S, Belzer C, Plovier H, Ouwerkerk JP, et al. Akkermansia muciniphila induces gut microbiota remodelling and controls islet autoimmunity in NOD mice. Gut. 2018;67(8):1445-53.

19. Hansen CH, Krych L, Nielsen DS, Vogensen FK, Hansen LH, Sorensen SJ, et al. Early life treatment with vancomycin propagates Akkermansia muciniphila and reduces diabetes incidence in the NOD mouse. Diabetologia. 2012;55(8):2285-94.

20. Zhang H, Liao X, Sparks JB, Luo XM. Dynamics of gut microbiota in autoimmune lupus. Appl Environ Microbiol. 2014;80(24):7551-60.

21. Manfredo Vieira S, Hiltensperger M, Kumar V, Zegarra-Ruiz D, Dehner C, Khan N, et al. Translocation of a gut pathobiont drives autoimmunity in mice and humans. Science. 2018;359(6380):1156-61.

22. Vidal S, Kono DH, Theofilopoulos AN. Loci predisposing to autoimmunity in MRL-Fas lpr and C57BL/6-Faslpr mice. J Clin Invest. 1998;101(3):696-702.

23. Wang X, Wang G, Zhang X, Dou Y, Dong Y, Liu D, et al. Inhibition of microRNA-182-5p contributes to attenuation of lupus nephritis via Foxo1 signaling. Exp Cell Res. 2018;373(1-2):91-8.

24. Stittrich AB, Haftmann C, Sgouroudis E, Kuhl AA, Hegazy AN, Panse I, et al. The microRNA miR-182 is induced by IL-2 and promotes clonal expansion of activated helper T lymphocytes. Nat Immunol. 2010;11(11):1057-62.

25. Wan C, Ping CY, Shang XY, Tian JT, Zhao SH, Li L, et al. MicroRNA 182 inhibits CD4(+)CD25(+)Foxp3(+) Treg differentiation in experimental autoimmune encephalomyelitis. Clin Immunol. 2016;173:109-16.

26. Ichiyama K, Gonzalez-Martin A, Kim BS, Jin HY, Jin W, Xu W, et al. The MicroRNA-183-96-182 Cluster Promotes T Helper 17 Cell Pathogenicity by Negatively Regulating Transcription Factor Foxo1 Expression. Immunity. 2016;44(6):1284-98.

27. Johnston DGW, Williams MA, Thaiss CA, Cabrera-Rubio R, Raverdeau M, McEntee C, et al. Loss of MicroRNA-21 Influences the Gut Microbiota, Causing Reduced Susceptibility in a Murine Model of Colitis. J Crohns Colitis. 2018;12(7):835-48.

28. Santos AA, Afonso MB, Ramiro RS, Pires D, Pimentel M, Castro RE, et al. Host miRNA-21 promotes liver dysfunction by targeting small intestinal Lactobacillus in mice. Gut Microbes. 2020;12(1):1-18.

29. Edwards MR, Dai R, Heid B, Cecere TE, Khan D, Mu Q, et al. Commercial rodent diets differentially regulate autoimmune glomerulonephritis, epigenetics and microbiota in MRL/lpr mice. Int Immunol. 2017;29(6):263-76.

30. Abdelhamid L, Cabana-Puig X, Mu Q, Moarefian M, Swartwout B, Eden K, et al. Quaternary Ammonium Compound Disinfectants Reduce Lupus-Associated Splenomegaly by Targeting Neutrophil Migration and T-Cell Fate. Front Immunol. 2020;11:575179.

Figures

Figure 1

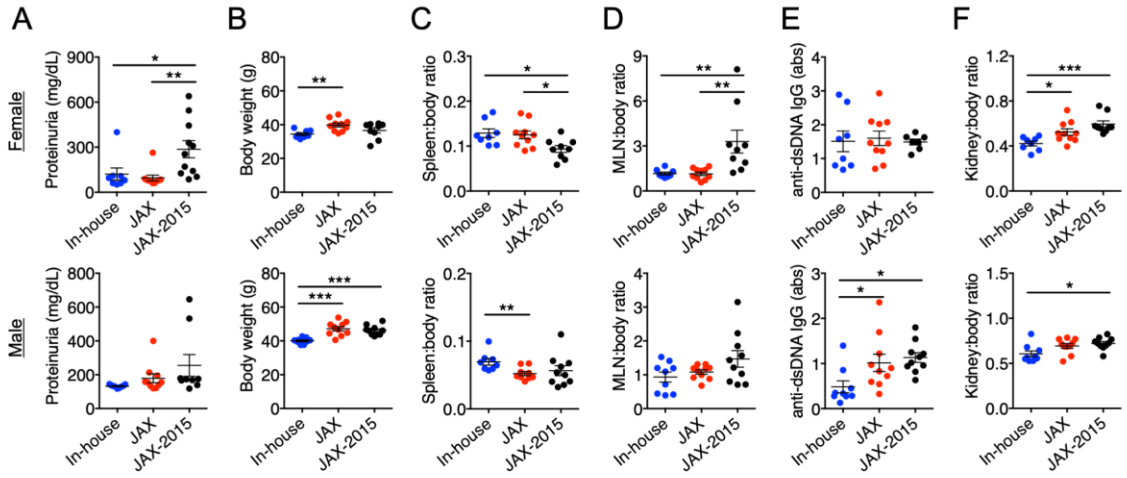

Figure 1. Phenotypic drift in MRL/*lpr* mice. Female (top) and male (bottom) MRL/lpr from our in-house colony were compared to those newly purchased from JAX in 2018 (JAX) and those purchased 3 years prior (JAX-2015). In females, n = 8, 10, 9 for in-house, JAX, and JAX-2015 groups, respectively. In males, n = 9, 10, 10 for the 3 respective groups. Characterization of the disease phenotype was performed when mice were 15 weeks of age. Historical data were used for JAX-2015. (**A**) Level of proteinuria. (**B**) Body weight. (**C**) Spleen-to-body weight ratio. (**D**) Mesenteric lymph node-to-body weight ratio. (**E**) Serum level of anti-dsDNA IgG. (**F**) Kidney-to-body weight ratio. Statistical significance (*p<0.05, **p<0.01, ***p<0.001) is shown based on one-way ANOVA.

Figure 2

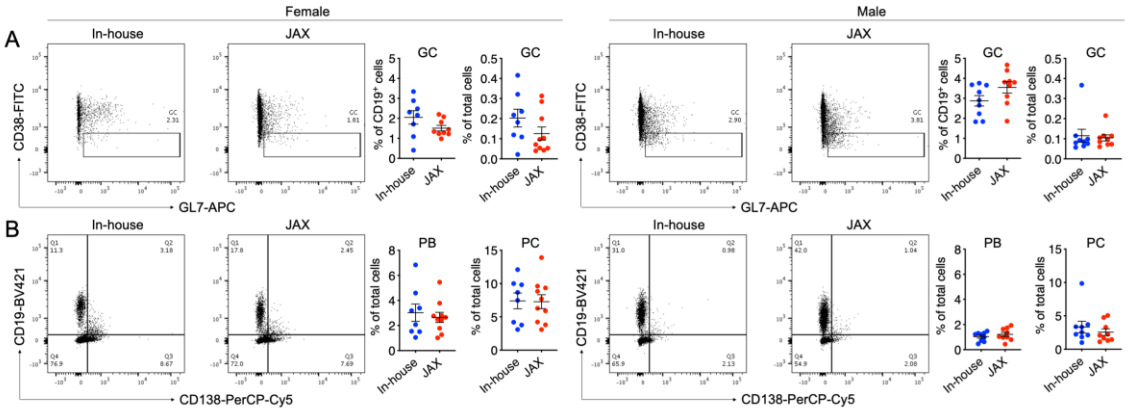

Figure 2. Splenic differences between in-house and new JAX mice as assessed with flow cytometry. (**A**) Frequency of $GL7^{+}CD38^{-}$ germinal center B (GC) cells in B cells or total live cells in the spleen of female (left) and male (right) MRL/lpr mice. The FACS plots were re-gated on $CD19^{+}$ cells. (**B**) Frequencies of $CD19^{+}CD138^{+}$ plasmablasts (PB) and $CD19^{-}CD138^{+}$ plasma cells (PC) in total live cells in the spleen of female (left) and male (right) MRL/lpr mice.

Figure 3

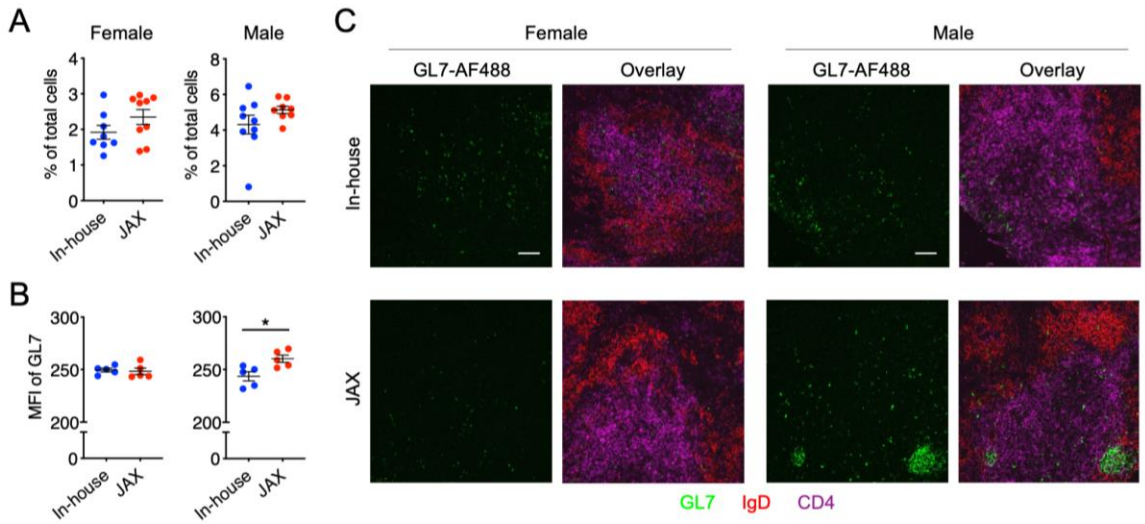

Figure 3. Splenic differences between in-house and new JAX mice as assessed with immunohistochemistry. (**A**) Frequency of $GL7^{+}$ cells in total splenocytes based on flow cytometry. (**B**) Mean fluorescence intensity (MFI) of GL7 based on immunohistochemistry. Splenic sections from 5 randomly selected mice per group were stained and quantified. Statistical significance (*p<0.05) is shown based on Student's *t*-test. (**C**) Representative images of splenic sections stained with fluorescent conjugated antibodies (GL7, IgD, CD4).

Figure 4

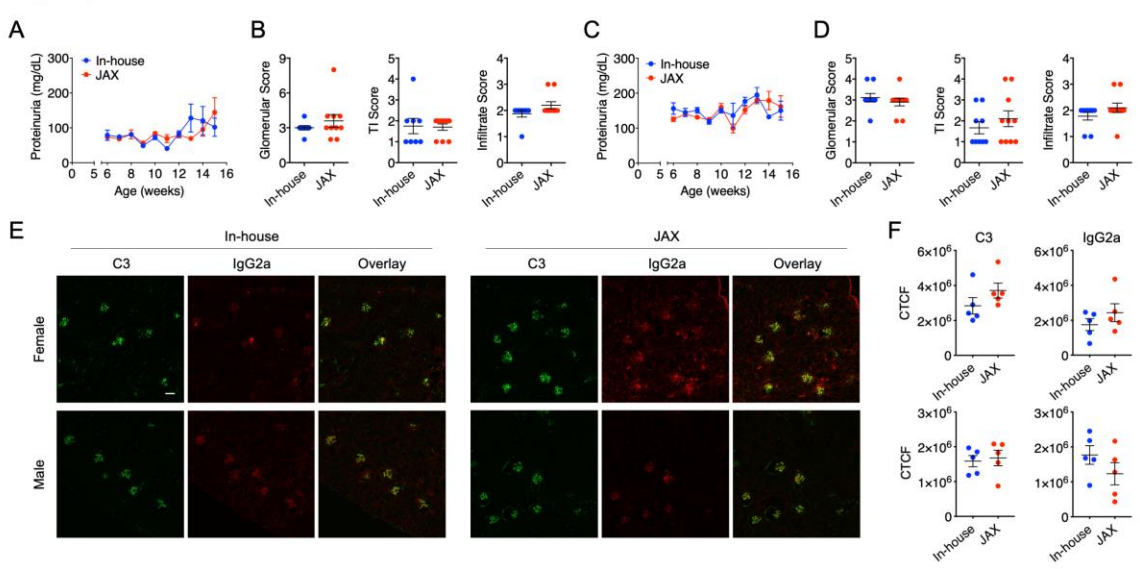

Figure 4. Renal differences between in-house and new JAX mice. (**A**-**D**) Time course of proteinuria (A for females, C for males) and kidney histopathological scores (B for females, D for males) are shown. TI, tubulointerstitial. (**E**) Representative images of kidney sections stained with fluorescent conjugated antibodies (complement C3, IgG2a). (**F**) Quantification of kidney immunohistochemistry data for female (top) and male (bottom) MRL/lpr mice.

Figure 5

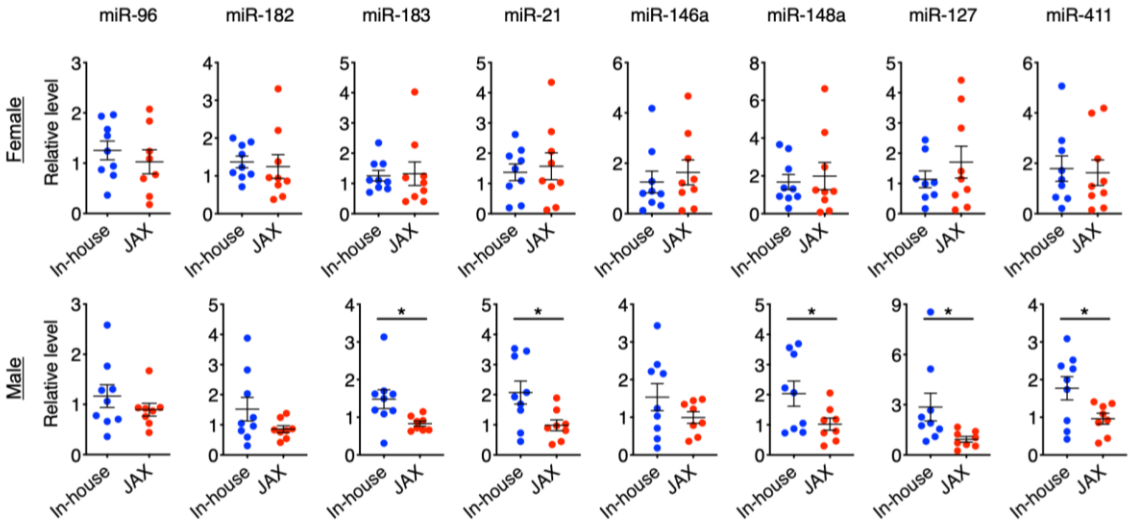

Figure 5. Analysis of lupus-associated microRNAs. Relative levels of microRNA expression in the spleen of female (top) and male (bottom) MRL/lpr mice are shown. Statistical significance (*p<0.05) is shown based on Student's t-test.

Figure 6

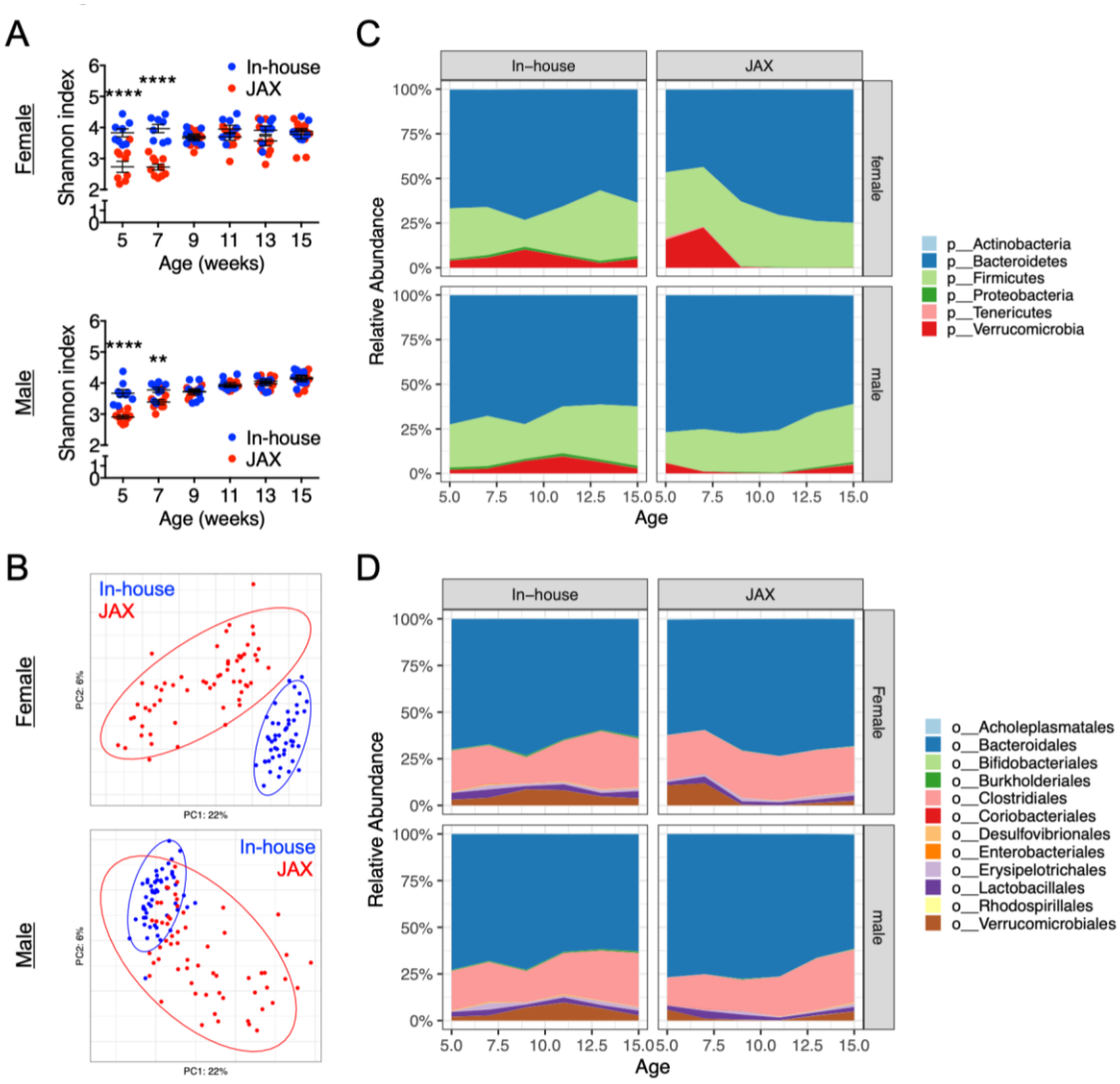

Figure 6. Analysis of gut microbiota composition. (**A**) Shannon diversity index over time for the fecal microbiota of female (top) and male (bottom) MRL/lpr mice. Statistical significance between groups (**p<0.01, ****p<0.0001) is shown based on two-way ANOVA. (**B**) Principal coordinate analysis of fecal microbiota composition for female (top) and male (bottom) MRL/lpr mice. (**C**) Changes of relative bacterial abundance over time at the Phylum level in the fecal microbiota of female (top) and male (bottom)

MRL/lpr mice. (**D**) Changes of relative bacterial abundance over time at the Order level in the fecal microbiota of female (top) and male (bottom) MRL/lpr mice.

Figure 7

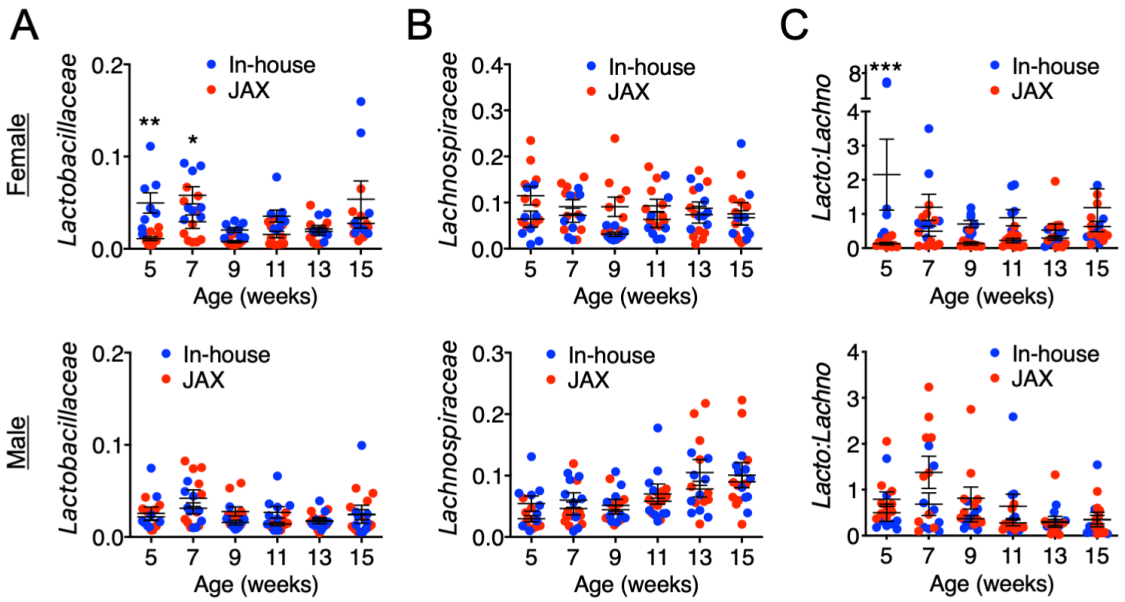

Figure 7. Analysis of gut microbiota with a focus on *Lactobacillaceae* and *Lachnospiraceae*. (**A**) Relative abundance of *Lactobacillaceae* over time in the fecal microbiota of female (top) and male (bottom) MRL/lpr mice. (**B**) Relative abundance of *Lachnospiraceae* over time in the fecal microbiota of female (top) and male (bottom) MRL/lpr mice. (**C**) The ratio of *Lactobacillaceae* to *Lachnospiraceae*. Statistical significance between groups (*p<0.05, **p<0.01, ***p<0.001) is shown based on two-way ANOVA.

Supplemental Figures

Supplemental Figure S1

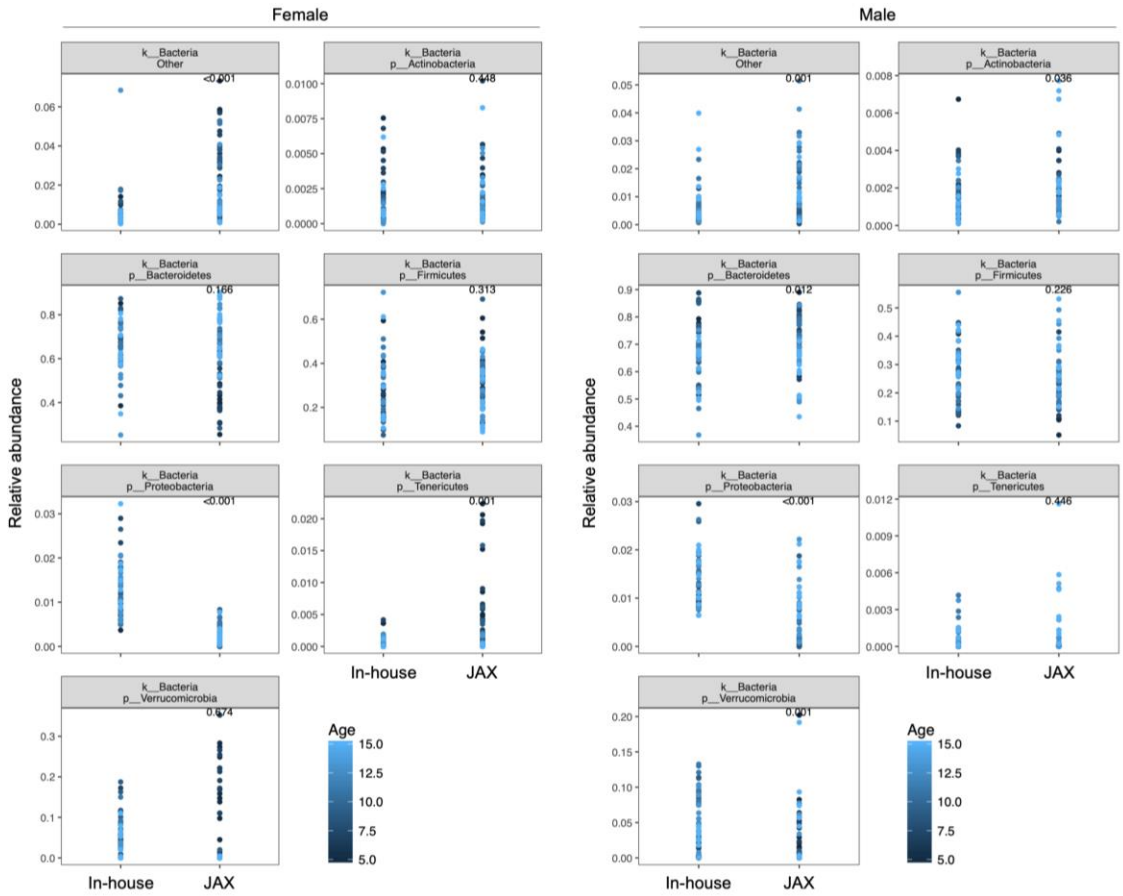

Figure S1. Differences in relative abundance at the Phylum level. Different shades of blue color represent different ages, and *p*-values are shown as numbers on the graphs.

Supplemental Figure S2

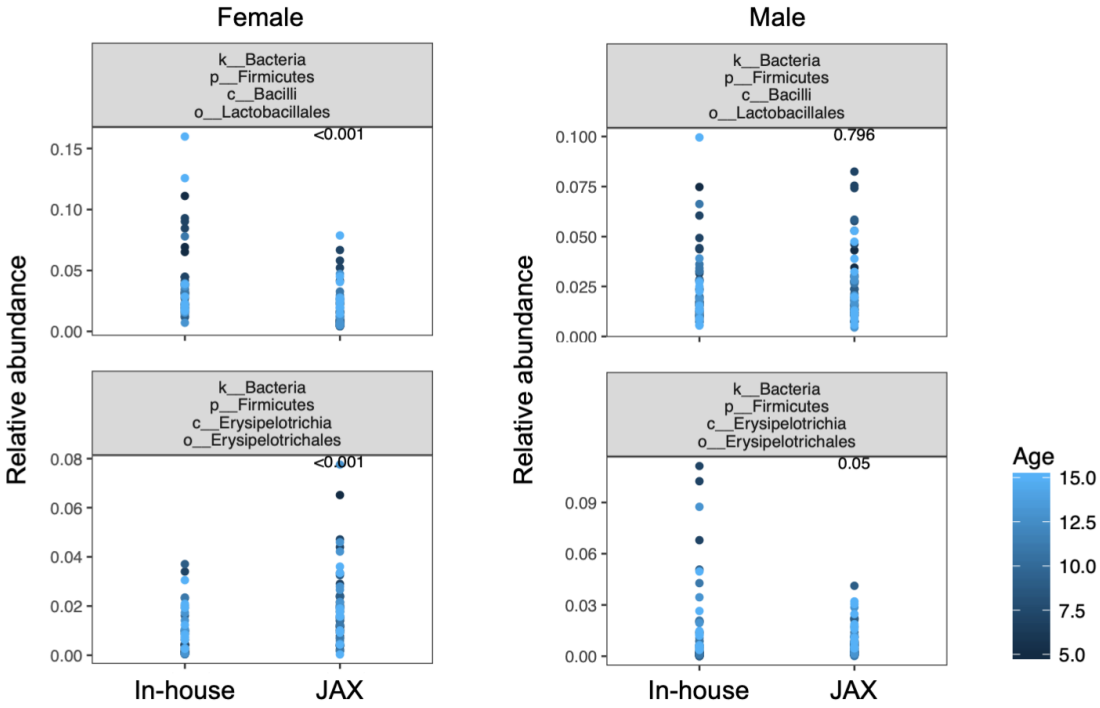

Figure S2. Differences in relative abundance for the Orders *Lactobacillales* and *Erysipelotrichales*. Different shades of blue color represent different ages, and p-values are shown as numbers on the graphs.

CHAPTER 3

Lactobacillus spp. act in synergy to attenuate splenomegaly and lymphadenopathy in lupus-prone MRL/*lpr* mice

Xavier Cabana-Puig[1], Qinghui Mu[1], Ran Lu[1], Brianna Swartwout[2], Leila Abdelhamid[1], Jing Zhu[1], Meeta Prakash[3], Thomas E. Cecere[1], Zhuang Wang[1], Sabrina Callaway[1], Sha Sun[4], Christopher M. Reilly[5], S. Ansar Ahmed[1], Xin M. Luo[1]

[1]Department of Biomedical Sciences and Pathobiology, College of Veterinary Medicine, Virginia Tech, Blacksburg, VA, USA

[2]Graduate Program in Translational Biology, Medicine, and Health, Virginia Tech, Roanoke, VA, USA

[3]Carilion School of Medicine, Virginia Tech, Roanoke, VA, USA

[4]Department of Development and Cell Biology, University of California, Irvine, CA, USA

[5]Edward Via College of Osteopathic Medicine, Blacksburg, VA, USA

Published in Frontiers of Immunology, July 2022

Abstract

Commensal bacteria and the immune system have a close and strong relationship that maintains a balance to control inflammation. Alterations of the microbiota, known as dysbiosis, can direct reactivity to self-antigens not only in the intestinal mucosa but also at the systemic level. Our laboratory previously reported gut dysbiosis, particularly lower abundance of bacteria in the family *Lactobacillaceae*, in lupus-prone MRL/*lpr* mice, a model of systemic autoimmunity. Restoring the microbiota with a mix of 5 different *Lactobacillus* species (spp.), *L. reuteri, L. oris, L. johnsonii, L. gasseri* and *L. rhamnosus*, attenuated lupus-liked clinical signs, including splenomegaly and lymphadenopathy. However, our understanding of the mechanism was limited. In this study, we first investigated the effects of individual species. Surprisingly, none of the species individually recapitulated the benefits of the mix. Instead, *Lactobacillus* spp. acted synergistically to attenuate splenomegaly and renal lymphadenopathy through secreted factors and a CX_3CR1-dependent mechanism. Interestingly, oral administration of MRS broth exerted the same benefits likely through increasing the relative abundance of endogenous *Lactobacillus* spp. Mechanistically, we found increased percentages of FOXP3-negative type 1 regulatory T cells with administration of the mix in both spleen and mesenteric lymph nodes. In addition, oral gavage of *Lactobacillus* spp. decreased the percentage of central memory T cells while increasing that of effector memory T cells in the lymphoid organs. Furthermore, a decreased percentage of double negative T cells was observed in the spleen with the mix. These results suggest that *Lactobacillus* spp. might act on T cells to attenuate splenomegaly and lymphadenopathy. Together, this study advances our understanding of how *Lactobacillus* spp. attenuate lupus in MRL/*lpr* mice.

The synergistic action of these bacteria suggests that multiple probiotic bacteria in combination may dampen systemic autoimmunity and benefit lupus patients.

Introduction

Recently generated evidence suggested that gut microbiota and the immune system interact to maintain tissue homeostasis (1-5), but it is unclear how disturbances in this interaction contribute to the pathogenesis of systemic lupus erythematosus (SLE). Our research team was the first to describe changes of gut microbiota in lupus-prone compared to control mice. Specifically, MRL/*lpr* lupus-prone mice have a decrease in *Lactobacillaceae* and an increase of *Lachnospiraceae* species (6), and administration of a mixture of 5 strains of *Lactobacillus* spp. into lupus-prone MRL/*lpr* mice via oral gavage corrected the gut microbiota and attenuated the disease (7). Our studies, along with two recent studies using additional models of murine lupus (8, 9), have established that gut microbiota is causative rather than the result of the disease. In SLE patients, one cross-sectional study showed that a greater *Bacteroidetes* to *Firmicutes* ratio was present in the fecal microbiota of SLE patients (10), whereas another cross-sectional study showed a strong association between SLE disease activity and expansion of *Ruminococcus gnavus* in the gut microbiota (11). Moreover, the fecal microbiota of SLE patients induced more Th17 differentiation than the control microbiota from healthy individuals (12).

Furthermore, human studies and investigations of different mouse models have identified a couple of SLE-driving pathobionts such as *Enterococcus gallinarum* (13). It has been suggested that translocation of pathobionts due to a leaky gut leads to systemic inflammation. This is supported by evidence that the gut in mice and people with SLE is leaky (7, 11, 13-15) and evidence of bacterial translocation into extraintestinal tissues (13). Notably, *Lactobacillus* spp. are capable of reversing the leaky gut, thus attenuating lupus (7). However, it remains unclear how the mixture of 5 strains of *Lactobacillus* spp.

modulated the interaction between gut microbiota and the immune system to affect disease. Specifically, whether individual *Lactobacillus* species could recapitulate the benefits of the mix had not been investigated.

In this study, we started with investigating the effects of individual *Lactobacillus* spp. in female MRL/*lpr* mice. Surprisingly, none of them was able to reproduce the benefits; instead, all 5 species acted in synergy to attenuate lupus-like disease. In addition, while the gut microbiota changes mostly did not correlate with the disease outcome, the relative abundance of two genera, *Clostridium* and *Oscillibacter*, at earlier time points was negatively correlated with lymphadenopathy. Mechanistically, we found that the mixed *Lactobacillus* spp. attenuated splenomegaly and lymphadenopathy through secreted factors and a CX_3CR1-dependent manner. Finally, we characterized alterations of immune cell populations in lymphoid organs demonstrating that the mixed *Lactobacillus* treatment might act on multiple T cell subsets to attenuate lupus in MRL/*lpr* mice. These results suggest synergistic actions of multiple *Lactobacillus* spp. that may benefit SLE patients as a combination therapy.

Material and Methods

Ethics statement

We followed the recommendations in the Guide for the Care and Use of Laboratory Animals of the NIH. The protocol was approved by the Institutional Animal Care and Use Committee (IACUC) of Virginia Tech College of Veterinary Medicine. All experiments with animals followed the guidelines provided by the IACUC protocol #18-060 and #21-003, including performing euthanasia with CO_2.

Mice

MRL/*lpr* (MRL/Mp-*Fas*$^{lpr/lpr}$, stock number 00485) mice were purchased from The Jackson Laboratory (JAX). MRL/*lpr*-*Cx3cr1*$^{gfp/gfp}$ mice were generated in-house as previously described (16). Mice were bred and maintained in a specific pathogen-free facility under the requirements of IACUC at Virginia Polytechnic Institute and State University. All *Lactobacillus* strains, *L. reuteri* (CF48-3A), *L. oris* (F0423), *L. johnsonii* (135-1-CHN), *L. gasseri* (JV-V03) and *L. rhamnosus* (LMS201), were obtained from BEI Resources. All 5 strains were freshly and separately cultured every week, then inoculated to mice as a mix or individually, twice a week at 10^9 total CFU, from 3 weeks of age until dissection. The inoculation volume increased with age, with 100µL at 3 weeks of age, 150µL at 4 weeks of age, and 200µL for the remaining weeks. The combined culture supernatant was obtained after spinning down the bacteria and transferring the supernatant to a new tube in sterile conditions, then filtered through a 0.22µm syringe filter and stored at -80ºC. The supernatant from10^9 total CFU of bacteria was orally gavaged at 200µL at a frequency of twice a week. The same volume and frequency were used for MRS broth oral gavage. All mice were continuously monitored every week for body weight and level of proteinuria, and euthanized at 15 weeks of age. Once mouse dissection was performed, body and organ weights were recorded.

Analysis of proteinuria, endotoxin, and antibodies

Proteinuria was determined with a Pierce Coomassie Protein Assay Kit (Thermo Scientific). Blood endotoxin was measured by using a Pierce LAL Chromogenic Endotoxin Quantitation Kit (Thermo Scientific). Anti-dsDNA IgG was measured as

previously described (17). Serum total IgG concentration was determined with mouse IgG ELISA kit (Bethyl Laboratories).

16S rRNA sequencing analysis

Fecal samples were collected weekly directly from the anus for each mouse. Samples were stored at -80°C till being processed at the same time. Samples were homogenized, cell lysed, and DNA extracted as previously described (6, 7, 18-21). PCR were performed and purified amplicons were sequenced bidirectionally (V4 region) on an Illumina MiSeq at Argonne National Laboratory. Data analysis was performed as described previously (22, 23).

Flow cytometry

Spleen and mesenteric lymph node (MLN) were collected and mashed in 70-μm cell strainers with C10 media (RPMI-1640 containing L-glutamine, 10% fetal bovine serum, 100 U/ml penicillin-streptomycin, 10 mM HEPES, 1 mM sodium pyruvate, 1% 100X MEM non-essential amino acids, 55 μM 2-mercaptoethanol, all from Life Technologies). For splenocytes, red blood cells were lysed with RBC lysis buffer (eBioscience). For FACS staining, cells were blocked by anti-mouse CD16/32 (eBioscience), stained with fluorochrome-conjugated antibodies, and analyzed with BD FACSAria Fusion flow cytometer (BD Biosciences). Anti-mouse antibodies used in this study include: CD3-FITC and B220-FITC (eBioscience), CD4-PerCP/Cy5.5, CD8-PE/Dazzle, PD-1-APC/Cy7, CXCR5-BV605, CD25-BV421, FOXP3-PE, CD44-APC, CD62L-APC/Cy7, CD138-PerCP/Cy5.5, CD19-BV421, CD273-PE/Dazzle, CD38-PE/Cy7 and GL7-APC

(Biolegend). For intracellular staining, Foxp3/Transcription Factor Staining Kit was used to fix the cells (Biolegend). For intracellular staining of IL-10 producing cells, splenocytes or MLN cells were pre-stimulated for 4 hours with 500X Cell Stimulation Cocktail (Invitrogen) plus protein transport inhibitor (eBioscience) containing phorbol 12-myristate 13-acetate (PMA), ionomycin, brefeldin A and monensin; then stained with CD19-AF700, CD138-BV711, Foxp3-AF647 and IL-10-PE. FlowJo was used to analyze data.

Kidney Histopathology

Kidneys were fixed in formalin right after isolation. Fixed tissues were paraffin-embedded, sectioned, and stained for Periodic Acid-Schiff (PAS) at the Histopathology Laboratory at Virginia Tech College of Veterinary Medicine. Kidney histopathology score were graded by a board-certified pathologist in a blindly fashion using the following categories: glomerular lesions (cellularity, mesangial matrix, necrosis, percentage of sclerotic glomeruli, and presence of crescents, tubulointerstitial lesions and vasculitis inflammation (24).

Analysis of tight junction transcripts

Isolated intestinal epithelial cells (IECs) were obtained as described previously (7). Reverse transcription and quantitative PCR were performed as we reported (25). Relative quantities were calculated using 18S and GAPDH as the housekeeping genes. Primer sequences for mouse *Cldn1*, *Cldn2*, *ZO1* are available upon request.

Statistical analyses.

For the comparison of two groups, unpaired student's *t*-test was used. For the comparison of three or more groups, one-way ANOVA was used. Two-way ANOVA was used to reveal time- and group-dependent effects. Results were considered statistically significant when $p<0.05$. All analyses were performed with the GraphPad Prism software.

Results

Five Lactobacillus species act synergistically to attenuate splenomegaly and lymphadenopathy.

Previously, we reported alterations of the gut microbiota in MRL/*lpr* mice that exhibited a state of dysbiosis characterized by lower abundance of the *Lactobacillaceae* bacterial family (6). This dysbiosis disrupted the balance between commensal bacteria and the immune system leading to a permanent state of inflammation. We next reported that restoring the microbiota with a mix of 5 different *Lactobacillus* species (spp.), *L. reuteri, L. oris, L. johnsonii, L. gasseri* and *L. rhamnosus*, attenuated lupus-liked clinical signs, including splenomegaly and lymphadenopathy (7). However, the underlying mechanisms were not clear. In this study, we first investigated the effects of individual species. As we showed *L. reuteri* together with an uncultured *Lactobacillus* dominated the gut microbiota of *Lactobacillus*-treated MRL/*lpr* mice (7), we hypothesized that *L. reuteri* would be the best candidate to reproduce the same beneficial effects.

Female MRL/*lpr* female mice were orally gavaged, twice a week at 10^9 CFU/mouse, freshly cultured *Lactobacillus* spp. either individually or as a mix from 3 weeks of age (pre-disease) till 15 weeks of age (late disease). Upon euthanasia, the

weight of different organs including spleen, mesenteric lymph node (MLN), and renal lymph node (RLN) was measured, and the organ-to-body weight ratios were calculated. There were no differences except for the mix, which significantly reduced the combined weight of all 3 lymphoid organs compared to the PBS control (Fig. 1A), suggesting that only the mix was beneficial against splenomegaly and lymphadenopathy. When looking at the lymphoid organs individually, we observed similar results with significantly smaller organs for the mix (Fig. 1B-D). Each strain individually did not have enough impact to exert a beneficial effect; instead, the 5 species worked synergistically to attenuate splenomegaly and lymphadenopathy.

We previously reported that lupus nephritis was linked to gut microbiota dysbiosis (7). We thus tested the levels of proteinuria, but no differences were found except for *L. johnsonii*, which significantly exacerbated glomerulonephritis over the PBS control (Fig. 1E). Notably, the MRL/*lpr* mice in our in-house colony, similar to those housed at The Jackson Laboratory, have lost the kidney disease phenotype (26), leading to low levels of proteinuria throughout the experiment. As expected, kidney histopathological analysis revealed no difference in glomerular and tubulointerstitial lesions as well as leukocyte infiltration (Suppl. Fig. 1). However, the serum level of anti-dsDNA IgG, a typical pathogenic autoantibody in lupus, as well as the anti-dsDNA IgG to total IgG ratio in the blood, were moderately decreased by the mix, although *L. johnsonii* and *L. gasseri* individually had similar effects (Fig. 1F-G).

These results indicate that none of the species individually recapitulated the benefits of the mix. Instead, these *Lactobacillus* spp. acted synergistically to attenuate splenomegaly and lymphadenopathy.

Gut microbiota during early disease is associated with the decrease of gut-draining lymph node size.

To study the associations between changes of disease phenotype and the composition of gut microbiota, we analyzed the fecal samples collected from mice treated with each *Lactobacillus* individually or in combination by using 16S rRNA sequencing. Looking at the observed operational taxonomic units (OTUs), we found that the gut microbiota from mice treated with the mix was significantly less diverse than that treated with the PBS control (Fig. 2A), likely due to the enrichment of *Lactobacillus* spp. In addition, we performed principal coordinate analysis and found the gut microbiotas from PBS, *L. reuteri* and *L. oris* treated groups were clustered together, whereas the gut microbiotas from the mix, *L. johnsonii, L. gasseri* and *L. rhamnosus* treated groups were clustered together (Fig. 2B). Analysis at the order level confirmed these observations (Fig. 2C). The order of *Lactobacillales*, in particular, followed this pattern with the *L. rhamnosus* treated group harboring significantly more *Lactobacillales* than the *L. oris* group (Fig. 2D). These results did not correlate with the observed disease phenotype, where only the mix was beneficial. However, it was evident that the relative abundance of genera *Clostridium* and *Oscillibacter* at earlier time points of 5 and 7 weeks of age was negatively correlated with the size of MLNs at 15 weeks of age (Fig. 2E; Suppl. Table 1). No correlation was observed between the size of endpoint MLNs and the relative abundance of these genera at 13 weeks of age (Suppl. Fig. 2A), suggesting that the changes of gut microbiota may precede the change of disease.

Lactobacillus spp. attenuate splenomegaly and renal lymphadenopathy through secreted factors and a CX_3CR1-dependent mechanism.

After uncovering that only the mix exerted beneficial effects, we further investigated whether it was the bacteria themselves or their secretion that improved the disease outcome. We thus treated female MRL/*lpr* mice with the combined culture supernatant of all 5 *Lactobacillus* spp. using the optimal culture medium of *Lactobacillus*, MRS broth, as the negative control. Interestingly, MRS broth transiently but significantly expanded endogenous *Lactobacillales* when mice were 11 weeks of age, whereas the gut microbiota following supernatant treatment was similar to that of the PBS control (Fig. 3A-B), even though the bacterial diversity of the gut microbiota was significantly lower upon treatment with the culture supernatant (Suppl. Fig. 2B). Nonetheless, the culture supernatant was effective in reducing splenomegaly and renal lymphadenopathy, although no differences were observed for the size of MLN, proteinuria and anti-dsDNA IgG to total IgG ratio (Fig. 3C-G). The latter was consistent with no differences in the endotoxin level (Suppl. Fig. 2C) and tight junction gene expression (Suppl. Fig. 2D). The MRS broth, presumably through enriching endogenous *Lactobacillus* spp., exerted similar benefits on splenomegaly and renal lymphadenopathy (Fig. 3C and 3E).

Furthermore, we were interested in CX_3CR1, a receptor that helps to present commensal bacterial antigens to the proximal lymph nodes, limiting the immune response against beneficial bacteria while removing harmful bacteria (27). We previously generated MRL/*lpr*-*Cx3cr1*$^{gfp/gfp}$ mice where *GFP* replaced the coding region of the *Cx3cr1* gene leading to global knockout of CX_3CR1 (16). By gavaging these mice with the MRS broth, we found that the benefits of the broth were eliminated in the knockout

mice (Fig. 3C and 3E), suggesting a CX_3CR1-dependent mechanism by which *Lactobacillus* spp. improve splenomegaly and renal lymphadenopathy.

Together, these results suggest that *Lactobacillus* spp. attenuate splenomegaly and renal lymphadenopathy through secreted factors and a CX_3CR1-dependent mechanism.

Lactobacillus spp. control inflammation through regulating splenic and MLN immune cell populations.

After observing the beneficial effects of mixed *Lactobacillus* spp., their culture supernatant, and MRS Broth, we sought to understand the immunological mechanism by which these treatments inhibited inflammation towards to a more balanced environment leading to decreased lymphoid organ sizes. We first analyzed the germinal center (GC) reaction in the spleen and MLN. Gating on $CD4^+PD\text{-}1^+CXCR5^+$ follicular T helper (Tfh) cells (Suppl. Fig. 3A) and $CD19^+GL7^+CD38^{-/low}$ GC-B cells (Suppl. Fig. 3B), we found mostly no difference in these populations (Suppl. Fig. 3C-D), although the mixed *Lactobacillus* spp. significantly induced more GC-B cells over the PBS control in the MLN (Suppl. Fig. 3D). We also gated on the recently identified $CD273^+$ regulatory B (Breg) cells (28-30) (Suppl. Fig. 3E), and the mixed *Lactobacillus* spp. was able to significantly induce more of these Breg cells in the MLN (Suppl. Fig. 3F). It is possible that the antibody-producing GC-B cells and immunosuppressive Breg cells counter their respective effects; therefore, overall, we did not observe significant alterations of spleen or MLN GC reaction by the treatment groups.

Next, we analyzed several populations of IL-10 producing immunoregulatory cells. These included $CD4^+Foxp3^-IL\text{-}10^+$ type 1 regulatory T (Tr1) cells (Fig. 4A),

$CD4^+Foxp3^+IL\text{-}10^+$ regulatory T (Treg) cells, $CD19^+IL\text{-}10^+$ Breg cells, and $CD138^+IL\text{-}10^+$ plasma cell (PC)-derived Breg cells (Suppl. Fig. 4A). We found consistent upregulation of Tr1 cells in the spleen and MLN with the mixed *Lactobacillus* treatment (Fig. 4A and 4E). This observation aligns well with our published results on Tr1 cells as IL-10 producers in MRL/*lpr* mice (7). Interestingly, the combined culture supernatant of all 5 *Lactobacillus* spp. was also able to significantly increase the percentage of Tr1 cells in the MLN (Fig. 4E). In addition, we observed decreased percentages of $FOXP3^+IL\text{-}10^+$ Treg cells and $CD138^+$ PC-Breg cells in the MLN with both the mixed *Lactobacillus* and MRS broth treatments (Suppl. Fig. 4B). These results suggest that Tr1 cells may be responsible for the immunoregulatory effects of the mixed *Lactobacillus* treatment. Notably, while $CD4^+Foxp3^+IL\text{-}10^+$ Treg cells were reduced in the MLN (Suppl. Fig. 4B), $CD25^+FOXP3^+$ Treg cells were significantly increased in the MLN with the mixed *Lactobacillus* treatment (Suppl. Fig. 4C), suggesting that Treg cells may produce cytokines other than IL-10, such as TGFβ, to suppress inflammation.

Moreover, oral gavage of *Lactobacillus* spp. decreased the percentage of central memory T (T_{CM}) cells while increasing that of effector memory T (T_{EM}) cells in both $CD4^+$ and $CD8^+$ compartments in the spleen (Fig. 4B-C) and MLN (Fig. 4F-G). Since T_{CM} cells are known to sustain persistent inflammation (31), the conversion of them into short-lived T_{EM} cells may be beneficial. Notably, the MRS broth exerted similar benefits within the $CD8^+$ compartment in the spleen (Fig. 4C), whereas the combined culture supernatant regulated T_{CM} and T_{EM} cells in a similar fashion as mixed *Lactobacillus* spp. in the MLN (Fig. 4F-G). Naïve T cells, on the other hand, were suppressed by mixed *Lactobacillus* spp. or MRS broth in the spleen (Fig. 4B-C). These results suggest that

Lactobacillus spp. may target memory T cells to suppress inflammation in MRL/*lpr* mice.

Furthermore, the mixed *Lactobacillus* treatment significantly downregulated the percentage of double-negative T (DNT) cells in the spleen (Fig. 4D), which play a proinflammatory role by secreting IL-17 that aggravates the autoimmune environment, particularly in lupus patients (32-35). The percentage of DNT cells in the MLN, on the other hand, did not change (Fig. 4H).

Together, these results suggest that *Lactobacillus* spp. might act on T cells to attenuate splenomegaly and lymphadenopathy.

Discussion

In this study, we showed that restoring the microbiota with a mix of 5 different *Lactobacillus* spp., *L. reuteri, L. oris, L. johnsonii, L. gasseri* and *L. rhamnosus*, was able ameliorate lupus-like clinical signs, reducing splenomegaly and lymphadenopathy. However, none of the strains individually could replicate the same positive effects that the mix *Lactobacillus* spp. showed, suggesting a potential cooperation among the species that helps to multiply each individual strength. In addition, the combined culture supernatant of *Lactobacillus* spp. attenuated splenomegaly and renal lymphadenopathy suggesting that the bacteria benefit by releasing certain secreted factors. Interestingly, oral administration of MRS broth exerted the same benefits probably by creating a favorable environment that increased the relative abundance of endogenous *Lactobacilliales*. Moreover, *Cx3cr1* deficiency in MRL/*lpr* mice abrogated the benefits showing a comparable level of disease as the control group, suggesting that the MRS

broth, and thus the endogenous *Lactobacillus* spp., may exert protective effects through a CX_3CR1-dependent mechanism. The mechanistic pathway of the mix of *Lactobacillus* spp. increasing the percentages of FOXP3-negative Tr1 cells in both spleen and MLN suggests a possible probiotic-mediated control of inflammation that may happen in both MRL/*lpr* mice and lupus patients. Furthermore, oral gavage of *Lactobacillus* spp. increased the relative abundance of T_{EM} cells in the lymphoid organs while decreasing T_{CM} cells. Finally, a lower percentage of DN T cells, which plays a detrimental role in SLE, was observed in the spleen, suggesting an additional protective mechanism provided by the mix of *Lactobacillus* spp.

Our novelty resides in the fact that individual *Lactobacillus* strains could not replicate the effects of the mix. This result was surprising to us and was not reported previously. In addition, while we did report the effect of the mixed *Lactobacillus* spp. on Tr1 cells, the new information we are presenting is the effects of the mixed culture supernatant and MRS broth. The mixed *Lactobacillus* group was used as the positive control. We advance the previous findings by explaining how *Lactobacillus* spp. could potentially exert the beneficial effects. Here we show data suggesting that they do so through secreted factors produced by the administered probiotics. We also show similar benefits due to MRS broth-mediated enrichment of local *Lactobacillus* spp. found in the gut microbiota.

MRL/*lpr* mice have been extensively used as a murine model of lupus. These mice spontaneously develop autoimmune disease resembling SLE patients due to multiple SLE susceptibility loci present in the MRL background as well as a spontaneous mutation in the *Fas* gene (36). Fas is a type I membrane protein of the tumor necrosis

factor receptor (TNFR) superfamily that is expressed on activated lymphocytes and in the thymus which induces lymphocyte apoptosis upon ligation by the Fas ligand. The *Fas* defect triggers the survival of self-reactive lymphocytes common in autoimmunity (37). Therefore, the *Fas* mutation accelerates the disease in MRL mice leading lymphoproliferation with progressive organ failures. Many features of the MRL/*lpr* mouse, including autoantibodies, glomerulonephritis, and infiltrates of proinflammatory B and T cells in peripheral tissues such as the kidney, resemble clinical symptoms in SLE patients. In addition, like human SLE, the MRL/*lpr* mouse develops progressive nonmalignant lymphoproliferation that contributes to an early mortality (38).

We recently published a study where disease manifestations in MRL/*lpr* mice can differ among animal facilities, suggesting a role for environment factors (26). Notably, the gene loci responsible for splenomegaly and lymphadenopathy, which are chromosomes 4, 5 and 7, are not the same as that for glomerulonephritis, which is chromosome 10. We found that comparing our in-house mice with those obtained from The Jackson Laboratory, there were differences in lymphoproliferation (splenomegaly and lymphadenopathy), but the loss of kidney disease (glomerulonephritis) was a shared phenomenon. Due to this significant phenotypic drift, we decided to focus on the splenomegaly and lymphadenopathy in the current study.

To further investigate the mechanism by which the gut microbiota modulates lupus disease progression, we characterized the gut microbiota and established correlations between gut bacteria and disease phenotype. Although less diversity traditionally means unhealthier gut microbiota (39), in the context of autoimmune disease, *Lactobacillus* spp. induces a positive change in the ecosystem, supporting

microbiota stability through their metabolic activities, interacting with the host to provide a low inflammatory state or to revert a proinflammatory state, and resisting the colonization from pathogens. In contrast, higher microbiota diversity in this setting seems to be associated with disease or dysfunction, leading to competition instead of cooperation, which undermines the stability of the microbial community. *Lactobacillus* spp., on the other hand, corrects this. Notably, the introduction of probiotics such as *Lactobacillus* spp. can be a starting point to redirect the gut microbiota towards to a better and healthier profile. It has been reported that major interventions in gut microbiota can temporarily reduce diversity, as the process of enriching certain bacteria could lead to a change in composition and, through competitive interactions, reduce diversity (40).

Interestingly, the relative abundance of genera *Clostridium* and *Oscillibacter* was negatively correlated to the size of MLN. *Clostridium* is a genus with butyrate-producing gram-positive bacteria (41). Known to exert beneficial effects for intestinal homeostasis, *Clostridium* spp. can have an important role in attenuating inflammation due to their cellular components and metabolites, likely through energizing intestinal epithelial cells, stimulating intestinal barrier health, and educating the immune system. Moreover, a member of the *Oscillibacter* genus, *O. valericigenes*, is a valerate- and butyrate-producing anaerobic gram-negative non-sporulating bacterium (42). *O. valericigenes* has been found in the human gut microbiota. In particular, *O. valericigenes* was found more abundant in healthy individuals compared to patients diagnosed with Crohn's disease (43). An important short-chain fatty acid (SCFA), butyrate has been shown to successfully prevent inflammation through Treg induction (44) and down-regulating the expression of pro-inflammatory cytokines (45). Therefore, it is conceivable, while yet to

be elucidated, that the negative correlation between mesenteric lymphadenopathy and the genera *Clostridium* and *Oscillibacter* may be due to the ability of the bacteria to produce the anti-inflammatory butyrate. It is likely that the presence or products of *Lactobacillus* spp. facilitated the proliferation and/or survival of these two genera, even though we do not know the mechanisms at this time. It is known, however, that *Lactobacillus* spp. are SCFA producers and can be butyrate-producing bacteria that alleviate intestinal permeability and maintain barrier function. Butyrate can not only inhibit pathogenic bacteria but also stimulate the growth of beneficial bacteria (46), a notion that could be associated with the enhancement of the relative abundance of *Oscillibacter* and *Clostridium*.

The secreted factors in the culture supernatant, potentially bacterial metabolites, showed the same benefits as the mixed *Lactobacilli* themselves. Bacterial metabolites are important particularly for food digestion and metabolic pathways of dietary carbohydrates, protein, fat and vitamins (47). SCFAs such as acetate, propionate and butyrate are bacterial metabolites generated from the fermentation of dietary fiber by the gut microbiota. They play immune modulatory roles and are involved in the maintenance of colonic mucosal health by stimulating the mucous layer, producing antimicrobial peptides, and serving as anti-inflammatory agents due to their regulatory effects on gene expression (48). Besides SCFAs, *Lactobacillus* spp. are known for their production of antimicrobial compounds, including biosurfactants, lactic acid, hydrogen peroxide, bacteriocins and bacteriocin-like peptides that could inhibit pathogen growth (49). It is likely that the metabolites of *Lactobacillus* spp., such as indole molecules, bind to the aryl hydrocarbon receptor (AhR) of T cells leading to Tr1 differentiation (50-53). Further

research is necessary to identify specific secreted factors that recapitulate the benefits of *Lactobacillus* spp. on lupus.

CX_3CR1 is important for maintaining intestinal homeostasis and controlling pathogen challenges (54, 55). CX_3CR1, or the fractalkine receptor, in conjunction with its ligand CX_3CL1, mediates the translocation of the antigen-presenting cells from the blood to the gut, MLN, kidney and brain. The role of CX_3CR1-expressing cells in the intestinal epithelium is to capture bacteria and antigens present in the gut lumen and to transport them to the MLN, where T cells are activated (56). Interestingly, however, *Cx3cr1*-deficient mice display markedly increased translocation of commensal bacteria into the MLN leading to gut inflammation (57), suggesting that CX_3CR1-expressing cells also have a regulatory function and promote homeostasis between commensal bacteria and immune system. Our study supports the important role of CX_3CR1 as an antigen carrier and an immune regulator, where the lack of the receptor abrogates the protective effects of *Lactobacillus* spp. enriched by the MRS broth leading to aggravated lupus.

Type 1 regulatory T (Tr1) can prevent and downregulate undesired immune responses to pathogenic and non-pathogenic antigens (such as autoantigens) and are associated with long-term tolerance. Tr1 cells produce IL-10 as well as TGF-β, but they can also produce variable amounts of other cytokines depending on the microenvironment and disease context (58). Notably, the ability to produce IL-10 does not equal to suppressor activity (59); however, IL-10-producing Tr1 cells do have suppressor functions that are independent from FOXP3 (60). Our results suggest that *Lactobacillus* treatment can promote an anti-inflammatory environment in the gut of lupus-prone mice through increasing the frequency of Tr1 cells. T_{CM} and T_{EM} cells are

antigen-specific memory T cells to viruses or other microbial molecules and their primary function is to trigger an immune response upon reintroduction of relevant pathogen into the body (61). T_{CM} cells can sometimes react to novel antigens, potentially caused by intrinsic diversity and breadth of the T cell receptor (62). These memory T cells could cross-react to environmental or resident antigens in our body (such as commensal bacteria in the gut) and proliferate. The cross-reactivity mechanism may be important to help maintain the T_{CM} population at mucosal surfaces. However, through the same mechanism, T_{CM} cells can sustain autoimmune response by proliferating in the secondary lymphoid organs and producing a persistent inflammatory state (63). T_{EM} cells, in comparison, present an immediate, but not sustained, defense at the pathogen's sites of entry. *Lactobacillus* treatment promotes a T_{EM} response while suppressing T_{CM} cells, thereby present an immediate response with subsequent resolution instead of prolonging the autoimmune response. Notably, the frequencies of T_{CM} cells decreased in the spleen and MLN that decreased their weights. This suggests that decreases of T_{CM} cells may be more critical changes induced by *Lactobacillus* spp. than relatively increased frequencies of Tr1 cells, as the latter increased while the organ weight decreased, leading to no change in actual cell numbers. DNT cells are characteristically elevated in several autoimmune diseases including SLE, and expanded DNT cells in inflamed tissues contribute to disease pathogenesis (35). DNT cells can produce inflammatory cytokines IL-17 and IFN-γ, which contribute to the pathogenesis of kidney damage in patients with SLE (64). Therefore, the suppression of DNT cells may be another reason that lupus-like clinical signs are improved by *Lactobacillus* treatment. Altogether, our results suggest the

probiotic bacteria may target T cells to control the autoimmune response in MRL/*lpr* mice.

In conclusion, this study advances our understanding of the mechanisms of how changes of the gut microbiota regulate SLE-associated immune responses in mice. Future studies will determine if these results can be replicated in human SLE patients. The ultimate goal is to uncover novel, gut microbiota-related pathogenic pathways of SLE that enable the identification of new therapeutic targets, for which the modification of gut microbiota—through diet modulation and/or probiotic supplementation—can be a cost-effective approach to complement the current SLE treatment strategies.

Ethics

This study was carried out in accordance to the recommendations in the Guide for the Care and Use of Laboratory Animals of the NIH. The Institutional Animal Care and Use Committee (IACUC) of Virginia Tech College of Veterinary Medicine approved this protocol (Animal Welfare Assurance Number: A3208-01). All animal experiments were conducted under IACUC protocol #18-060 and protocol #21-003.

Data Availability Statement

The 16S rRNA sequences are available in the National Institutes of Health SRA database (PRJNA827847).

Conflict of Interest

The authors declare that the research was conducted in the absence of any commercial or financial relationships that could be construed as a potential conflict of interest.

Author Contributions

XML designed the study. XCP, QM, RL, BS, LA, JZ, MP and SC performed the experiments. XCP, SS, CMR, SAA and XML analysed the data. TEC scored the pathology slides. XCP and XML wrote the manuscript.

Funding

This work was supported by internal funding from VMCVM and NIH grants AR067418 and AR073240 (Luo).

Acknowledgments

We thank to Sarah Owens and Husen Zhang for assistance on Illumina MiSeq sequencing and bioinformatics analysis. In addition, we thank Melissa Makris for flow cytometry analysis.

Supplementary Material

Additional files are provided.

References

1. Kamada N, Seo SU, Chen GY, Nunez G. Role of the gut microbiota in immunity and inflammatory disease. Nature reviews Immunology. 2013;13(5):321-35.

2. Kuhn KA, Stappenbeck TS. Peripheral education of the immune system by the colonic microbiota. Seminars in immunology. 2013;25(5):364-9.

3. Strober W. Impact of the gut microbiome on mucosal inflammation. Trends in immunology. 2013;34(9):423-30.

4. Yeoh N, Burton JP, Suppiah P, Reid G, Stebbings S. The role of the microbiome in rheumatic diseases. Current rheumatology reports. 2013;15(3):314.

5. Brown EM, Sadarangani M, Finlay BB. The role of the immune system in governing host-microbe interactions in the intestine. Nature immunology. 2013;14(7):660-7.

6. Zhang H, Liao X, Sparks JB, Luo XM. Dynamics of gut microbiota in autoimmune lupus. Applied and environmental microbiology. 2014;80(24):7551-60.

7. Mu Q, Zhang H, Liao X, Lin K, Liu H, Edwards MR, et al. Control of lupus nephritis by changes of gut microbiota. Microbiome. 2017;5(1):73.

8. Zegarra-Ruiz DF, El Beidaq A, Iñiguez AJ, Lubrano Di Ricco M, Manfredo Vieira S, Ruff WE, et al. A Diet-Sensitive Commensal Lactobacillus Strain Mediates TLR7-Dependent Systemic Autoimmunity. Cell host & microbe. 2019;25(1):113-27.e6.

9. Choi SC, Brown J, Gong M, Ge Y, Zadeh M, Li W, et al. Gut microbiota dysbiosis and altered tryptophan catabolism contribute to autoimmunity in lupus-susceptible mice. Sci Transl Med. 2020;12(551).

10. Hevia A, Milani C, López P, Cuervo A, Arboleya S, Duranti S, et al. Intestinal dysbiosis associated with systemic lupus erythematosus. mBio. 2014;5(5):e01548-14.

11. Azzouz D, Omarbekova A, Heguy A, Schwudke D, Gisch N, Rovin BH, et al. Lupus nephritis is linked to disease-activity associated expansions and immunity to a gut commensal. Ann Rheum Dis. 2019.

12. López P, de Paz B, Rodríguez-Carrio J, Hevia A, Sánchez B, Margolles A, et al. Th17 responses and natural IgM antibodies are related to gut microbiota composition in systemic lupus erythematosus patients. Scientific reports. 2016;6:24072.

13. Manfredo Vieira S, Hiltensperger M, Kumar V, Zegarra-Ruiz D, Dehner C, Khan N, et al. Translocation of a gut pathobiont drives autoimmunity in mice and humans. Science. 2018;359(6380):1156-61.

14. Luo XM, Edwards MR, Mu Q, Yu Y, Vieson MD, Reilly CM, et al. Gut microbiota in human SLE and a mouse model of lupus. Applied and environmental microbiology. 2017.

15. Mu Q, Kirby J, Reilly CM, Luo XM. Leaky Gut As a Danger Signal for Autoimmune Diseases. Frontiers in immunology. 2017;8:598.

16. Liao X, Ren J, Reihl A, Pirapakaran T, Sreekumar B, Cecere TE, et al. Renal-infiltrating CD11c(+) cells are pathogenic in murine lupus nephritis through promoting CD4(+) T cell responses. Clin Exp Immunol. 2017;190(2):187-200.

17. Liao X, Ren J, Wei CH, Ross AC, Cecere TE, Jortner BS, et al. Paradoxical effects of all-trans-retinoic acid on lupus-like disease in the MRL/lpr mouse model. PloS one. 2015;10(3):e0118176.

18. Mu Q, Tavella VJ, Kirby JL, Cecere TE, Chung M, Lee J, et al. Antibiotics ameliorate lupus-like symptoms in mice. Scientific Reports. 2017;7(1):13675.

19. Mu Q, Edwards MR, Swartwout BK, Cabana Puig X, Mao J, Zhu J, et al. Gut Microbiota and Bacterial DNA Suppress Autoimmunity by Stimulating Regulatory B Cells in a Murine Model of Lupus. Frontiers in immunology. 2020;11.

20. Mu Q, Cabana-Puig X, Mao J, Swartwout B, Abdelhamid L, Cecere TE, et al. Pregnancy and lactation interfere with the response of autoimmunity to modulation of gut microbiota. Microbiome. 2019;7(1):1-13.

21. Mu Q, Swartwout BK, Edwards M, Zhu J, Lee G, Eden K, et al. Regulation of neonatal IgA production by the maternal microbiota. Proceedings of the National Academy of Sciences. 2021;118(9).

22. Zhang H, Liao X, Sparks JB, Luo XM, Schloss PD. Dynamics of Gut Microbiota in Autoimmune Lupus. Applied and environmental microbiology. 2014;80(24):7551-60.

23. Zhang H, Sparks JB, Karyala SV, Settlage R, Luo XM. Host adaptive immunity alters gut microbiota. The ISME Journal. 2015;9(3):770-81.

24. De Lema GP, Lucio-Cazaña FJ, Molina ANA, Luckow B, Schmid H, de Wit C, et al. Retinoic acid treatment protects MRL/lpr lupus mice from the development of glomerular disease. Kidney International. 2004;66(3):1018-28.

25. Abdelhamid L, Cabana-Puig X, Swartwout B, Lee J, Li S, Sun S, et al. Retinoic Acid Exerts Disease Stage-Dependent Effects on Pristane-Induced Lupus. Frontiers in Immunology. 2020;11.

26. Cabana-Puig X, Bond JM, Wang Z, Dai R, Lu R, Lin A, et al. Phenotypic Drift in Lupus-Prone MRL/lpr Mice: Potential Roles of MicroRNAs and Gut Microbiota. Immunohorizons. 2022;6(1):36-46.

27. Niess JH, Brand S, Gu X, Landsman L, Jung S, McCormick BA, et al. CX3CR1-Mediated Dendritic Cell Access to the Intestinal Lumen and Bacterial Clearance. Science. 2005;307(5707):254-8.

28. Mielle J, Audo R, Hahne M, Macia L, Combe B, Morel J, et al. IL-10 Producing B Cells Ability to Induce Regulatory T Cells Is Maintained in Rheumatoid Arthritis. Frontiers in Immunology. 2018;9.

29. Pennati A, Ng S, Wu Y, Murphy JR, Deng J, Rangaraju S, et al. Regulatory B Cells Induce Formation of IL-10-Expressing T Cells in Mice with Autoimmune Neuroinflammation. The Journal of neuroscience : the official journal of the Society for Neuroscience. 2016;36(50):12598-610.

30. Tomayko MM, Steinel NC, Anderson SM, Shlomchik MJ. Cutting edge: Hierarchy of maturity of murine memory B cell subsets. J Immunol. 2010;185(12):7146-50.

31. Restifo NP, Gattinoni L. Lineage relationship of effector and memory T cells. Curr Opin Immunol. 2013;25(5):556-63.

32. Li H, Adamopoulos IE, Moulton VR, Stillman IE, Herbert Z, Moon JJ, et al. Systemic lupus erythematosus favors the generation of IL-17 producing double negative T cells. Nature communications. 2020;11(1):2859.

33. Koga T, Ichinose K, Kawakami A, Tsokos GC. The role of IL-17 in systemic lupus erythematosus and its potential as a therapeutic target. Expert review of clinical immunology. 2019;15(6):629-37.

34. Edgerton C, Crispín JC, Moratz CM, Bettelli E, Oukka M, Simovic M, et al. IL-17 producing CD4+ T cells mediate accelerated ischemia/reperfusion-induced injury in autoimmunity-prone mice. Clinical immunology (Orlando, Fla). 2009;130(3):313-21.

35. Crispín JC, Oukka M, Bayliss G, Cohen RA, Van Beek CA, Stillman IE, et al. Expanded double negative T cells in patients with systemic lupus erythematosus produce IL-17 and infiltrate the kidneys. J Immunol. 2008;181(12):8761-6.

36. Chu JL, Drappa J, Parnassa A, Elkon KB. The defect in Fas mRNA expression in MRL/lpr mice is associated with insertion of the retrotransposon, ETn. Journal of Experimental Medicine. 1993;178(2):723-30.

37. Gulinello M, Putterman C. The MRL/lpr mouse strain as a model for neuropsychiatric systemic lupus erythematosus. J Biomed Biotechnol. 2011;2011:207504-.

38. Andrews BS, Eisenberg RA, Theofilopoulos AN, Izui S, Wilson CB, McConahey PJ, et al. Spontaneous murine lupus-like syndromes. Clinical and immunopathological manifestations in several strains. The Journal of experimental medicine. 1978;148(5):1198-215.

39. Lozupone CA, Stombaugh JI, Gordon JI, Jansson JK, Knight R. Diversity, stability and resilience of the human gut microbiota. Nature. 2012;489(7415):220-30.

40. Zhao L, Zhang F, Ding X, Wu G, Lam YY, Wang X, et al. Gut bacteria selectively promoted by dietary fibers alleviate type 2 diabetes. Science. 2018;359(6380):1151-6.

41. Guo P, Zhang K, Ma X, He P. Clostridium species as probiotics: potentials and challenges. Journal of Animal Science and Biotechnology. 2020;11(1):24.

42. Katano Y, Fujinami S, Kawakoshi A, Nakazawa H, Oji S, Iino T, et al. Complete genome sequence of Oscillibacter valericigenes Sjm18-20(T) (=NBRC 101213(T)). Stand Genomic Sci. 2012;6(3):406-14.

43. Mondot S, Kang S, Furet JP, Aguirre de Carcer D, McSweeney C, Morrison M, et al. Highlighting new phylogenetic specificities of Crohn's disease microbiota. Inflammatory bowel diseases. 2011;17(1):185-92.

44. Furusawa Y, Obata Y, Fukuda S, Endo TA, Nakato G, Takahashi D, et al. Commensal microbe-derived butyrate induces the differentiation of colonic regulatory T cells. Nature. 2013;504(7480):446-50.

45. Chang PV, Hao L, Offermanns S, Medzhitov R. The microbial metabolite butyrate regulates intestinal macrophage function via histone deacetylase inhibition. Proceedings of the National Academy of Sciences of the United States of America. 2014;111(6):2247-52.

46. Hsiao Y-P, Chen H-L, Tsai J-N, Lin M-Y, Liao J-W, Wei M-S, et al. Administration of Lactobacillus reuteri Combined with Clostridium butyricum Attenuates Cisplatin-Induced Renal Damage by Gut Microbiota Reconstitution, Increasing Butyric Acid Production, and Suppressing Renal Inflammation. Nutrients. 2021;13(8):2792.

47. Rowland I, Gibson G, Heinken A, Scott K, Swann J, Thiele I, et al. Gut microbiota functions: metabolism of nutrients and other food components. European journal of nutrition. 2018;57(1):1-24.

48. Wong JM, de Souza R, Kendall CW, Emam A, Jenkins DJ. Colonic health: fermentation and short chain fatty acids. Journal of clinical gastroenterology. 2006;40(3):235-43.

49. Petrova MI, Lievens E, Malik S, Imholz N, Lebeer S. Lactobacillus species as biomarkers and agents that can promote various aspects of vaginal health. Frontiers in physiology. 2015;6:81.

50. Mascanfroni ID, Takenaka MC, Yeste A, Patel B, Wu Y, Kenison JE, et al. Metabolic control of type 1 regulatory T cell differentiation by AHR and HIF1-α. Nature Medicine. 2015;21(6):638-46.

51. Aoki R, Aoki-Yoshida A, Suzuki C, Takayama Y. Indole-3-Pyruvic Acid, an Aryl Hydrocarbon Receptor Activator, Suppresses Experimental Colitis in Mice. The Journal of Immunology. 2018;201(12):3683-93.

52. Scott SA, Fu J, Chang PV. Microbial tryptophan metabolites regulate gut barrier function via the aryl hydrocarbon receptor. Proceedings of the National Academy of Sciences. 2020;117(32):19376-87.

53. Wu HY, Quintana FJ, da Cunha AP, Dake BT, Koeglsperger T, Starossom SC, et al. In vivo induction of Tr1 cells via mucosal dendritic cells and AHR signaling. PloS one. 2011;6(8):e23618-e.

54. Blander JM, Longman RS, Iliev ID, Sonnenberg GF, Artis D. Regulation of inflammation by microbiota interactions with the host. Nature immunology. 2017;18(8):851-60.

55. Niess JH, Brand S, Gu X, Landsman L, Jung S, McCormick BA, et al. CX3CR1-mediated dendritic cell access to the intestinal lumen and bacterial clearance. Science. 2005;307(5707):254-8.

56. Niess JH. What are CX3CR1+ mononuclear cells in the intestinal mucosa? Gut Microbes. 2010;1(6):396-400.

57. Medina-Contreras O, Geem D, Laur O, Williams IR, Lira SA, Nusrat A, et al. CX3CR1 regulates intestinal macrophage homeostasis, bacterial translocation, and colitogenic Th17 responses in mice. The Journal of clinical investigation. 2011;121(12):4787-95.

58. Bacchetta R, Bigler M, Touraine JL, Parkman R, Tovo PA, Abrams J, et al. High levels of interleukin 10 production in vivo are associated with tolerance in SCID patients transplanted with HLA mismatched hematopoietic stem cells. The Journal of experimental medicine. 1994;179(2):493-502.

59. Roncarolo MG, Gregori S, Bacchetta R, Battaglia M. Tr1 Cells and the Counter-Regulation of Immunity: Natural Mechanisms and Therapeutic Applications. In: Fillatreau S, O'Garra A, editors. Interleukin-10 in Health and Disease. Berlin, Heidelberg: Springer Berlin Heidelberg; 2014. p. 39-68.

60. Roncarolo MG, Gregori S, Bacchetta R, Battaglia M, Gagliani N. The Biology of T Regulatory Type 1 Cells and Their Therapeutic Application in Immune-Mediated Diseases. Immunity. 2018;49(6):1004-19.

61. Gehad A, Teague JE, Matos TR, Huang V, Yang C, Watanabe R, et al. A primary role for human central memory cells in tissue immunosurveillance. Blood Advances. 2018;2(3):292-8.

62. Klebanoff CA, Gattinoni L, Torabi-Parizi P, Kerstann K, Cardones AR, Finkelstein SE, et al. Central memory self/tumor-reactive CD8+ T cells confer superior

antitumor immunity compared with effector memory T cells. Proceedings of the National Academy of Sciences. 2005;102(27):9571-6.

63. Sallusto F, Geginat J, Lanzavecchia A. Central Memory and Effector Memory T Cell Subsets: Function, Generation, and Maintenance. Annual Review of Immunology. 2004;22(1):745-63.

64. Nemenoff RA, Kleczko EK, Hopp K. Renal double negative T cells: unconventional cells in search of a function. Annals of Translational Medicine. 2019:S342.

Figures

Figure 1

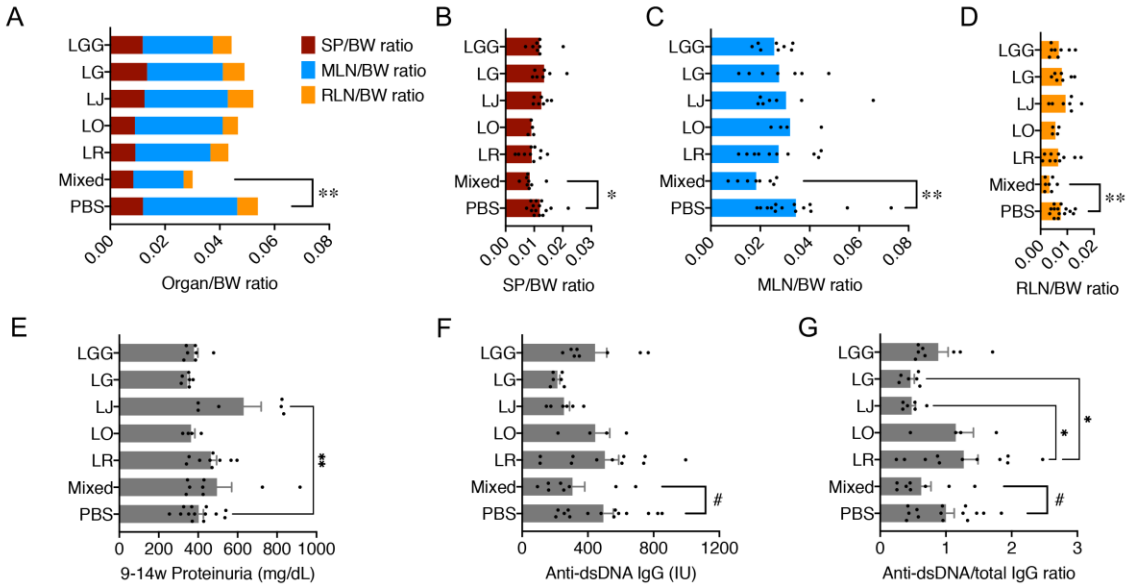

Figure 1. Five *Lactobacillus* species act synergistically to attenuate splenomegaly and lymphadenopathy. Female MRL/*lpr* mice were treated with indicated *Lactobacillus* spp. at 10^9 total CFU/mouse twice a week from 3 weeks to 15 weeks of age. PBS, phosphate buffered saline control. Mixed, the mix of all 5 species. LR, LO, LJ, LG and LGG represent *L. reuteri*, *oris*, *johnsonii*, *gasseri* and *rhamnosus*, respectively. (**A**) Combined organ weight-to-body weight ratio. SP, spleen; MLN, mesenteric lymph node; RLN, renal lymph node. (**B**) SP-to-body weight ratio. (**C**) MLN-to-body weight ratio. (**D**) RLN-to-body weight ratio. (**E**) Accumulated proteinuria level from 9 weeks to 14 weeks of age. (F) Serum level of anti-dsDNA IgG at 15 weeks of age. IU, international units. (**G**) Serum level of anti-dsDNA IgG-to-total IgG weight ratio at 15 weeks of age. n ≥ 7 mice per group. Statistical significance (*p<0.05, **p<0.01) is shown based on one-way

ANOVA. Nearly significant differences between PBS and Mixed are shown as $^{\#}p<0.1$.

Figure 2

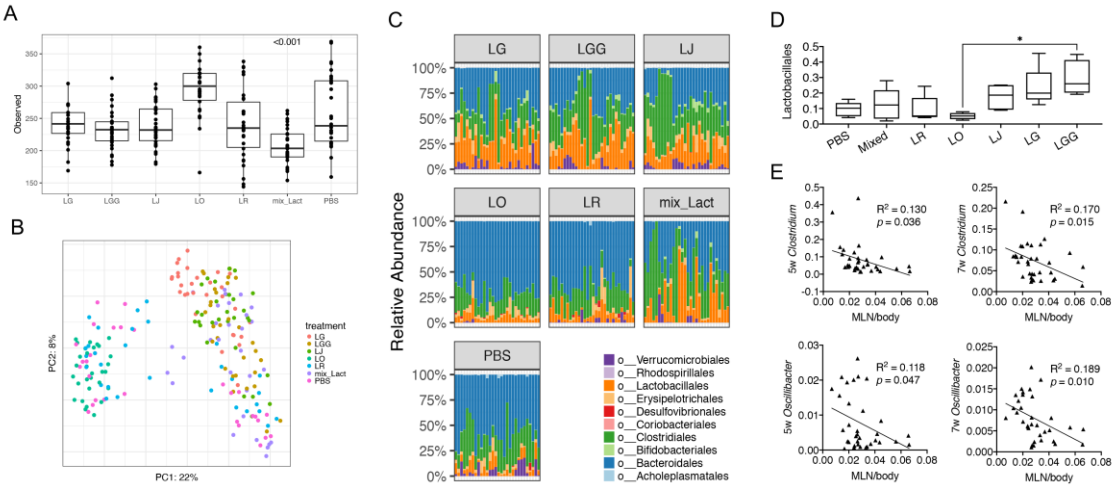

Figure 2. Gut microbiota at early stage is associated with the decrease of gut-draining lymph node size. Fecal microbiota samples were collected at 3, 5, 7, 9, 11 and 13 weeks of age (n = 5 mice per group) and subjected to 16S rRNA sequencing. (**A**) Observed OTUs (p<0.001). (**B**) Principal coordinate analysis of fecal microbiota composition. (**C**) Time-dependent changes of fecal microbiota at the order level. (**D**) The relative abundance of the order *Lactobacillales*. Statistical significance (*p<0.05) is shown based on one-way ANOVA. (**E**) Correlation analysis of the relative abundance of the genera *Clostridium* and *Oscillibacter* at 5 and 7 weeks of age against the MLN-to-body weight ratio at 15 weeks of age.

Figure 3

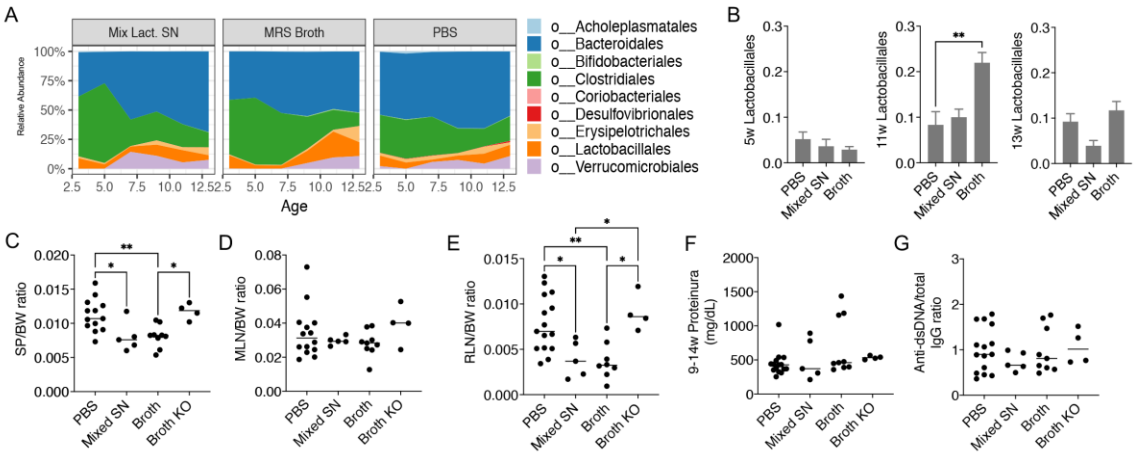

Figure 3. *Lactobacillus* spp. attenuate splenomegaly and renal lymphadenopathy through secreted factors and a CX$_3$CR1-dependent mechanism. Female MRL/*lpr* mice were orally gavaged with PBS, the combined culture supernatant of the 5 *Lactobacillus* spp. (Mixed SN), or MRS broth (Broth) twice a week at 200 μL/mouse from 3 weeks to 15 weeks of age. In some experiments, female MRL/*lpr*-*Cx3cr1*$^{gfp/gfp}$ mice were treated with MRS broth (Broth KO) following the same protocol. (**A**) Time-dependent changes of fecal microbiota (n = 5 mice per group). (**B**) The relative abundance of the order *Lactobacillales* at 5, 11 and 13 weeks of age. (**C**) SP-to-body weight ratio. (**D**) MLN-to-body weight ratio. (**E**) RLN-to-body weight ratio. (**F**) Accumulated level of proteinuria from 9 to 14 weeks of age. (D) Anti-dsDNA-to-total IgG ratio. n ≥ 7 mice per group. Statistical significance (*p<0.05, **p<0.01) is shown based on one-way ANOVA.

Figure 4

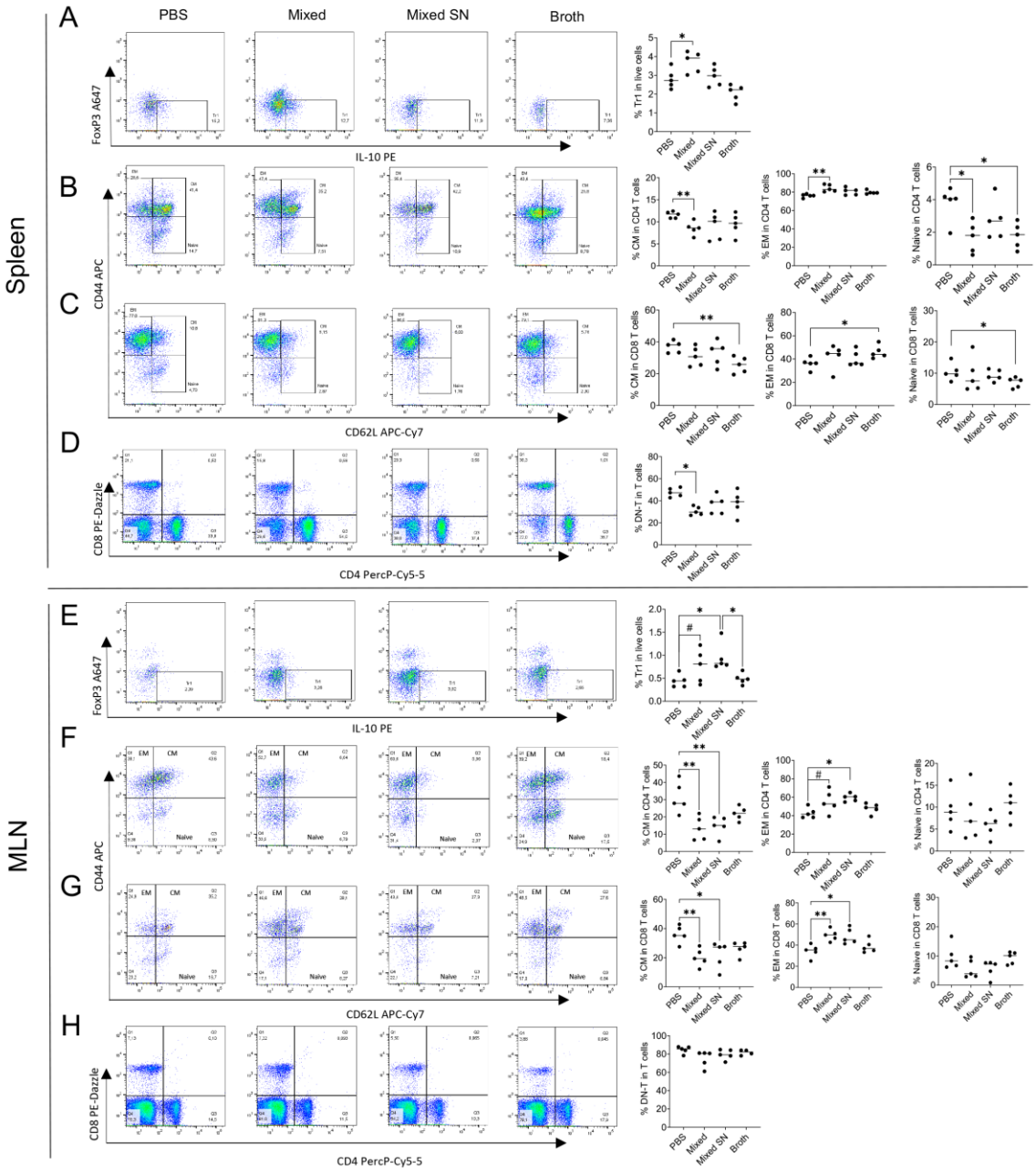

Figure 4: *Lactobacillus* spp. control inflammation through regulating splenic and MLN immune cell populations. (**A-D**) Flow cytometry analysis of splenocytes. (**E-H**) Flow cytometry analysis of MLN cells. (A and E) Frequency of IL-10-expressing type 1 regulatory T (Tr1) cells. Plots were pre-gated on $CD4^+$ T cells. (B and F) Frequencies of

central memory (CM) and effector memory (EM) T cells as well as naïve T cells within $CD4^+$ T cells. Plots were pre-gated on $CD4^+$ T cells. (C and G) Frequencies of CM and EM T cells as well as naïve T cells within $CD8^+$ T cells. Plots were pre-gated on $CD8^+$ T cells. (D and H) Frequency of double-negative T (DNT) cells. Plots were pre-gated on T cells. Statistical significance (*p<0.05, **p<0.01) is shown based on one-way ANOVA. Nearly significant differences are shown as $^{\#}p$<0.1.

Supplemental Figures

Supplemental Figure 1

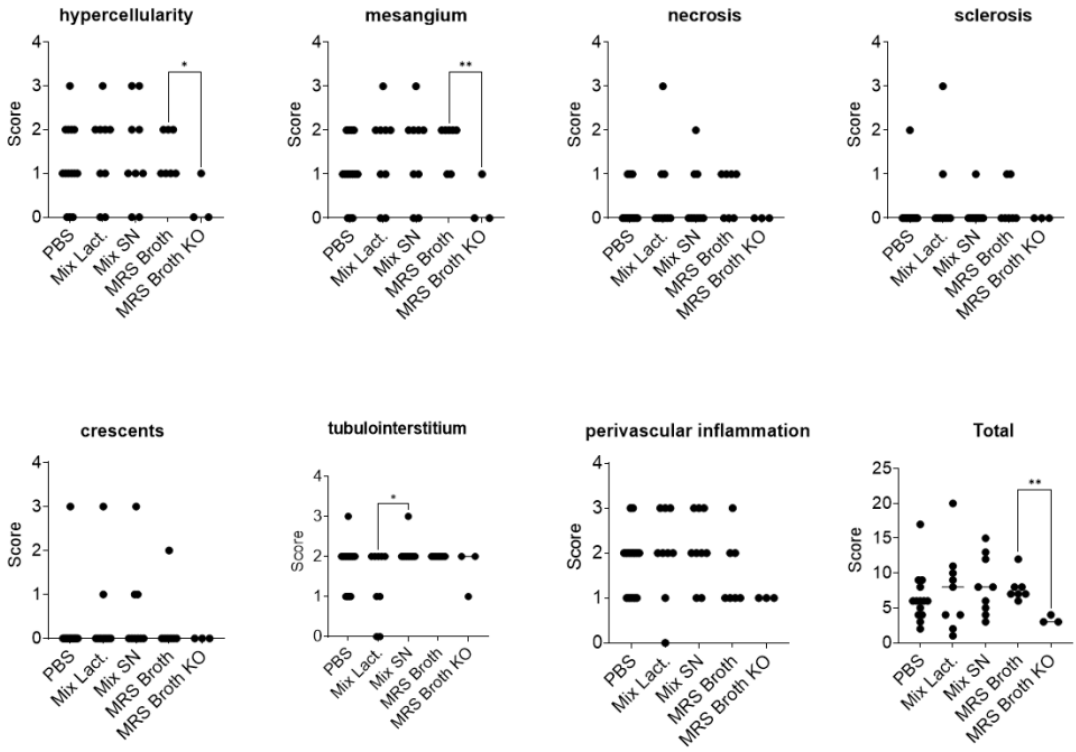

Figure S1. kidney histopathological scores for female mice are shown. Total score is the sum of all the other scores. n = 3, 7 or 8 mice per group; *$p < 0.05$, **$p < 0.01$.

Supplemental Figure 2

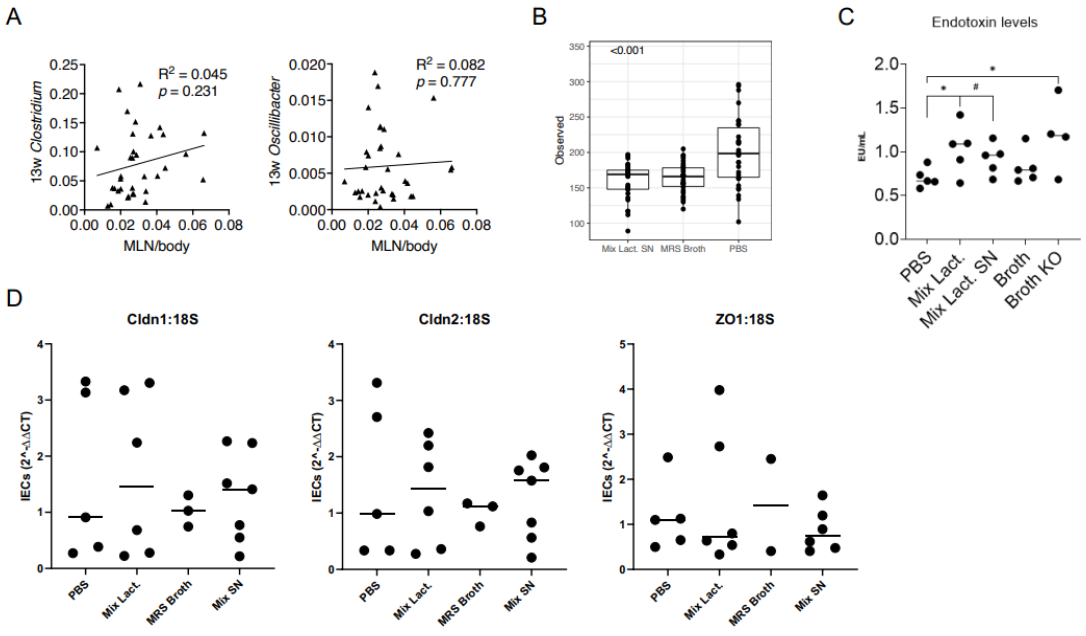

Figure S2. Fecal microbiota samples were collected at 3, 5, 7, 9, 11 and 13 weeks of age (n = 5 mice per group) and subjected to 16S rRNA sequencing. (**A**) Lack of correlation between the relative abundance of two genera at 13 weeks of age and the size of endpoint MLNs (p>0.05). (**B**) Alpha-diversity shown as observed OTUs (p <0.001). (**C**) Level of endotoxin in the serum. (**D**) Transcript levels of tight junction proteins in intestinal epithelial cells of 15-week-old mice. n = 5 mice per group; #$p < 0.1$, *$p < 0.05$.

Supplemental Figure 3

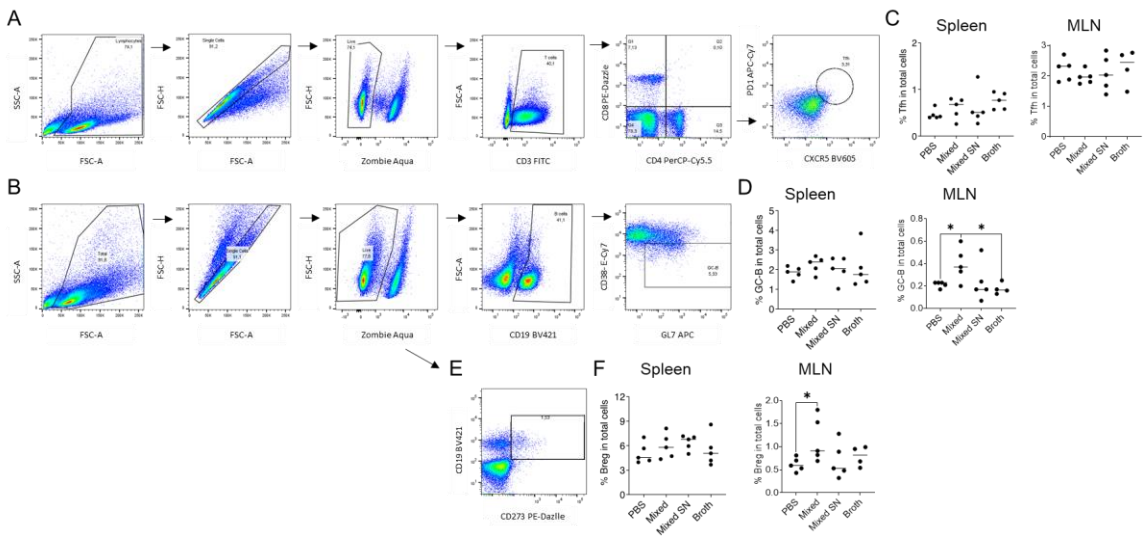

Figure S3. (**A**) Gating strategy for PD1^{+} CXCR5^{+} T follicular helper cells (Tfh) as determined by flow cytometry. (**B**) Gating strategy for CD38^{+}GL7^{+} germinal center B cells (GC-B). (**C**) Frequencies of Tfh in the spleen and mesenteric lymph node (MLN). (**D**) Frequencies of GC-B in the spleen and MLN. (**E**) Gating strategy for CD19^{+}CD273^{+} B regulatory cells (Breg). (**F**) Frequencies of Bregs in the spleen and MLN. n = 5 mice per group; *$p < 0.05$.

Supplemental Figure 4

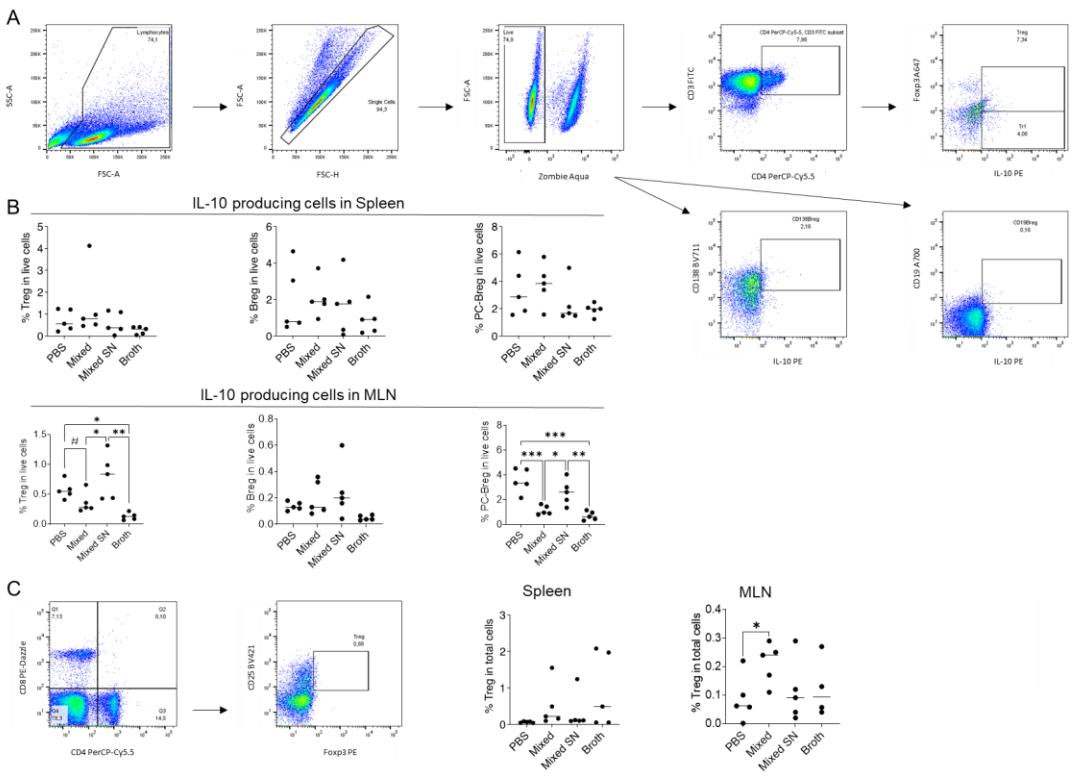

Figure S4. (**A**) Gating strategy for Foxp3^{+}IL-10+ cells T regulatory cells (Treg), CD138+ IL-10+ B regulatory plasma cells (PC-Breg) and CD19^{+}IL-10^{+} Breg as determined by flow cytometry. (**B**) Frequency of each cell population in the spleen and MLN. (**C**) Gating strategy for CD25^{+}Foxp3^{+} Treg and frequencies of such Tregs in the spleen and MLN. n = 5 mice per group; *$p < 0.05$.

Supplemental Table 1

Table S1. Relative abundance of *Clostridium* and *Oscillibacter* in each group at 5 and 7 weeks of age.

Treatment	Age	Clostridium	Oscillibacter	MLN/body
PBS	w5	0.014350308	0.000919646	0.0287602
PBS	w5	0.042757404	0.002807379	0.0404596
PBS	w5	0.055500525	0.020471259	0.0337574
PBS	w5	0.05224002	0.019389487	0.0186728
PBS	w5	0.0896239	0.01333689	0.0200933
mix_Lact	w5	0.437595862	0.026209738	0.026746
mix_Lact	w5	0.356416206	0.017512939	0.0069759
mix_Lact	w5	0.023222797	0.000709867	0.0239791
mix_Lact	w5	0.03223376	0.002456841	0.0561644
mix_Lact	w5	0.040181691	0.003983229	0.0254487
LR	w5	0.017231153	0.002216326	0.0435884
LR	w5	0.028242455	0.004618397	0.0417251
LR	w5	0.092980296	0.002531472	0.0266725
LR	w5	0.15643395	0.015587491	0.012844
LR	w5	0.114696795	0.020895103	0.0145545
LO	w5	0.013628875	0.003482103	0.0282562
LO	w5	0.017421665	0.00155962	0.0662156
LO	w5	0.0346746	0.001226973	0.024343
LO	w5	0.043254328	0.011254709	0.0308266
LO	w5	0.098126694	0.008371111	0.0447002
LJ	w5	0.041881776	0.002516779	0.0190722
LJ	w5	0.045611276	0.00414373	0.065684
LJ	w5	0.04994454	0.002310821	0.0199824
LJ	w5	0.031391837	0.004502631	0.0265772
LJ	w5	0.125661517	0.020103001	0.0237164
LG	w5	0.019881211	0.001778284	0.0368098
LG	w5	0.058245601	0.000950173	0.0340301
LG	w5	0.140728711	0.005743068	0.0154668
LG	w5	0.056526461	0.005381122	/
LG	w5	0.077215504	0.001661986	0.0270821
LGG	w5	0.165056059	0.021050266	0.0272093
LGG	w5	0.047785578	0.007229167	0.0201571
LGG	w5	0.068422828	0.005470934	0.02651
LGG	w5	0.040040366	0.000423191	0.0166446
LGG	w5	0.084211226	0.000797581	0.0331622
PBS	w7	0.041604118	0.002380442	0.0287602
PBS	w7	0.069691172	0.005173154	0.0404596
PBS	w7	0.113187384	0.017184612	0.0337574
PBS	w7	0.10989011	0.010501333	0.0186728
PBS	w7	0.191723246	0.014225671	0.0200933
mix_Lact	w7	0.111098614	0.008182662	0.026746
mix_Lact	w7	0.216211401	0.00807601	0.0069759
mix_Lact	w7	0.0722065	0.005981477	0.0239791
mix_Lact	w7	0.092917098	0.005826088	0.0561644
mix_Lact	w7	0.043493076	0.014931384	0.0254487
LR	w7	0.027169003	0.002500473	0.0435884
LR	w7	0.046051808	0.008092437	0.0417251
LR	w7	0.033870362	0.006578196	0.0266725
LR	w7	0.08465952	0.010422333	0.012844
LR	w7	0.086848921	0.013544365	0.0145545
LO	w7	0.027104737	0.001525299	0.0282562
LO	w7	0.059526579	0.005379784	0.0662156
LO	w7	0.06631162	0.005652542	0.024343
LO	w7	0.079447576	0.006349938	0.0308266
LO	w7	0.031020298	0.001888192	0.0447002
LJ	w7	0.083762737	0.015012979	0.0190722
LJ	w7	0.014482991	0.001751431	0.065684
LJ	w7	0.10860041	0.013619696	0.0199824
LJ	w7	0.023741993	0.001083527	0.0265772
LJ	w7	0.115325133	0.006162412	0.0237164
LG	w7	0.126463295	0.004805567	0.0368098
LG	w7	0.025864133	0.002774008	0.0340301
LG	w7	0.083266243	0.009379277	0.0154668
LG	w7	0.02866891	0.001219625	/
LG	w7	0.028437612	0.001546253	0.0270821
LGG	w7	0.042862421	0.013214154	0.0272093
LGG	w7	0.036043836	0.007198872	0.0201571
LGG	w7	0.07934465	0.020175317	0.02651
LGG	w7	0.071351323	0.012160059	0.0166446
LGG	w7	0.046289875	0.003987517	0.0331622

Table S1. Relative abundance of Clostridium and Oscillibacter in each group at 5 and 7 weeks of age.

CHAPTER 4

CX_3CR1 modulates SLE-associated glomerulonephritis and cardiovascular disease in MRL/*lpr* mice

Xavier Cabana-Puig[1,], Ran Lu[1,2,], Shuo Geng[2,], Jacquelyn S. Michaelis[3], Vanessa Oakes[1], Caitlin Armstrong[1,2], James C. Testerman[1], Xiaofeng Liao[1], Razan Alajoleen[1], Michael Appiah[1], Yao Zhang[2], Christopher M. Reilly[4], Liwu Li[2,], Xin M. Luo[1,]

[1]Department of Biomedical Sciences and Pathobiology, Virginia Tech, Blacksburg, VA, USA

[2]Department of Biological Sciences, Virginia Tech, Blacksburg, VA, USA

[3]Center for Bioinformatics and Computational Biology, University of Maryland, College Park, MD, USA

[4]Edward Via College of Osteopathic Medicine, Blacksburg, VA, USA

Under Review

Abstract

Patients with systemic lupus erythematosus (SLE) often develop multi-organ damages including heart and kidney complications, with poorly defined underlying mechanisms. We generated a *Cx3cr1*-deficient MRL/*lpr* lupus-prone mouse which exhibits a distinct phenotype of exacerbated glomerulonephritis with concurrent change of the gut microbiota composition compared to *Cx3cr1*$^{+/+}$ MRL/*lpr* littermates. Interestingly, upon correction of the gut microbiota with *Lactobacillus* administration, the phenotype of exacerbated glomerulonephritis was reversed, suggesting that CX_3CR1 controls glomerulonephritis in MRL/*lpr* mice through a gut microbiota-dependent mechanism. Additional results showed a decrease of spleen tolerogenic marginal zone macrophages and an increase of $CD3^+CD4^-CD8^-$ double-negative T cells in *Cx3cr1*$^{-/-}$ MRL/*lpr* mice. Furthermore, upon treatment with a high-fat diet, *Cx3cr1*$^{-/-}$ MRL/*lpr* mice developed significantly more atherosclerotic plaques that were promoted by *Cx3cr1* deficiency-mediated activation of $Ly6C^{++}$ monocytes. The activated monocytes expressed ICOS-L that interacted with ICOS-expressing follicular T helper cells, which in turn facilitated a germinal center reaction to produce more autoantibodies. Through a positive feedback mechanism, the increased circulatory autoantibodies further promoted the activation of Ly6C-expressing monocytes and their display of ICOS-L. Together, we uncovered novel, *Cx3cr1* deficiency-mediated pathogenic mechanisms contributing to SLE-associated glomerulonephritis and cardiovascular disease in MRL/*lpr* mice. The results of these studies will lead to the identification of new therapeutic targets for the treatment of two severe manifestations accounting for most of the morbidity and mortality in SLE.

Introduction

Systemic lupus erythematosus (SLE) is a prototypic autoimmune disease for which there is no known cure. It is characterized by systemic inflammation that damages numerous organs of the body, including kidney and heart (1). The SLE-associated inflammation of the kidney, known as lupus nephritis, affects more than half of SLE patients and represents one of the leading causes of morbidity and mortality (1, 2). Among the more severe manifestations of SLE, cardiovascular events are also a leading cause of death for SLE patients, who have a relative risk of 1.98 of symptomatic cardiovascular events compared to non-SLE controls based on a 2021 meta-analysis (3). A recent longitudinal prospective study involving 342 patients with SLE have found that 20% of these patients experienced major adverse cardiovascular events, among which a quarter of them died (4). Current standard-of-care treatments for SLE are primarily nonselective immunosuppressants and not specific for treating or preventing cardiovascular events (2). Although current therapies can treat acute symptoms and reduce the risk of renal failure associated with SLE, side effects are a major cause of concern. For example, patients taking long-term immunosuppressants are prone to higher incidence of severe infections (5). There is an imperative need to develop new treatment strategies against the development of SLE-associated kidney and heart disease, for which a thorough understanding of the pathogenesis is required.

CX_3CR1 (6) and its ligand CX_3CL1 (7, 8) were both discovered in 1997. They were initially found to mediate lymphocyte and monocyte chemotaxis. CX_3CL1 is induced upon LPS or TNF/IL-1 stimulation through NF-κB signaling indicating a role of the receptor/ligand in inflammation (9). CX_3CR1 is highly expressed in human $CD16^+$

and mouse Ly6C$^-$ non-classical monocytes (10). CX_3CR1 and its ligand are found to be elevated in the circulation of SLE patients (receptor in the peripheral blood mononuclear cells/PBMCs (11) and soluble ligand in the serum (12)). Studies of human kidney biopsies have shown that renal infiltrates of CX_3CR1^+ cells are T cells and monocyte/macrophages (13). In mouse models of SLE, elevations of the receptor and ligand have been shown to be associated with proliferative lupus nephritis (14). In lupus-prone MRL/*lpr* mice, CX_3CL1 antagonism can attenuate lupus nephritis (15). In the anti-glomerular basement membrane glomerulonephritis model, antibody neutralization of CX_3CR1 attenuates disease severity (16). We have also shown that renal infiltrates of CX_3CR1^+ cells are CD11b$^+$ conventional dendritic cells (cDCs) in MRL/*lpr* mice (17). In fact, CX_3CR1 mediates the homing of cDCs (18) and monocytes/macrophages (19) to the kidney. Furthermore, the CX_3CL1-CX_3CR1 axis is implicated in chronic kidney disease (CKD) (20), and CX_3CR1 is expressed in the developing kidney (21). Therefore, many have hypothesized that CX_3CR1^+ cells contribute to the development of kidney inflammation in SLE.

In contrast, the role of CX_3CR1 in SLE-associated cardiovascular disease is significantly understudied, although there are many CX_3CR1 studies on atherosclerosis unrelated to SLE. In general, *CX3CR1* polymorphisms are risk factors for atherosclerosis (22). This is with the exception of homozygous *CX3CR1* M280 mutation, which leads to loss-of-function and thus protection against atherosclerotic cardiovascular disease (23). Consistent with a pathogenic role of human *CX3CR1* in atherosclerosis, *Cx3cr1* deficiency in mice leads to rapid turnover (survival disadvantage) of myeloid cells including monocytes within atherosclerotic plaques, suggesting that CX_3CL1-CX_3CR1

signaling provides a survival signal for monocytes and/or foam cells (9, 22). However, it has also been shown that CX_3CR1 is important for T cell survival (24) and mediates regulatory T cell (Treg) migration to the aorta in atherosclerosis to improve disease (25, 26). As mentioned earlier, how CX_3CR1 modulates SLE-associated cardiovascular disease is unknown.

People have resorted to loss-of-function genetic approaches to elucidate the putative pathogenic role of CX_3CR1 in several autoimmune disease models. Previous studies of *Cx3cr1* deficiency in autoimmunity had been focused on inducible models. For example, *Cx3cr1* deficiency led to more severe disease in C57BL/6 (B6) mice upon induction of experimental autoimmune uveitis due to increased recruitment of monocytes to the retina (27). The deficiency also accelerated retinopathy in streptozotocin (STZ) induced type 1 diabetes in B6 mice (28), and injection of CX_3CR1 antagonist induced cognitive deficits in STZ-treated B6 mice (29). Notably, these results are contradictory to those presented earlier, where blockade of CX_3CR1 signaling tends to attenuate autoimmunity with kidney involvement. Likewise, while *Cx3cr1* deficiency led to more severe disease in an experimental autoimmune encephalomyelitis (EAE) mouse model of multiple sclerosis (MS) with accumulation of DCs in the brain (30), inhibition of CX_3CR1 attenuated EAE in a myelin oligodendrocyte glycoprotein-induced rat model of MS (31). The role of CX_3CR1 in autoimmunity is thus complex, possibly due to the fact that it is expressed by various immune cell types. In humans, there are two common single nucleotide polymorphisms (SNPs) in *CX3CR1*, V249I and T280M, with the latter conferring loss-of-function for the gene. Both SNPs have been recently shown to be associated with increased risk of CKD (32).

In this study, we have generated global knockout of *Cx3cr1* in lupus-prone MRL/*lpr* mice and directly assessed the roles of this chemokine receptor in the pathogenesis of glomerulonephritis and SLE-associated heart disease. Our results indicate exacerbation of both in the absence of *Cx3cr1*, suggesting CX_3CR1-mediated control of kidney and cardiovascular disease in SLE. In addition, we have uncovered the regulatory mechanisms that account for the effects of *Cx3cr1* deficiency on these two clinically relevant SLE manifestations.

Materials and Methods

Animals

MRL/*lpr* [MRL/Mp-*Fas*$^{lpr/lpr}$, stock number 000485] and B6/*Cx3cr1*$^{gfp/gfp}$ [B6.129P2(Cg)- *Cx3cr1*^{tm1Litt}, stock number 005582] mice were purchased from The Jackson Laboratory. All mice were maintained in a specific pathogen-free environment under the requirements of Institutional Animal Care and Use Committee (IACUC) at Virginia Polytechnic Institute and State University. MRL/*lpr*-*Cx3cr1*$^{gfp/gfp}$ (or *Cx3cr1*$^{-/-}$ MRL/*lpr*) mice were obtained after backcrossing the loss-of-function *Cx3cr1*$^{gfp/gfp}$ locus to MRL/*lpr* for 12 generations, reaching at least 99% similarity to MRL/*lpr* background, which was confirmed with genome scanning using mouse SNP panels. For all experiments, we first crossed MRL/*lpr* to *Cx3cr1*$^{-/-}$ MRL/*lpr* to obtain *Cx3cr1*$^{+/-}$ MRL/*lpr*. The heterozygous mice were then intercrossed to generate littermate experimental animals of 3 different genotypes (+/+, +/-, -/-). The *Lactobacillus* strains, *L. reuteri* (CF48-3A), *L. oris* (F0423), *L. johnsonii* (135-1-CHN) and *L. gasseri* (JV-V03) and *L. rhamnosus* (LMS201), were obtained from BEI Resources. All 5 strains were

freshly cultured every week individually, then mixed, washed, and resuspended in PBS, and finally orally administered to female *Cx3cr1*$^{-/-}$ MRL/*lpr* and *Cx3cr1*$^{+/+}$ MRL/*lpr* littermates, weekly at 2×10^8 CFU/*Lactobacillus* strain per dose, from 3 weeks of age till euthanasia at 17 weeks of age. In experiments involving diet modulations, female *Cx3cr1*$^{-/-}$ MRL/*lpr* and *Cx3cr1*$^{+/-}$ MRL/*lpr* littermates were fed with a high fat diet (HFD; Envigo, TD88137) or a control diet (CD; Envigo, TD05230) for 10 weeks starting at 4 weeks of age, followed by sample collection at 14 weeks of age. All mice were continuously monitored every week for body weight and proteinuria. Upon euthanasia, the body and organ weights were recorded.

Analyses of renal function

All fixed kidney tissues were paraffin-embedded, sectioned, and stained for Periodic Acid-Schiff (PAS) at the Histopathology Laboratory at Virginia-Maryland College of Veterinary Medicine. Kidney histopathology was graded on a scale of 0–3 each for glomerular nephritis (GN; including cellularity, mesangial matrix, necrosis, percentage of sclerotic glomeruli, and presence of crescents), tubulointerstitial nephritis (TI), and perivascular infiltration (PV). Scores were assigned by a board-certified veterinary pathologist in a blinded fashion (33). Proteinuria was determined with a Pierce Coomassie Protein Assay Kit (Thermo Fisher Scientific, Waltham, MA). Urine samples were also used for the measurement of urinary albumin and creatinine with a mouse Albumin ELISA kit (Bethyl Laboratories/Fortis Life Sciences, Waltham, MA), and a Creatinine Assay kit (Cayman Chemical, Ann Arbor, MI), respectively, according to the

instructions provided in the kits. The Albumin to Creatinine Ratio (ACR, mg/g) was then calculated.

Immunohistochemistry

Kidneys and spleens were embedded in Tissue-Tek OCT Compound (Sakura Finetek, Torrance, CA) and rapidly frozen in a freezing bath of dry ice and 2-methylbutane. Frozen OCT samples were cryosectioned and unstained slides were stored at -80°C. Frozen slides were warmed to room temperature and let dry for 30 min, followed by fixation in -20°C cold acetone at room temperature for 10 min. After washing in phosphate buffered saline (PBS), slides were blocked with PBS containing 1% bovine serum albumin (BSA) and anti-mouse CD16/32 (1:100, BioLegend, San Diego, CA) for 40 min at room temperature. Slides were then incubated with fluorochrome-conjugated antibody mixture overnight at 4°C in a dark humid box. Slides were mounted with Prolong Gold containing DAPI (Life Technologies, Carlsbad, CA). The following anti-mouse antibodies were used in immunohistochemical analysis: complement C3-APC (1:200, Cedarlane, Cat# 1850362A); IgG2a-PE (1:200, BioLegend, Cat# 407107); Ly6C-APC (1:200, eBiosciences, Cat# 17-5932-80); ICOS-L-PE (1:200, BioLegend, Cat# 107405); CD3-PE (BD Pharmingen, Cat# 555275); and GL7-AF647 (1:100, BioLegend, Cat# 144606). Slides were read and pictured with KEYENCE BZ-X810 Fluorescence Microscope (KEYENCE Corporation of America, Itasca, IL) and a 20× objective.

16S rRNA sequencing and analysis

Fecal pellets were collected weekly directly from the anus for each mouse to maintain sterile conditions. Samples were stored immediately at -80°C until processed. Samples

were homogenized, cell lysed, and DNA was extracted using a phenol-chloroform method as previously described (34-38). DNA was amplified by PCR and amplicons were purified and sequenced bidirectionally (V4 region) on an Illumina MiSeq at Argonne National Laboratory using 150 bp PE chemistry. Reads were quality trimmed using Trimmomatic (39), specifying ILLUMINACLIP:TruSeq3-PE.fa:2:30:10 SLIDINGWINDOW:4:20 MAXINFO:140:0.9 MINLEN:130. Amplicon sequence variants (ASVs) were generated using DADA2 (40) in R. Reads were quality trimmed and filtered using the command fastqPairedFilter using parameters truncLen=c(140,140), maxEE=c(2,2), rm.phix=TRUE, maxN=0, compress=TRUE, multithread=FALSE. DADA2 was used to learn error rates, perform sample inference, dereplicate and merge paired end reads, and construct a sequence table. Taxonomy was assigned using the SILVA 138 ribosomal RNA (rRNA) database training set (10.5281/zenodo.4587946) using the DADA2 functions, assignTaxonomy and addSpecies.

Samples were analyzed using the R package phyloseq (41) v 1.34.0. A total of 3698 ASVs were detected in 140 total samples. ASVs seen fewer than three times in at least 20% of samples and samples with fewer than 1000 reads were removed from the dataset, resulting in 139 samples and 286 ASVs used for downstream analyses. ASVs were aggregated at the genus level using the phyloseq function *tax_glom*. For each comparison, ASVs seen fewer than three times in at least 20% of samples were removed from the analyses. Counts were used for alpha diversity and differential abundance tests, while proportions were used to calculate Bray-Curtis dissimilarity. Differentially abundant and variable taxa between groups were identified using the function *differentialTest* in corncob (42) v 0.2.0 and significance was assessed using a Wald test

with an FDR cutoff of 0.05. Bray-Curtis distances were calculated using the phyloseq function *ordinate*, specifying "method="NMDS", distance="bray", trymax=1000, k=3". Significance was assessed using the adonis test in the vegan (43) package v 2.5.7 with 999 permutations. Figures were generated using the functions ordiplot3d and ordiellipse in the library vegan3d.

Flow cytometry

Spleen and mesenteric lymph nodes (MLN) were collected and mashed in 70-μm cell strainers with C10 media (RPMI-1640 containing L-glutamine, 10 mM HEPES, 1 mM sodium pyruvate, 1% 100X MEM non-essential amino acids, 55 μM 2-mercaptoethanol, 10% fetal bovine serum, 100 U/ml penicillin-streptomycin, all from Life Technologies). For splenocytes, red blood cells were lysed with RBC lysis buffer (eBioscience/Thermo Fisher Scientific). For cell staining, cells were blocked by anti-mouse CD16/32 (1:100, BioLegend), stained with fluorochrome-conjugated antibodies, and analyzed with BD FACS Aria Fusion flow cytometer (BD Biosciences, San Jose, CA). For intracellular staining, Foxp3/Transcription Factor Staining kit was used (eBioscience/Thermo Fisher Scientific). Dead cells were stained with Zombie Aqua (1:100, Biolegend, Cat# 423101). Anti-mouse antibodies used in this study include: CD3-APC (1:80, BioLegend, Cat# 100235); CD3-APC/Cy7 (1:200, BD Pharmingen, Cat# 559596); CD4-PE/Cy7 (1:160, BioLegend, Cat# 100421); CD8-PE/Dazzle 594 (1:300, BioLegend, Cat# 126621); PD-1-APC/Cy7 (1:300, BioLegend, Cat# 135223); CXCR5-BV605 (1:160, BioLegend, Cat# 145513); CD25-BV421 (1:200, BioLegend, Cat# 102033); CD25-Pacific Blue (1:160, BioLegend, Cat# 102201); Foxp3-PE (1:80, BioLegend, Cat# 320007); CD44-

PerCP/Cy5.5 (1:160, BDbiosciences, Cat# 560570); CD62L-APC/Cy7 (1:300, eBioscience, Cat# 25-0621-82); RORγT-PE (1:300, eBioscience, Cat# 12-6981-82); CD3-APC/Cy7 (1:200, BD Pharmingen, Cat# 559596); B220-PE (1:160, BioLegend, Cat# 103207); CD138-PerCP/Cy5.5 (1:200, BioLegend, Cat# 142509); CD19-AF700 (1:200, eBioscience, Cat# 56-0193-82); CD38-PE/Cy7 (1:160, BioLegend, Cat# 102717); GL7-AF647 (1:100, BioLegend, Cat# 144606); XCR1-BV650 (1:200, BioLegend, Cat# 148220); CD11c-APC (1:80, eBioscience, Cat# 17-0114-82); MHC-II-PE (1:80, BioLegend, Cat# 107607); CD172a-PE/Dazzle 594 (1:200, BioLegend, Cat# 144015); CD21/35-APC/Cy7 (1:200, BioLegend, Cat# 123417); F4/80-BV421 (1:200, BioLegend, Cat# 123131); Siglec-H-PerCP/Cy5.5 (1:200, BioLegend, Cat# 129614); CD138-PerCP/Cy5.5 (1:200, BioLegend, Cat# 142509); GL7-AF647 (1:100, BioLegend, Cat# 144606). Flow cytometry data were analyzed with FlowJo.

Bone marrow (BM) and spleen were harvested from *Cx3cr1*$^{+/-}$ MRL/*lpr* mice and *Cx3cr1*$^{-/-}$ MRL/*lpr* mice fed with HFD or CD. BM and spleen samples were disassociated with mechanical processes and then filtered through 70-μm cell strainers to obtain single-cell suspension. Red blood cells were lysed with ACK buffer (Thermo Fisher Scientific). The samples were incubated with anti-CD16/32 antibodies (1:100, BD Biosciences) to block Fc receptors followed by staining with fluorochrome-conjugated CD11b-APC/Cy7 (1:200, BioLegend, Cat# 101226), Ly6C-PE/Cy7 (1:200, BioLegend, Cat# 128018), Ly6G-PerCP/Cy5.5 (1:200, BioLegend, Cat# 127616), CCR2-APC (1:200, BioLegend, Cat# 150628), CD14-APC (1:200, BioLegend, Cat# 123312), CD24-PE (1:200, BioLegend, Cat# 138503), CD38 (1:200, BioLegend, Cat# 102712), CD86-APC (1:200, BioLegend, Cat# 159203), CD200R-APC (1:200, BioLegend, Cat# 123916), ICAM-1-PE

(1:200, BioLegend, Cat# 116108), and PD-L1-APC (1:200, BioLegend, Cat# 124312) antibodies. The surface phenotype of $Ly6G^+$ neutrophils, $Ly6G^-CD11b^+Ly6C^{++}$ monocytes, $Ly6G^-CD11b^+Ly6C^+$ monocytes, and $Ly6G^-CD11b^+Ly6C^-$ monocytes was examined using FACSCanto II (BD Biosciences). The data were analyzed with FlowJo.

Analysis of atherosclerotic lesions

Histological analyses of murine atherosclerotic lesions were performed as previously described (44, 45). Briefly, freshly frozen and OCT-embedded proximal aortic sections were fixed in 4% neutral buffered formalin, followed by Oil Red O staining was performed using a kit (Newcomer Supply, Middleton, WI). The samples were observed under a light microscope, and the percentages of total lesion area were calculated.

ELISAs

Serum was separated from blood after clotting at room temperature for 2 hours, then collected and stored at -80°C. Anti-dsDNA IgG was measured as previously described (46). Serum total IgG concentration was determined with mouse IgG ELISA kit (Bethyl Laboratories). Blood endotoxin was measured by using a Pierce LAL Chromogenic Endotoxin Quantitation kit (Thermo Fisher Scientific, Cat# A39552).

BM cell isolation and in vitro stimulation

BM cells isolated from C57BL/6 (B6) mice were cultured in complete RPMI 1640 medium supplemented with M-CSF (10 ng/mL) as described previously (44, 45). BM cultures were incubated with serum (5% of total volume) collected from B6 mice,

Cx3cr1$^{+/-}$ MRL/lpr mice, or *Cx3cr1*$^{-/-}$ MRL/*lpr* mice. Fresh serum was added every 2 days. After 5 days, BMMs were harvested, filtered through 70-μm cell strainers, and incubated with anti-CD16/32 antibodies (1:100, BD Biosciences, Cat# 553141) to block Fc receptors. The cells were then stained with fluorochrome-conjugated CD11b-APC/Cy7 (1:200, BioLegend, Cat# 101226), Ly6C-PE/Cy7 (1:200, BioLegend, Cat# 128018), and ICOS-L-PE (1:200, BioLegend, Cat# 107405) antibodies. The samples were examined using FACSCanto II, and the data were analyzed using FlowJo.

Statistical analysis

For the comparison of two groups, unpaired student's *t*-test was used. For the comparison of three or more groups, one-way ANOVA was used. Two-way ANOVA was used to reveal time- and group-dependent effects. Results were considered statistically significant when $p<0.05$. All analyses were performed with the GraphPad Prism software.

Results

Cx3cr1 deficiency exacerbates lymphoproliferation and glomerulonephritis in female MRL/lpr mice.

To directly elucidate the role of CX_3CR1^+ cells in spontaneous SLE, we backcrossed the *Cx3cr1-gfp/gfp* locus from B6 background (The Jackson Laboratory/JAX Stock Number 005582) to lupus-prone MRL/*lpr* mice (JAX Stock Number 000485). The *Cx3cr1-gfp/gfp* mice have *EGFP* knock-in replacing the first 390 bp of the coding exon of the *Cx3cr1* gene. After 12 generations of speed congenic backcrossing (17, 47), we confirmed with genome scanning using mouse SNP panels that the purity of MRL background reached at

least 99.9%. Using heterozygous intercross, we generated littermate MRL/*lpr* mice that were either wildtype (+/+) or global knockout (-/-, or *gfp/gfp* knock-in) for the gene *Cx3cr1*. Littermates were separated upon weaning, and those with the same genotype were housed together.

We had hypothesized that the deficiency of *Cx3cr1* would attenuate disease in MRL/*lpr* mice given its potentially pathogenic role especially for kidney inflammation as discussed earlier. Surprisingly, *Cx3cr1* deficiency exacerbated lupus-like disease in both MRL/*lpr* females (**Fig. 1** and Suppl. Fig. S1A-B) and males (Suppl. Fig. S1C-D). Female MRL/*lpr* mice lacking *Cx3cr1* exhibited significantly worse splenomegaly and lymphadenopathy (**Fig. 1A**), as well as significantly exacerbated glomerulonephritis (**Fig. 1B**), compared to $Cx3cr1^{-/-}$ MRL/*lpr* mice. Of note, $Cx3cr1^{+/+}$ MRL/*lpr* mice did not have a significant elevation of proteinuria even at 17 weeks of age due to the loss of this phenotype in both JAX and our colony (48). Heterozygous mice (+/*gfp*) mostly exhibited an intermediate phenotype between $Cx3cr1^{+/+}$ and $Cx3cr1^{-/-}$ mice (Suppl. Fig. S1A-C).

Consistent with the increase of proteinuria, the urine albumin-to-creatinine ratio (ACR) at the late disease stage was significantly higher in $Cx3cr1^{-/-}$ MRL/*lpr* mice (**Fig. 1C**), indicating more severe glomerulonephritis. We next performed kidney histopathological analysis to characterize glomerulonephritis (GN), tubulointerstitial nephritis (TI), and perivascular infiltration (PV). While no statistical significance was observed, 50% of $Cx3cr1^{-/-}$ MRL/*lpr* mice (3 out of 6), compared to none of $Cx3cr1^{+/+}$ MRL/*lpr* mice, exhibited severe glomerulonephritis (**Fig. 1D**) that was characterized by glomerular necrosis, sclerosis, and formation of crescents (**Fig. 1E**). TI nephritis and PV infiltration scores, on the other hand, were largely comparable between $Cx3cr1^{+/+}$ and

Cx3cr1$^{-/-}$ MRL/*lpr* mice (Suppl. Fig. S2A). Furthermore, we performed immunohistochemical analysis of renal deposition of complement C3 as well as IgG2a, the pathogenic Ig isotype in MRL/*lpr* mice. While the deposition of C3 was comparable among all images taken, renal deposition of IgG2a was noticeably higher for the three *Cx3cr1*$^{-/-}$ MRL/*lpr* mice with worse GN scores (**Fig. 1F**), leading to an overall trending increase of the IgG2a/C3 intensity ratio with *Cx3cr1* deficiency (**Fig. 1G**). Other measurements, including the serum endotoxin level, the ratio of anti-double stranded (ds)DNA IgG to total IgG in the blood, and serum levels of typical pro-inflammatory and anti-inflammatory cytokines, were comparable between *Cx3cr1*$^{+/+}$ and *Cx3cr1*$^{-/-}$ MRL/*lpr* mice (Suppl. Fig. S2B-D).

Together, these results suggest exacerbation of lupus-like signs, including glomerulonephritis and lymphoproliferation (splenomegaly, lymphadenopathy), in MRL/*lpr* mice lacking *Cx3cr1* globally.

Exacerbation of glomerulonephritis with Cx3cr1 deficiency is gut microbiota-dependent, but exacerbation of lymphoproliferation is not.

It is known that *Cx3cr1* deficiency compromises the gut barrier (49). Indeed, *Cx3cr1* deficiency causes bacterial translocation to mesenteric lymph nodes (MLN) and more severe DSS-induced colitis through an IL-17A-dependent mechanism (50). We have previously shown that a mixture of 5 *Lactobacillus* spp. can decrease intestinal permeability and enhance gut barrier function while reshaping the gut microbiota of MRL/*lpr* mice (35). Therefore, we tested the hypothesis that the same 5 species of lactobacilli (*L. reuteri*, *oris*, *johnsonii*, *gasseri* and *rhamnosus*) (35) could render the

phenotypes of *Cx3cr1*$^{+/+}$ and *Cx3cr1*$^{-/-}$ MRL/*lpr* mice indistinguishable by repairing the leaky gut caused by *Cx3cr1* deficiency.

We first mapped the composition of the gut microbiota using 16S rRNA sequencing with or without *Lactobacillus* treatment. As anticipated, the probiotic bacteria were able to neutralize the gut microbiota differences between female *Cx3cr1*$^{+/+}$ and *Cx3cr1*$^{-/-}$ MRL/*lpr* mice (**Fig. 2A-B**). Analysis of amplicon sequence variants revealed 10 differentially abundant taxa between *Cx3cr1*$^{+/+}$ and *Cx3cr1*$^{-/-}$ MRL/*lpr* mice (**Fig. 2C**). In contrast, only 3 genera were minimally different in abundance with *Lactobacillus* treatment (**Fig. 2D**), confirming that *Lactobacillus* equalized the gut microbiota differences between the two mouse genotypes. Interestingly, the 5 genera enriched in *Cx3cr1*$^{-/-}$ MRL/*lpr* mice in the absence of *Lactobacillus* spp., namely *Lachnospiraceae unclassified*, *Lachnospiraceae FCS020 group*, *Desulfovibrio*, *Butyricicoccus* and *Romboutsia*, all have commensal species capable of producing short-chain fatty acids (SCFAs). However, preliminary testing showed no difference in fecal levels of acetate, butyrate, and propionate between *Cx3cr1*$^{+/+}$ and *Cx3cr1*$^{-/-}$ MRL/*lpr* mice (data not shown). This suggests that the bacterial species enriched in the gut microbiota of *Cx3cr1*$^{-/-}$ MRL/*lpr* mice may not be primary producers of SCFAs. Future studies involving metagenomic shotgun sequencing will reveal the identities of these bacterial species. Surprisingly, however, oral administration of *Lactobacillus* spp. did not affect the degree of splenomegaly and lymphadenopathy in female *Cx3cr1*$^{-/-}$ MRL/*lpr* mice (**Fig. 2E**). This observation suggests that a gut microbiota-independent mechanism is responsible for the CX_3CR1-mediated exacerbation of splenomegaly and lymphadenopathy in the MRL/*lpr* mouse. In contrast, treatment with *Lactobacillus* reversed the exacerbated renal disease

(proteinuria levels) caused by *Cx3cr1* deficiency (**Fig. 2F**). Given that *Lactobacillus* spp. equalized the gut microbiotas between *Cx3cr1*$^{+/+}$ and *Cx3cr1*$^{-/-}$ MRL/*lpr* mice, this finding suggests a gut microbiota-dependent mechanism that *Cx3cr1* deficiency exacerbates glomerulonephritis in the female MRL/*lpr* mouse.

Together, these results suggest a novel concept of dissociation between glomerulonephritis and lymphoproliferation in MRL/*lpr* mice, where gut dysbiosis in the lupus-prone mouse contributes to the development of renal inflammation but not to lymphoproliferation.

Significant differences in several splenic populations between Cx3cr1*$^{+/+}$ *and Cx3cr1*$^{-/-}$ *MRL/lpr mice are equalized by Lactobacillus treatment.

To elucidate the cellular mechanisms by which *Cx3cr1* deficiency contributes to the development of glomerulonephritis, we analyzed the splenocytes of *Cx3cr1*$^{+/+}$ and *Cx3cr1*$^{-/-}$ MRL/*lpr* mice with or without *Lactobacillus* treatment. Subsets of B cells, T cells and myeloid cells were quantified with flow cytometry. Three subsets of immune cells were significantly modulated by *Cx3cr1*. They were $CD3^+CD4^-CD8^-$ double-negative T (DNT) cells and two populations of MHC-II^+ cells ($CD11c^{high}$ and $CD11c^{low}$). DNT cells were significantly expanded in *Cx3cr1*$^{-/-}$ MRL/*lpr* mice, which accounted for over 50% of total splenocytes (~70% of T cells were DNT cells as shown in **Fig. 3A**, whereas ¾ of splenocytes were T cells). With the spleens of *Cx3cr1*$^{-/-}$ MRL/*lpr* mice being significantly larger, this represented a large number of DNT cells. The two populations of MHC-II^+ cells, on the other hand, were significantly decreased in frequency (**Fig. 3C**). Interestingly, all these differences were equalized with

Lactobacillus treatment (**Fig. 3B** and **3D**). This may have contributed to the same level of proteinuria in *Cx3cr1*$^{+/+}$ and *Cx3cr1*$^{-/-}$ MRL/*lpr* mice with *Lactobacillus* treatment. A fraction of the two populations of MHC-II^{+} cells express a specific marker of marginal zone macrophages (MZM), SIGN-R1 (51), which were almost completely depleted in *Cx3cr1*$^{-/-}$ MRL/*lpr* mice (**Fig. 3E**). Interestingly, both CD11c^{high}SIGN-R1^{+} and CD11c^{low}SIGN-R1^{+} MZM cells were restored in *Cx3cr1*$^{-/-}$ MRL/*lpr* mice in the presence of *Lactobacillus* spp. (**Fig. 3F**). Together, these results suggest that *Cx3cr1* deficiency exacerbates lupus-like disease in MRL/*lpr* mice via suppression of MZM cells that leads to the generation of DNT cells, thus exacerbating SLE.

A high-fat diet exacerbates cardiovascular inflammation in Cx3cr1*$^{-/-}$ *MRL/lpr mice.

To define the role of CX_3CR1 in SLE-associated cardiovascular disease, we used a high-fat diet (HFD) to accelerate the progression of atherosclerotic inflammation (45). In this experiment, we employed the heterozygous *Cx3cr1*$^{+/-}$ MRL/*lpr* mice that co-expressed GFP with CX_3CR1. As anticipated, the HFD increased the body weight of both *Cx3cr1*$^{+/-}$ and *Cx3cr1*$^{-/-}$ MRL/*lpr* mice (Suppl. Fig. S3A-B). However, HFD did not exacerbate glomerulonephritis (Suppl. Fig. S3C) or the enlargement of lymphoid tissues (Suppl. Fig. S3D-E). Strikingly, while the HFD was able to slightly increase the plaque size in *Cx3cr1*$^{+/-}$ MRL/*lpr* mice over the control diet (CD), the atherosclerotic plaque size was significantly larger when HFD was given to *Cx3cr1*$^{-/-}$ MRL/*lpr* mice (**Fig. 4A**), suggesting CX_3CR1 as a suppressor of cardiovascular inflammation in SLE.

As both neutrophils (52) and monocytes (45) are capable of releasing pro-inflammatory mediators that contribute to the development of atherosclerotic plaques, we

assessed the frequencies of these two types of myeloid cells in the bone marrow and spleen. While no significant differences were observed among treatment groups in the bone marrow (Suppl. Fig. S4), in the spleen, neutrophils were expanded with HFD; but the expansion was comparable between *Cx3cr1*$^{+/-}$ and *Cx3cr1*$^{-/-}$ MRL/*lpr* mice (**Fig. 4B**). In contrast, the frequency of a subpopulation of monocytes expressing a high level of Ly6C (Ly6G^{-}CD11b^{+}Ly6C^{++} classical monocytes) was the highest in the spleen of *Cx3cr1*$^{-/-}$ MRL/*lpr* mice fed the HFD and significantly higher than their *Cx3cr1*$^{+/-}$ MRL/*lpr* counterparts (**Fig. 4C**). This suggests that the expansion of splenic Ly6C^{++} classical monocytes may be involved in the exacerbation of cardiovascular inflammation observed in *Cx3cr1*$^{-/-}$ MRL/*lpr* mice with HFD. Moreover, the splenic monocytes of HFD-fed *Cx3cr1*$^{-/-}$ MRL/*lpr* mice expressed a significantly increased level of CD38, an activation marker of enhanced inflammation (53), over those in mice treated with CD (**Fig. 4D**). Furthermore, the adhesion molecule ICAM-1 was significantly increased on splenic monocytes isolated from *Cx3cr1*$^{-/-}$ MRL/*lpr* mice with HFD compared with CD-fed *Cx3cr1*$^{-/-}$ MRL/*lpr* mice (**Fig. 4E**), suggesting the potential of these monocytes to undergo trans-endothelial migration/trafficking towards sites of inflammation such as the atherosclerotic plaques (45).

We also analyzed the frequencies of multiple T cell subsets (Suppl. Fig. S5A), B cell subsets (Suppl. Fig. S5B) and macrophage and dendritic cell subsets (Suppl. Fig. S5C). With the exception of macrophages and plasmacytoid dendritic cells, HFD did not significantly alter the frequencies of these cell populations in the spleen of *Cx3cr1*$^{-/-}$ MRL/*lpr* mice compared to CD-fed *Cx3cr1*$^{-/-}$ MRL/*lpr* mice or *Cx3cr1*$^{+/-}$ MRL/*lpr* mice.

Together, these results suggest *Cx3cr1* deficiency facilitated the activation and migration of $Ly6C^{++}$ classical monocytes leading to the exacerbation of cardiovascular inflammation in lupus-prone MRL/*lpr* mice.

Monocytes promote a positive feedback cycle of inflammation that involves germinal center reaction and autoantibody production in Cx3cr1$^{-/-}$ MRL/lpr mice fed a high-fat diet.

To elucidate the mechanism by which splenic monocytes contribute to the exacerbation of atherosclerotic inflammation in *Cx3cr1*$^{-/-}$ MRL/*lpr* mice with HFD, we first investigated the formation of germinal centers, as monocytes are known to promote $ICOS^{+}$ follicular T helper (Tfh) cells by expressing ICOS-L (54, 55). Indeed, we observed on splenic sections the co-localization of Ly6C with ICOS-L, which was most evident in *Cx3cr1*$^{-/-}$ MRL/*lpr* mice fed a HFD (**Fig. 5A**). Consequently, the frequency of $CXCR5^{+}PD1^{+}$ Tfh cells (**Fig. 5B**) and that of Tfh cells expressing a high level of ICOS (**Fig. 5C**) were significantly higher in HFD-fed *Cx3cr1*$^{-/-}$ MRL/*lpr* mice than their CD-fed counterparts, suggesting the promotion of germinal center reaction that involves the interaction between ICOS-L expressed by monocytes and ICOS expressed by Tfh cells.

The enhanced germinal center reaction led to a significantly higher level of anti-dsDNA IgG autoantibodies in the circulation (**Fig. 6A**). Therefore, we asked if the upregulation of autoantibodies had an impact on monocyte activation. To do this, we established *in vitro* bone marrow cultures treated with the sera from B6 mice, *Cx3cr1*$^{+/-}$ MRL/*lpr* mice and *Cx3cr1*$^{-/-}$ MRL/*lpr* mice, respectively, and quantified the expansion of $Ly6C^{-}$, $Ly6C^{+}$ and $Ly6C^{++}$ monocyte populations (**Fig. 6B**) as well as their expression of

ICOS-L. Strikingly, the serum from *Cx3cr1*$^{-/-}$ MRL/*lpr* mice was the most potent in converting Ly6C^{-} monocytes to Ly6C-expressing (Ly6C^{+} and Ly6C^{++}) monocytes (**Fig. 6C**). In addition, the serum from *Cx3cr1*$^{-/-}$ MRL/*lpr* mice significantly induced the expression of ICOS-L on all 3 monocyte populations over the B6 and *Cx3cr1*$^{+/-}$ MRL/*lpr* controls (**Fig. 6D**). This observation, coupled with the greater level of autoantibodies in the serum of *Cx3cr1*$^{-/-}$ MRL/*lpr* mice, suggests autoantibody-mediated expansion of Ly6C^{+}ICOS-L^{+} monocytes.

Together, these results suggest a positive feedback cycle of inflammation with *Cx3cr1* deficiency in MRL/*lpr* mice, where Ly6C^{+} monocytes facilitate germinal center reaction via ICOS—ICOS-L interaction leading to upregulation of circulatory autoantibodies, which in turn promote the activation of Ly6C^{+} monocytes and their expression of ICOS-L, thereby further activating ICOS-expressing Tfh cells. This cycle is then exacerbated by HFD leading to aggravated cardiovascular inflammation in *Cx3cr1*$^{-/-}$ MRL/*lpr* mice.

Discussion

In this study, we generated global *Cx3cr1* knockout on MRL/*lpr* background to model the role of the genetic deficiency on autoimmune lupus. Our results showed exacerbation of both glomerulonephritis and HFD-facilitated atherosclerotic inflammation with the deficiency, suggesting that the chemokine receptor CX_3CR1, which was originally discovered to function in chemotaxis, also plays an important role in controlling peripheral inflammation associated with SLE. Mechanistically, we uncovered that *Cx3cr1* deficiency-mediated exacerbation of renal disease was gut microbiota-dependent,

as the difference in phenotype was abrogated when the gut microbiotas of *Cx3cr1*$^{+/+}$ and *Cx3cr1*$^{-/-}$ MRL/*lpr* mice were equalized by *Lactobacillus* treatment. In addition, we provided evidence to support downregulation of immunosuppressive MZM cells with *Cx3cr1* deficiency, which then allowed for the generation of DNT cells known to be pathogenic by infiltrating the kidney in both human and mouse SLE. Moreover, we found that HFD-facilitated exacerbation of cardiovascular inflammation in *Cx3cr1*$^{-/-}$ MRL/*lpr* mice was mediated by a feed-forward mechanism involving monocyte activation and expression of ICOS-L, which stimulates ICOS-expressing Tfh cells leading to increased germinal center reaction, followed by enhancement of autoantibody production which in turn promotes further activation of monocytes and their expression of ICOS-L.

Our results showed that the exacerbation of glomerulonephritis in *Cx3cr1*$^{-/-}$ MRL/*lpr* mice was reversed following treatment with *Lactobacillus* spp., whereas the exacerbation of splenomegaly and lymphadenopathy was not affected. This suggests distinct regulatory mechanisms leading to glomerulonephritis and lymphoproliferation: one depends on the gut microbiota while the other does not. The next question is how the gut microbiota from *Cx3cr1*$^{-/-}$ MRL/*lpr* mice facilitates the exacerbation of glomerulonephritis. Interestingly, the conversion of CD8 T cells to DNT cells is increased in the presence of antigens (56). These antigens can be protein antigens like ovalbumin, or self-antigens provided by apoptotic cells. It is possible that gut bacteria can provide such antigens. Therefore, we hypothesize that the gut microbiota of *Cx3cr1* MRL/*lpr* mice provides antigens necessary for the stimulation of pathogenic lymphocytes (e.g., DNT cells) which lodge the kidneys to exacerbate glomerulonephritis.

DNT cells are T cell receptor (TCR)-$\alpha\beta^+$, IL-17 producing T cells well characterized in both human SLE and murine lupus models (56-62). Peripheral DNT cells can be derived directly from thymocytes, or from activated $CD8^+$ T cells that lose the expression of CD8 (58). In type 1 diabetes (T1D), DNT cells are considered regulatory cells (58). In SLE, however, these cells promote the activation of B cells to produce autoantibodies, represent a major source of IL-17A that is known to be pathogenic in SLE, and infiltrate the kidney to exacerbate lupus nephritis (58). Therefore, it is logical to interpret that the increase of splenic DNT cells in *Cx3cr1*$^{-/-}$ MRL/*lpr* mice may be the cause of disease exacerbation in these mice.

Contrary to DNT cells, the potential function of losing $CD11c^{high}MHC\text{-}II^+$ and $CD11c^{low}MHC\text{-}II^+$ cells in *Cx3cr1*$^{-/-}$ MRL/*lpr* mice was initially difficult to interpret. If they were antigen presenting cDCs that stimulate T cells, why would their change be opposite to that of DNT cells? In addition, neither of the $MHC\text{-}II^+$ populations expressed a significant amount of XCR-1 or CD172a (data not shown), respective markers of cDC1 and cDC2 cells (63). Nor did they express Siglec-H, a marker of plasmacytoid DCs. Therefore, we questioned if they were indeed DCs, as markers of DCs and macrophages are not mutually exclusive (63-67). While the expression of F4/80 was low, we postulated that the two $MHC\text{-}II^+$ populations were $F4/80^{-/low}$ splenic macrophages. A subset of such macrophages has been described, namely splenic MZM cells (68). MZM cells surround splenic follicles to clear dying cells through the expression of scavenger receptors MARCO, SR-A and SIGN-R1 (51). Importantly, these cells can induce tolerance (51) and have been recently described to possess the capability to control the generation of DNT cells by producing TGFβ (56). Indeed, we were able to detect SIGN-

R1^{+} MZM cells in both CD11c^{high}MHC-II^{+} and CD11c^{low}MHC-II^{+} cells, which were almost completely removed in the spleen of *Cx3cr1*$^{-/-}$ MRL/*lpr* mice unless mice were given *Lactobacillus* spp. This would explain why their change (decrease) was opposite to that of DNT cells (increase).

A recent publication from George Tsokos' group has described an elegant mechanism of SLE pathogenesis involving MZM and DNT, where the removal of TGFβ-producing MZM leads to conversion of CD8^{+} T cells to IL-17 producing DNT cells, thus promoting SLE (56). Our observation of decreased MZM cells (found in two cell populations, CD11c^{high}MHC-II^{+} and CD11c^{low}MHC-II^{+}) and increased DNT cells in *Cx3cr1*$^{-/-}$ MRL/*lpr* mice is consistent with this mechanism. Interestingly, when probing the cell types expressing CX_3CR1 using *Cx3cr1*$^{+/gfp}$ mice, which co-express GFP with the receptor, we found that CD11c^{high}MHC-II^{+} and CD8^{+} T cells express CX_3CR1, but CD11c^{low}MHC-II^{+} cells and DNT cells do not (data not shown). It is possible that CD8^{+} T cells downregulate CX_3CR1 when losing CD8 to become DNT cells, whereas in MZM cells, the downregulation of CD11c coincides with the loss of CX_3CR1. The loss of CX_3CR1 in MZM cells may have led to decreased production of TGFβ from these cells, as the expression of CX_3CR1 has been shown to serve as a marker of TGFβ production from macrophages (69, 70). Finally, decreased TGFβ would allow the generation of pathogenic DNT cells leading to exacerbation of SLE (56). Taken together (Suppl. Fig. S6A), our observations and the current literature suggest the hypothesis that *Cx3cr1* deficiency exacerbates lupus-like disease in MRL/*lpr* mice via suppressing the production of TGFβ from MZM cells leading to gut microbial antigen-facilitated conversion of CD8^{+} T cells to IL-17 producing DNT cells, thus exacerbating SLE.

Our data further complement emerging studies demonstrating a close connection between SLE and cardiovascular complications (3, 4). Mechanistically, our findings reveal that *Cx3cr1* deletion may contribute to the expansion of Ly6C^{++} monocytes which uniquely elevate the expression of ICOS-L both *in vitro* and *in vivo*. In turn, the expanded Ly6C^{++} monocytes may facilitate the expansion of Tfh cells and the increase of autoantibody-expressing B cells. This positive feedback circuitry (Suppl. Fig. S6B) may underlie the mechanistic connection between SLE and elevated cardiovascular risks observed in patients.

In conclusion, we present here a mechanistic study detailing the roles of CX_3CR1 in controlling SLE-associated kidney and cardiovascular inflammation. Future studies will include identifying the pathobionts in the gut microbiota of *Cx3cr1*$^{-/-}$ MRL/*lpr* mice and examine the role of these pathobionts in exacerbating glomerulonephritis, elucidating how *Cx3cr1* deficiency suppresses MZM cells while promoting monocyte activation, as well as delineating the mechanisms by which Ly6C^{++} monocytes and anti-dsDNA IgG autoantibodies contribute to SLE-associated cardiovascular disease. Together, these novel mechanisms will lead to identification of new pathogenic pathways and thus therapeutic targets in the treatment of two severe manifestations, lupus nephritis and lupus-associated cardiovascular disease, that account for most of the morbidity and mortality in SLE patients.

Acknowledgements

We thank to Sarah Owens and Argonne National Laboratory for assistance on Illumina MiSeq sequencing. In addition, we thank Melissa Makris for flow cytometry analysis.

This work was supported by NIH grants AR067418 and AR073240 (Luo) and HL163948 (Li).

Conflicts of Interest

There are no competing financial interests in relation to the work described.

Availability of Data and Materials

The 16S rRNA sequences are available in the National Institutes of Health SRA database (PRJNA835508).

References

1. Tsokos GC. Systemic lupus erythematosus. The New England journal of medicine. 2011;365(22):2110-21.

2. Lech M, Anders HJ. The pathogenesis of lupus nephritis. J Am Soc Nephrol. 2013;24(9):1357-66.

3. Restivo V, Candiloro S, Daidone M, Norrito R, Cataldi M, Minutolo G, et al. Systematic review and meta-analysis of cardiovascular risk in rheumatological disease: Symptomatic and non-symptomatic events in rheumatoid arthritis and systemic lupus erythematosus. Autoimmun Rev. 2021:102925.

4. Skaggs BJ, Grossman J, Sahakian L, Perry L, FitzGerald J, Charles-Schoeman C, et al. A Panel of Biomarkers Associates With Increased Risk for Cardiovascular Events in Women With Systemic Lupus Erythematosus. ACR Open Rheumatol. 2021;3(4):209-20.

5. Tektonidou MG, Wang Z, Dasgupta A, Ward MM. Burden of Serious Infections in Adults With Systemic Lupus Erythematosus: A National Population-Based Study, 1996-2011. Arthritis Care Res (Hoboken). 2015;67(8):1078-85.

6. Imai T, Hieshima K, Haskell C, Baba M, Nagira M, Nishimura M, et al. Identification and molecular characterization of fractalkine receptor CX3CR1, which mediates both leukocyte migration and adhesion. Cell. 1997;91(4):521-30.

7. Bazan JF, Bacon KB, Hardiman G, Wang W, Soo K, Rossi D, et al. A new class of membrane-bound chemokine with a CX3C motif. Nature. 1997;385(6617):640-4.

8. Pan Y, Lloyd C, Zhou H, Dolich S, Deeds J, Gonzalo JA, et al. Neurotactin, a membrane-anchored chemokine upregulated in brain inflammation. Nature. 1997;387(6633):611-7.

9. Garcia GE, Xia Y, Chen S, Wang Y, Ye RD, Harrison JK, et al. NF-kappaB-dependent fractalkine induction in rat aortic endothelial cells stimulated by IL-1beta, TNF-alpha, and LPS. J Leukoc Biol. 2000;67(4):577-84.

10. Hirose S, Lin Q, Ohtsuji M, Nishimura H, Verbeek JS. Monocyte subsets involved in the development of systemic lupus erythematosus and rheumatoid arthritis. Int Immunol. 2019;31(11):687-96.

11. Qiu F, Li Y, Zhu Y, Li G, Lei F, Zhang S, et al. CX3CR1 might be a promising predictor of systemic lupus erythematosus patients with pulmonary fibrosis. Scand J Immunol. 2021;94(1):e13038.

12. Yajima N, Kasama T, Isozaki T, Odai T, Matsunawa M, Negishi M, et al. Elevated levels of soluble fractalkine in active systemic lupus erythematosus: potential involvement in neuropsychiatric manifestations. Arthritis Rheum. 2005;52(6):1670-5.

13. Segerer S, Hughes E, Hudkins KL, Mack M, Goodpaster T, Alpers CE. Expression of the fractalkine receptor (CX3CR1) in human kidney diseases. Kidney Int. 2002;62(2):488-95.

14. Nakatani K, Yoshimoto S, Iwano M, Asai O, Samejima K, Sakan H, et al. Fractalkine expression and CD16+ monocyte accumulation in glomerular lesions: association with their severity and diversity in lupus models. Am J Physiol Renal Physiol. 2010;299(1):F207-16.

15. Inoue A, Hasegawa H, Kohno M, Ito MR, Terada M, Imai T, et al. Antagonist of fractalkine (CX3CL1) delays the initiation and ameliorates the progression of lupus nephritis in MRL/lpr mice. Arthritis Rheum. 2005;52(5):1522-33.

16. Feng L, Chen S, Garcia GE, Xia Y, Siani MA, Botti P, et al. Prevention of crescentic glomerulonephritis by immunoneutralization of the fractalkine receptor CX3CR1 rapid communication. Kidney Int. 1999;56(2):612-20.

17. Liao X, Ren J, Reihl A, Pirapakaran T, Sreekumar B, Cecere TE, et al. Renal-infiltrating CD11c+ cells are pathogenic in murine lupus nephritis through promoting CD4+ T cell responses. Clin Exp Immunol. 2017.

18. Hochheiser K, Heuser C, Krause TA, Teteris S, Ilias A, Weisheit C, et al. Exclusive CX3CR1 dependence of kidney DCs impacts glomerulonephritis progression. J Clin Invest. 2013;123(10):4242-54.

19. Liu F, Dai S, Feng D, Qin Z, Peng X, Sakamuri S, et al. Distinct fate, dynamics and niches of renal macrophages of bone marrow or embryonic origins. Nat Commun. 2020;11(1):2280.

20. Cormican S, Griffin MD. Fractalkine (CX3CL1) and Its Receptor CX3CR1: A Promising Therapeutic Target in Chronic Kidney Disease? Front Immunol. 2021;12:664202.

21. Grone HJ, Cohen CD, Grone E, Schmidt C, Kretzler M, Schlondorff D, et al. Spatial and temporally restricted expression of chemokines and chemokine receptors in the developing human kidney. J Am Soc Nephrol. 2002;13(4):957-67.

22. Landsman L, Bar-On L, Zernecke A, Kim KW, Krauthgamer R, Shagdarsuren E, et al. CX3CR1 is required for monocyte homeostasis and atherogenesis by promoting cell survival. Blood. 2009;113(4):963-72.

23. McDermott DH, Fong AM, Yang Q, Sechler JM, Cupples LA, Merrell MN, et al. Chemokine receptor mutant CX3CR1-M280 has impaired adhesive function and

correlates with protection from cardiovascular disease in humans. J Clin Invest. 2003;111(8):1241-50.

24. Mionnet C, Buatois V, Kanda A, Milcent V, Fleury S, Lair D, et al. CX3CR1 is required for airway inflammation by promoting T helper cell survival and maintenance in inflamed lung. Nat Med. 2010;16(11):1305-12.

25. Bonacina F, Martini E, Svecla M, Nour J, Cremonesi M, Beretta G, et al. Adoptive transfer of CX3CR1 transduced-T regulatory cells improves homing to the atherosclerotic plaques and dampens atherosclerosis progression. Cardiovasc Res. 2021;117(9):2069-82.

26. Dong L, Nordlohne J, Ge S, Hertel B, Melk A, Rong S, et al. T Cell CX3CR1 Mediates Excess Atherosclerotic Inflammation in Renal Impairment. J Am Soc Nephrol. 2016;27(6):1753-64.

27. Dagkalis A, Wallace C, Hing B, Liversidge J, Crane IJ. CX3CR1-deficiency is associated with increased severity of disease in experimental autoimmune uveitis. Immunology. 2009;128(1):25-33.

28. Beli E, Dominguez JM, 2nd, Hu P, Thinschmidt JS, Caballero S, Li Calzi S, et al. CX3CR1 deficiency accelerates the development of retinopathy in a rodent model of type 1 diabetes. J Mol Med (Berl). 2016;94(11):1255-65.

29. Kawamura N, Katsuura G, Yamada-Goto N, Novianti E, Inui A, Asakawa A. Reduced brain fractalkine-CX3CR1 signaling is involved in the impaired cognition of streptozotocin-treated mice. IBRO Rep. 2020;9:233-40.

30. Mai W, Liu X, Wang J, Zheng J, Wang X, Zhou W. Protective effects of CX3CR1 on autoimmune inflammation in a chronic EAE model for MS through modulation of antigen-presenting cell-related molecular MHC-II and its regulators. Neurol Sci. 2019;40(4):779-91.

31. Ridderstad Wollberg A, Ericsson-Dahlstrand A, Jureus A, Ekerot P, Simon S, Nilsson M, et al. Pharmacological inhibition of the chemokine receptor CX3CR1 attenuates disease in a chronic-relapsing rat model for multiple sclerosis. Proc Natl Acad Sci U S A. 2014;111(14):5409-14.

32. Yadav AK, Kumar V, Jha V. Association of chemokine receptor CX3CR1 V249I and T280M polymorphisms with chronic kidney disease. Indian J Nephrol. 2016;26(4):275-9.

33. De Lema GP, Lucio-Cazaña FJ, Molina ANA, Luckow B, Schmid H, de Wit C, et al. Retinoic acid treatment protects MRL/lpr lupus mice from the development of glomerular disease. Kidney Int. 2004;66(3):1018-28.

34. Zhang H, Liao X, Sparks JB, Luo XM, Schloss PD. Dynamics of Gut Microbiota in Autoimmune Lupus. Applied and environmental microbiology. 2014;80(24):7551-60.

35. Mu Q, Zhang H, Liao X, Lin K, Liu H, Edwards MR, et al. Control of lupus nephritis by changes of gut microbiota. Microbiome. 2017;5(1):73.

36. Mu Q, Edwards MR, Swartwout BK, Cabana Puig X, Mao J, Zhu J, et al. Gut Microbiota and Bacterial DNA Suppress Autoimmunity by Stimulating Regulatory B Cells in a Murine Model of Lupus. Front Immunol. 2020;11:593353.

37. Mu Q, Cabana-Puig X, Mao J, Swartwout B, Abdelhamid L, Cecere TE, et al. Pregnancy and lactation interfere with the response of autoimmunity to modulation of gut microbiota. Microbiome. 2019;7(1):105.

38. Mu Q, Swartwout BK, Edwards M, Zhu J, Lee G, Eden K, et al. Regulation of neonatal IgA production by the maternal microbiota. Proceedings of the National Academy of Sciences. 2021;118(9).

39. Bolger AM, Lohse M, Usadel B. Trimmomatic: a flexible trimmer for Illumina sequence data. Bioinformatics. 2014;30(15):2114-20.

40. Callahan BJ, McMurdie PJ, Rosen MJ, Han AW, Johnson AJ, Holmes SP. DADA2: High-resolution sample inference from Illumina amplicon data. Nat Methods. 2016;13(7):581-3.

41. McMurdie PJ, Holmes S. phyloseq: an R package for reproducible interactive analysis and graphics of microbiome census data. PLoS One. 2013;8(4):e61217.

42. Martin BD, Witten D, Willis AD. MODELING MICROBIAL ABUNDANCES AND DYSBIOSIS WITH BETA-BINOMIAL REGRESSION. Ann Appl Stat. 2020;14(1):94-115.

43. Oksanen J, Blanchet, F.G., Kindt, R., Legendre, P., Minchin, P.R., O'Hara, R.B., Simpson, G.L., Solymos, P., Stevens, M.H.H., Wagner, H. Vegan: Community Ecology Package. R Package Version 2.2-0. http://CRAN.Rproject.org/package=vegan. 2014.

44. Geng S, Zhang Y, Yi Z, Lu R, Li L. Resolving monocytes generated through TRAM deletion attenuate atherosclerosis. JCI Insight. 2021;6(20).

45. Geng S, Chen K, Yuan R, Peng L, Maitra U, Diao N, et al. The persistence of low-grade inflammatory monocytes contributes to aggravated atherosclerosis. Nat Commun. 2016;7:13436.

46. Liao X, Ren J, Wei CH, Ross AC, Cecere TE, Jortner BS, et al. Paradoxical Effects of All-Trans-Retinoic Acid on Lupus-Like Disease in the MRL/lpr Mouse Model. PLoS One. 2015;10(3):e0118176.

47. Reilly CM, Olgun S, Goodwin D, Gogal RM, Jr., Santo A, Romesburg JW, et al. Interferon regulatory factor-1 gene deletion decreases glomerulonephritis in MRL/lpr mice. Eur J Immunol. 2006;36(5):1296-308.

48. Cabana-Puig X, Bond JM, Wang Z, Dai R, Lu R, Lin A, et al. Phenotypic Drift in Lupus-Prone MRL/lpr Mice: Potential Roles of MicroRNAs and Gut Microbiota. Immunohorizons. 2022;6(1):36-46.

49. Schneider KM, Bieghs V, Heymann F, Hu W, Dreymueller D, Liao L, et al. CX3CR1 is a gatekeeper for intestinal barrier integrity in mice: Limiting steatohepatitis by maintaining intestinal homeostasis. Hepatology. 2015;62(5):1405-16.

50. Medina-Contreras O, Geem D, Laur O, Williams IR, Lira SA, Nusrat A, et al. CX3CR1 regulates intestinal macrophage homeostasis, bacterial translocation, and colitogenic Th17 responses in mice. J Clin Invest. 2011;121(12):4787-95.

51. McGaha TL, Chen Y, Ravishankar B, van Rooijen N, Karlsson MC. Marginal zone macrophages suppress innate and adaptive immunity to apoptotic cells in the spleen. Blood. 2011;117(20):5403-12.

52. Geng S, Zhang Y, Lee C, Li L. Novel reprogramming of neutrophils modulates inflammation resolution during atherosclerosis. Sci Adv. 2019;5(2):eaav2309.

53. Pradhan K, Yi Z, Geng S, Li L. Development of Exhausted Memory Monocytes and Underlying Mechanisms. Front Immunol. 2021;12:778830.

54. Aicher A, Hayden-Ledbetter M, Brady WA, Pezzutto A, Richter G, Magaletti D, et al. Characterization of human inducible costimulator ligand expression and function. J Immunol. 2000;164(9):4689-96.

55. Wikenheiser DJ, Stumhofer JS. ICOS Co-Stimulation: Friend or Foe? Front Immunol. 2016;7:304.

56. Li H, Adamopoulos IE, Moulton VR, Stillman IE, Herbert Z, Moon JJ, et al. Systemic lupus erythematosus favors the generation of IL-17 producing double negative T cells. Nat Commun. 2020;11(1):2859.

57. Rodriguez-Rodriguez N, Flores-Mendoza G, Apostolidis SA, Rosetti F, Tsokos GC, Crispin JC. TCR-alpha/beta CD4(-) CD8(-) double negative T cells arise from CD8(+) T cells. J Leukoc Biol. 2020;108(3):851-7.

58. Li H, Tsokos GC. Double-negative T cells in autoimmune diseases. Curr Opin Rheumatol. 2021;33(2):163-72.

59. Chen PM, Tsokos GC. The role of CD8+ T-cell systemic lupus erythematosus pathogenesis: an update. Curr Opin Rheumatol. 2021;33(6):586-91.

60. Shivakumar S, Tsokos GC, Datta SK. T cell receptor alpha/beta expressing double-negative (CD4-/CD8-) and CD4+ T helper cells in humans augment the production of pathogenic anti-DNA autoantibodies associated with lupus nephritis. J Immunol. 1989;143(1):103-12.

61. Crispin JC, Oukka M, Bayliss G, Cohen RA, Van Beek CA, Stillman IE, et al. Expanded double negative T cells in patients with systemic lupus erythematosus produce IL-17 and infiltrate the kidneys. J Immunol. 2008;181(12):8761-6.

62. Mizui M, Koga T, Lieberman LA, Beltran J, Yoshida N, Johnson MC, et al. IL-2 protects lupus-prone mice from multiple end-organ damage by limiting CD4-CD8- IL-17-producing T cells. J Immunol. 2014;193(5):2168-77.

63. Cabeza-Cabrerizo M, Cardoso A, Minutti CM, Pereira da Costa M, Reis e Sousa C. Dendritic Cells Revisited. Annu Rev Immunol. 2021;39:131-66.

64. Gottschalk C, Kurts C. The Debate about Dendritic Cells and Macrophages in the Kidney. Front Immunol. 2015;6:435.

65. Arnold IC, Mathisen S, Schulthess J, Danne C, Hegazy AN, Powrie F. CD11c(+) monocyte/macrophages promote chronic Helicobacter hepaticus-induced intestinal inflammation through the production of IL-23. Mucosal Immunol. 2016;9(2):352-63.

66. Lu L, Kuroishi T, Tanaka Y, Furukawa M, Nochi T, Sugawara S. Differential expression of CD11c defines two types of tissue-resident macrophages with different origins in steady-state salivary glands. Sci Rep. 2022;12(1):931.

67. Cao Q, Wang Y, Wang XM, Lu J, Lee VW, Ye Q, et al. Renal F4/80+ CD11c+ mononuclear phagocytes display phenotypic and functional characteristics of macrophages in health and in adriamycin nephropathy. J Am Soc Nephrol. 2015;26(2):349-63.

68. Borges da Silva H, Fonseca R, Pereira RM, Cassado Ados A, Alvarez JM, D'Imperio Lima MR. Splenic Macrophage Subsets and Their Function during Blood-Borne Infections. Front Immunol. 2015;6:480.

69. Helmke A, Nordlohne J, Balzer MS, Dong L, Rong S, Hiss M, et al. CX3CL1-CX3CR1 interaction mediates macrophage-mesothelial cross talk and promotes peritoneal fibrosis. Kidney Int. 2019;95(6):1405-17.

70. Kassianos AJ, Wang X, Sampangi S, Afrin S, Wilkinson R, Healy H. Fractalkine-CX3CR1-dependent recruitment and retention of human CD1c+ myeloid dendritic cells by in vitro-activated proximal tubular epithelial cells. Kidney Int. 2015;87(6):1153-63.

Figures

Figure 1

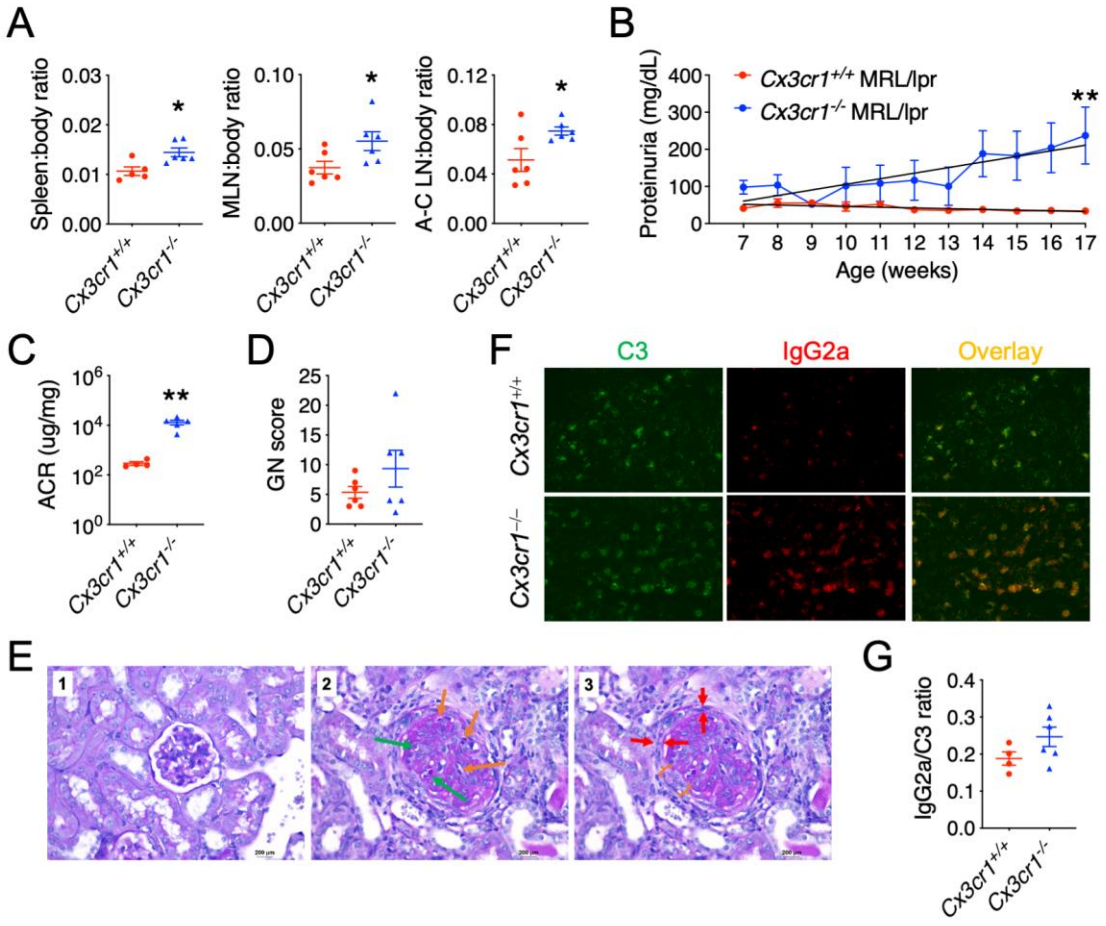

Figure 1. *Cx3cr1* deficiency exacerbates lymphoproliferation and glomerulonephritis in female MRL/*lpr* mice. (**A**) Lymphoid tissue-to-body weight ratios at 17 weeks of age. MLN, mesenteric lymph node; A-C LN, axillary-cervical lymph nodes. *p<0.05. (**B**) Level of proteinuria over time. n=6, **p<0.01. (**C**) Urinary albumin-to-creatinine ratio at late disease. (**D**) Histopathological scores at late disease stage. GN, glomerulonephritis. Note that three *Cx3cr1*$^{-/-}$ MRL/*lpr* mice had noticeably higher GN scores. (**E**) Representative images showing a normal glomerulus (1) *vs*. an abnormal glomerulus (2,3), the latter from a *Cx3cr1*$^{-/-}$ MRL/*lpr* mouse. 2: Glomerular

necrosis. Green arrows indicate cytoplasmic fragmentation; Orange arrows indicate nuclear pyknosis and karyorrhexis. 3: Glomerular sclerosis and crescent formation. Sclerosis is indicated by red arrows and surrounds the entire glomerulus; Crescent formation is indicated by the orange brackets and is segmental. (**F**) Representative images showing exacerbated renal deposition of pathogenic IgG2a. (**G**) Intensity ratio of IgG2a to complement C3 as determined with ImageJ. Note that three *Cx3cr1*$^{-/-}$ MRL/*lpr* mice had noticeably higher ratios leading to an overall trending increase with *Cx3cr1* deficiency (p=0.14).

Figure 2

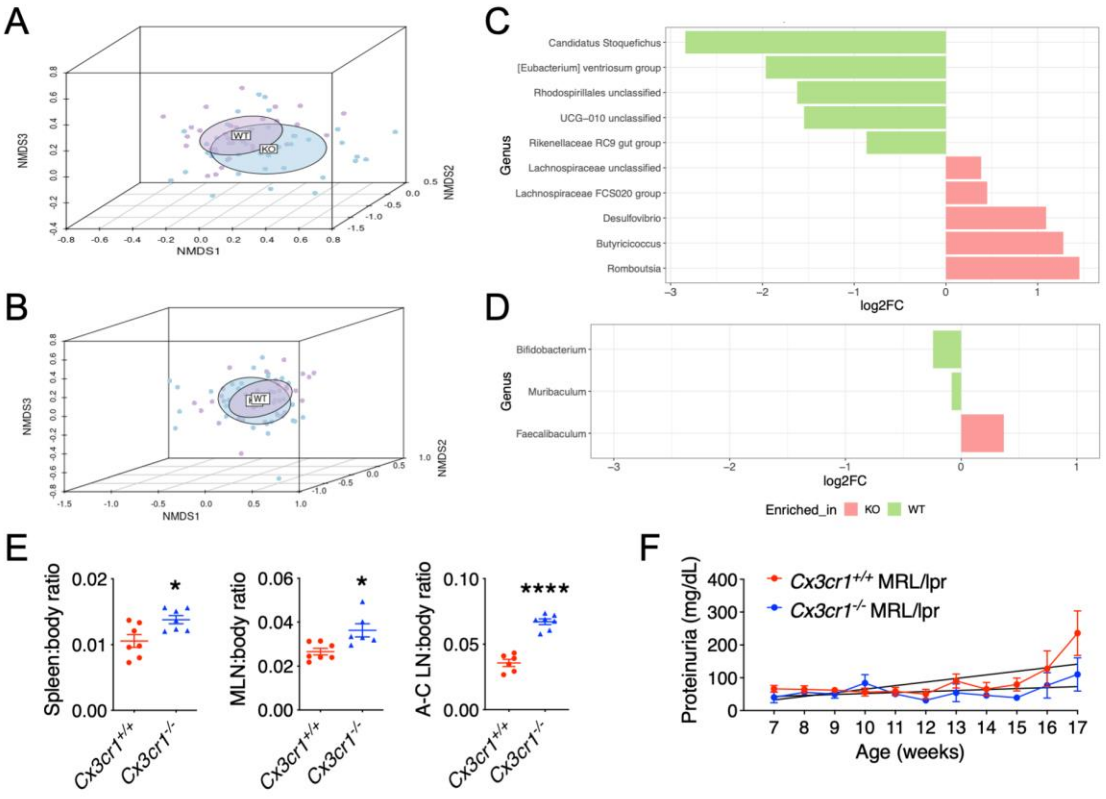

Figure 2. Exacerbation of glomerulonephritis with *Cx3cr1* deficiency is gut microbiota-dependent, but exacerbation of lymphoproliferation is not. (**A**-**B**) Non-metric multidimensional scaling (NMDS) ordination of gut microbiota communities in female *Cx3cr1*$^{+/+}$ (WT) and *Cx3cr1*$^{-/-}$ (KO) MRL/*lpr* littermates treated with either PBS (**A**) or *Lactobacillus* spp. (**B**). Data from fecal samples collected every 2 weeks from weaning till 15 weeks of age are shown (n=5/group/time point). For the PBS groups the differences were statistically significant (Adonis test, $p<0.001$). (**C**-**D**) Differentially abundant taxa at the genus level between WT and KO MRL/*lpr* mice upon PBS (**C**) or *Lactobacillus* treatment (**D**). (**E**) Lymphoid tissue-to-body weight ratios at 17 weeks of age following *Lactobacillus* treatment. MLN, mesenteric lymph node; A-C LN, axillary-cervical lymph nodes. *$p<0.05$; ****$p<0.0001$. (**B**) Level of proteinuria over time

(n=6/group) following *Lactobacillus* treatment. The difference was not statistically significant.

Figure 3

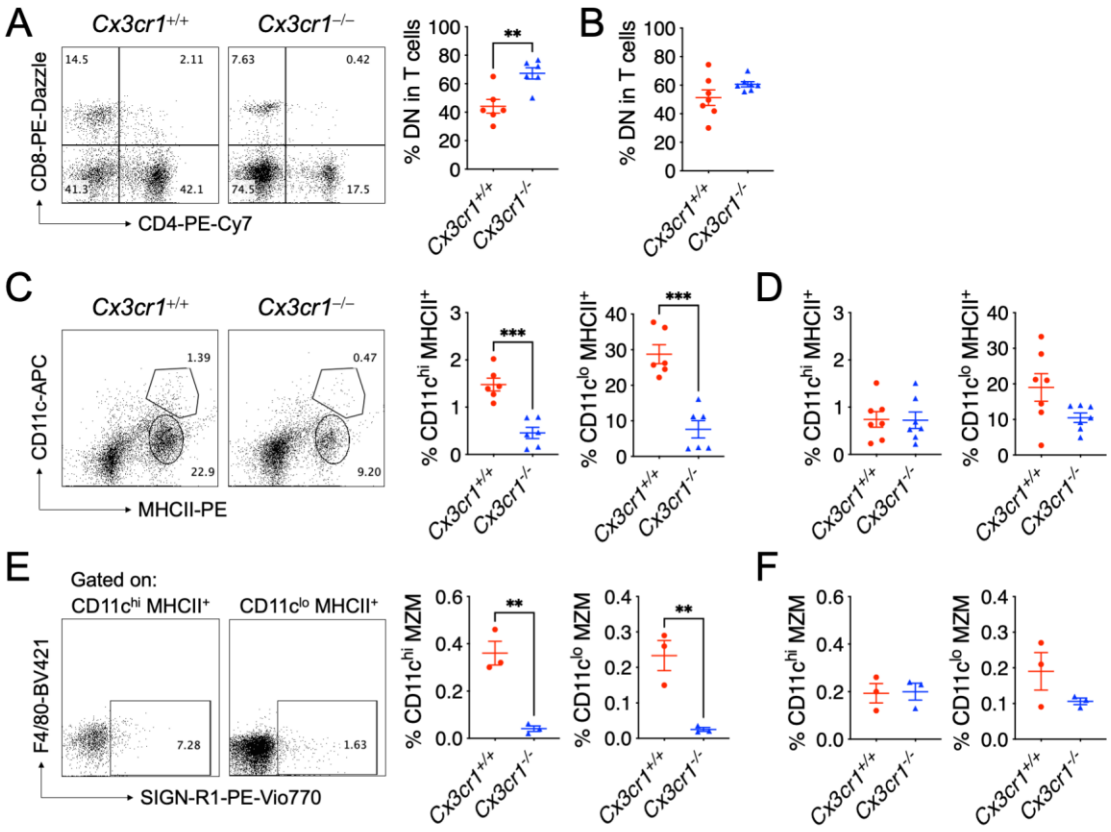

Figure 3. Significant differences in several splenic populations between *Cx3cr1*$^{+/+}$ and *Cx3cr1*$^{-/-}$ MRL/*lpr* mice are equalized by Lactobacillus treatment. (**A**) Analysis of DNT cells without *Lactobacillus.* Left: representative FACS plots. Right: frequency of DNT cells in total T cells. ***p*<0.01. (**B**) Analysis of DNT cells with *Lactobacillus*. (**C**) Analysis of MHC-II^{+} cells without *Lactobacillus*. Left: representative FACS plots. Right: frequencies of CD11c^{high}MHCII^{+} and CD11c^{low}MHCII^{+} cells in total splenocytes. ****p*<0.001. (**D**) Analysis of MHC-II^{+} cells with *Lactobacillus*. (**E**) Analysis of MZM cells without *Lactobacillus*. Left: gating strategy to identify SIGN-R1^{+} MZM cells. Right, frequencies of CD11c^{high} & CD11c^{low} MZM cells in total splenocytes. ***p*<0.01. (**F**) Analysis of MZM cells with *Lactobacillus*.

Figure 4

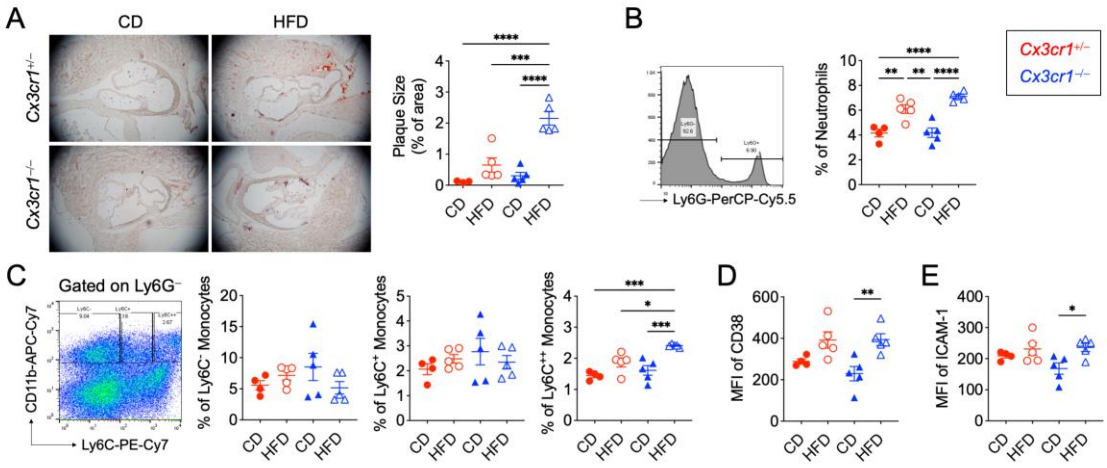

Figure 4. A high-fat diet exacerbates cardiovascular inflammation in *Cx3cr1*$^{-/-}$ MRL/*lpr* mice. *Cx3cr1*$^{+/-}$ and *Cx3cr1*$^{-/-}$ MRL/*lpr* mice were fed either a 42% fat high-fat diet (HFD) or its control diet (CD; 6% fat) starting 4 weeks of age. Mice were euthanized at 15 weeks of age for analyses. (**A**) Measurement of vasculitis. Left, representative Oil Red O (ORO) images. Right, quantification of plaque size. ***p<0.001, ****p<0.0001. (**B**) Frequency of splenic neutrophils. Left, representative histogram. **p<0.01, ****p<0.0001. (**C**) Frequencies of splenic monocytes. From left to right, representative FACS plot and frequencies of Ly6C^{-}, Ly6C^{+}, and Ly6C^{++} monocytes. *p<0.05, ***p<0.001. (**D**) Mean fluorescence intensity (MFI) of CD38 on total monocytes. **p<0.01. (**E**) MFI of ICAM-1 on total monocytes. *p<0.05. One-way ANOVA was performed for all statistical analyses.

Figure 5

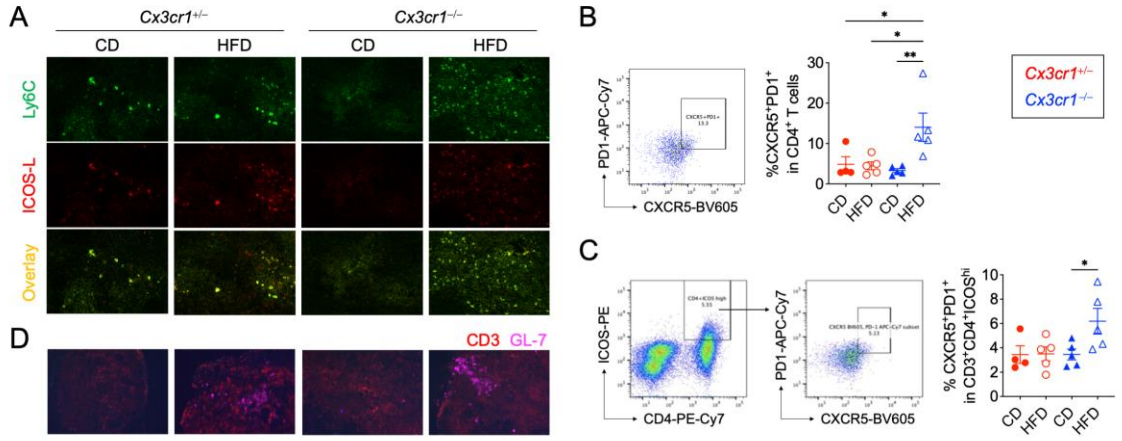

Figure 5. ICOS-L expressing Ly6C$^+$ monocytes promote germinal center reaction in *Cx3cr1*$^{-/-}$ MRL/*lpr* mice fed a high-fat diet. (**A**) Immunohistochemical analysis showing co-expression of Ly6C and ICOS-L. (**B**) Frequency of splenic CXCR5$^+$PD1$^+$ cells in CD4$^+$ T cells. Left, representative FACS plot pre-gated on CD4$^+$ T cells. *p<0.05, **p<0.01. (**C**) Frequency of splenic CXCR5$^+$PD1$^+$ cells in ICOS^{high} CD4$^+$ T cells. Left, representative FACS plot pre-gated on T cells. Middle, FACS plot within the CD4$^+$ICOS^{high} T cell gate. *p<0.05. One-way ANOVA was performed for all statistical analyses. (**D**) Immunohistochemical analysis showing GL7$^+$ germinal centers in relationship to CD3$^+$ T cells.

Figure 6

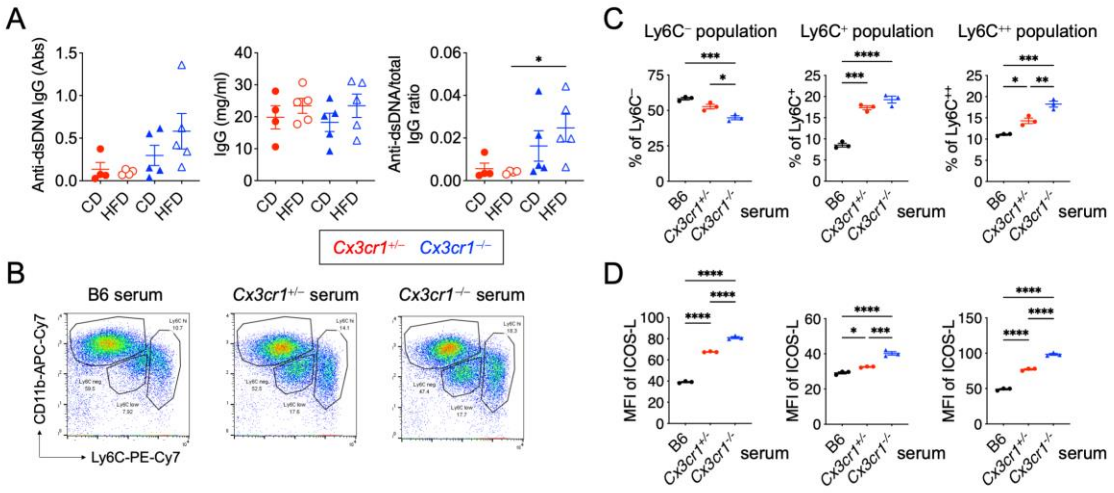

Figure 6. The high-fat diet induces anti-dsDNA IgG in *Cx3cr1*$^{-/-}$ MRL/*lpr* mice that in turn promotes monocyte expression of ICOS-L. (**A**) Levels of anti-dsDNA IgA, total IgG, and ratio of anti-dsDNA/total IgG. **p*<0.05. (**B**-**D**) Total bone marrow cells from B6 mice were incubated with the serum from B6, *Cx3cr1*$^{+/-}$ MRL/*lpr*, or *Cx3cr1*$^{-/-}$ MRL/*lpr* mice for 5 days in the presence of M-CSF. (**B**) Representative FACS plot showing gating strategy for Ly6C^{-}, Ly6C^{+} and Ly6C^{++} populations. (**C**) Frequencies of the 3 monocyte populations. **p*<0.05, ***p*<0.01, ****p*<0.001, *****p*<0.0001. (**D**) MFI of ICOS-L expression for the 3 monocyte populations. **p*<0.05, ****p*<0.001, *****p*<0.0001. One-way ANOVA was performed for all statistical analyses.

Supplemental Methods

Luminex assay To simultaneously quantify serum levels of BAFF, IFNγ, IL-17A, IL-6, TNFα, and IL-10 cytokines, the beadbased flow cytometric technique FLEXMAP 3D® was used (Luminex Corporation, Austin, TX). Cytokine profiles were characterized using a personalized ProcartaPlex Mouse Cytokine Panel (Life Technologies). According to the manufacturer's instructions, all washing steps were carried out using a magnetic plate carrier. Beads were added to the plate then washed, and liquid was removed by quickly inverting the plate over a sink. Samples and standards were added to the plate, sealed, and placed on an orbital shaker for 2 hours at room temperature. After washing, the biotinylated detection antibody mix was added, sealed, and shook at 600 rpm for 30 minutes at room temperature. The plate was washed again and Streptavidin-PE was added, sealed, and shook at 600 rpm for 30 minutes at room. After that, the plate was washed again, beads were resuspended with reading buffer and the plate was read by the FLEXMAP 3D® instrument. The concentration of the samples was calculated by extrapolating the concentration of the standards against their relative fluorescence intensity.

Supplemental Figures

Supplemental Figure S1

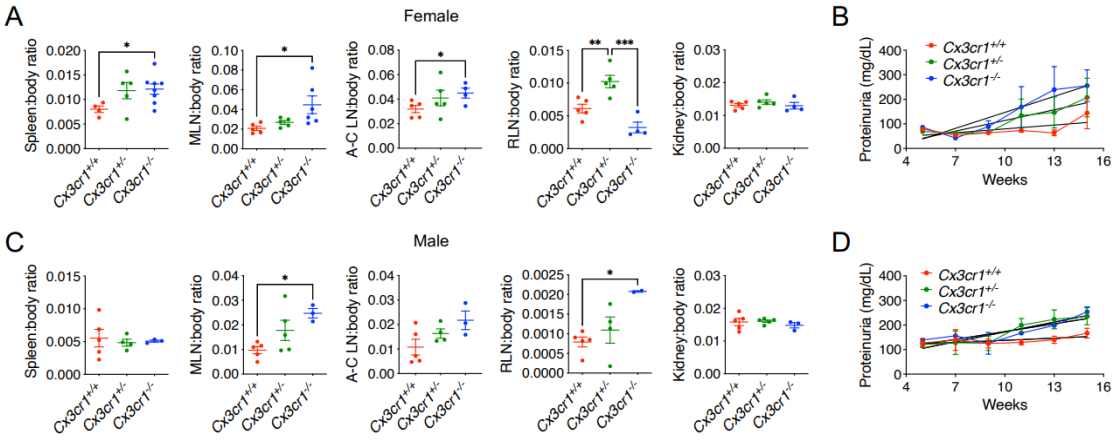

Figure S1. Disease phenotype of *Cx3cr1*$^{+/+}$, *Cx3cr1*$^{+/-}$, *Cx3cr1*$^{-/-}$ MRL/*lpr* female (**A-B**) and male (**C-D**) littermates. MLN, mesenteric lymph nodes; A-C LN, axillary-cervical lymph nodes; RLN, renal lymph nodes.

Supplemental Figure S2

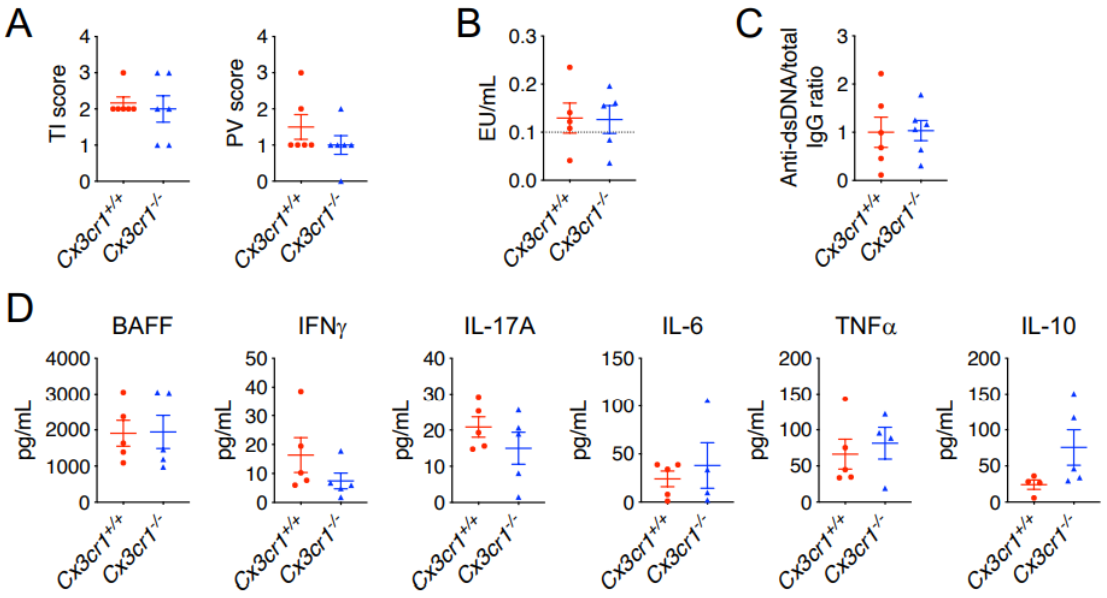

Figure S2. (**A**) Kidney histopathology scores. TI, tubulointerstitial nephritis; PV, perivascular infiltration. (**B**) Serum endotoxin levels. (**C**) Anti-dsDNA IgG to total IgG ratio. (**D**) Serum cytokine levels as determined by the Luminex assay.

Supplemental Figure S3

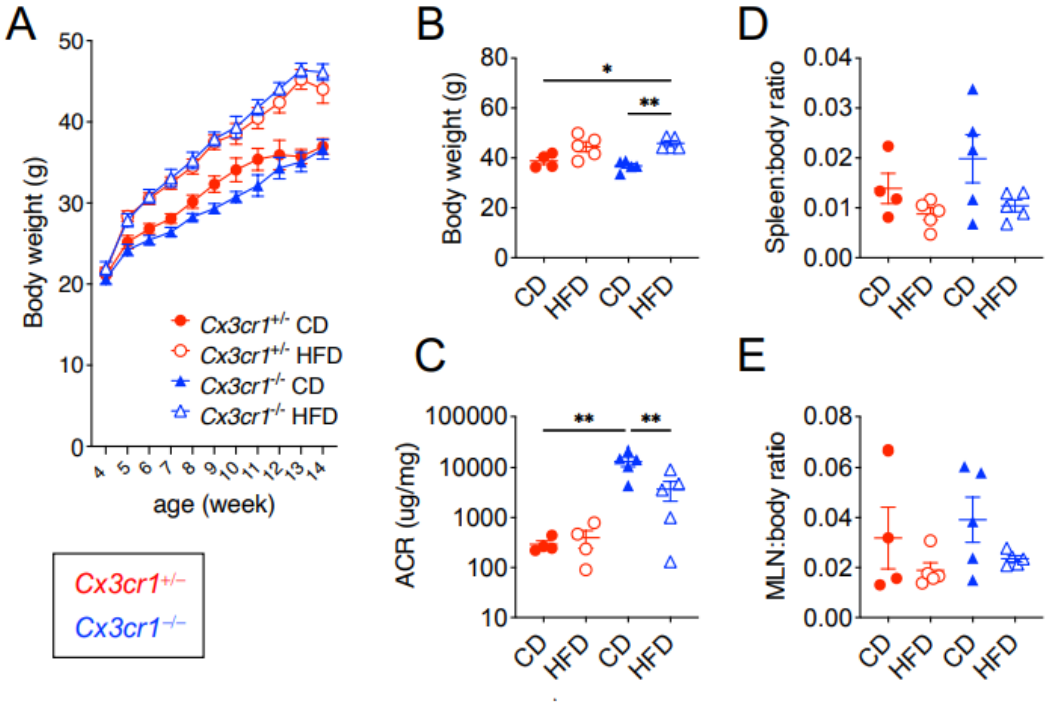

Figure S3. (**A**) Body weight over time. (**B**) Body weight at euthanasia. (C) Urinary albumin-to-creatinine ratio. (**D**) Spleen-to-body weight ratio. (**E**) MLN-to-body weight ratio.

Supplemental Figure S4

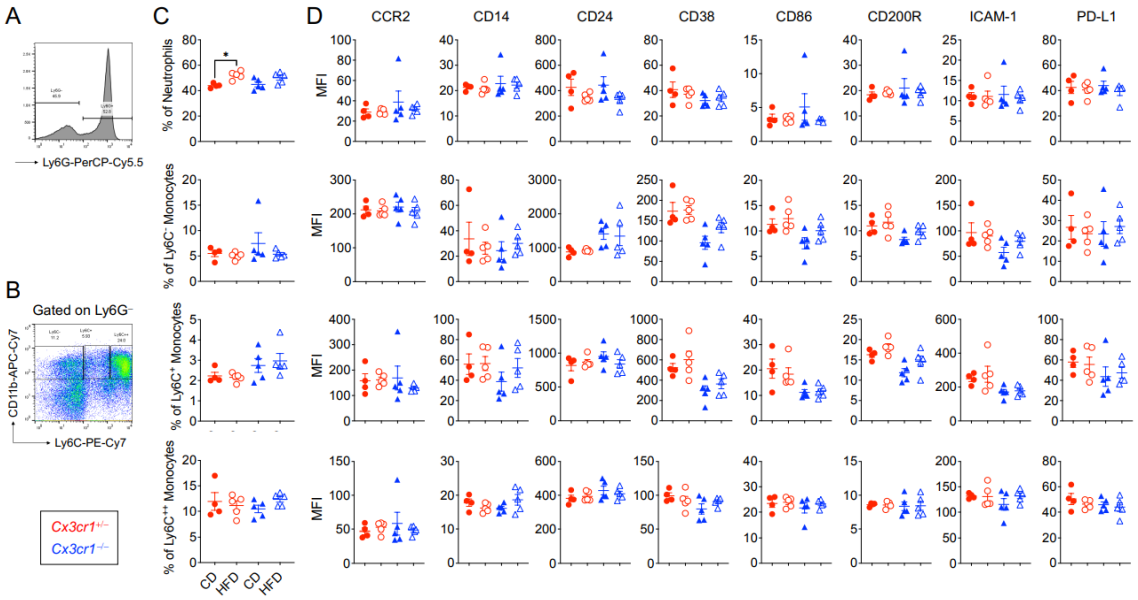

Figure S4. FACS analysis of bone marrow cells. (**A**) Representative gating of neutrophils. (**B**) Gating strategy of $Ly6C^{++}$, $Ly6C^{+}$ and $Ly6C^{-}$ monocytes. (**C**) Percentages of neutrophils and monocyte subsets in total bone marrow cells. (**D**) Mean fluorescence intensity (MFI) of the indicated markers on neutrophils and monocyte subsets.

Supplemental Figure S5

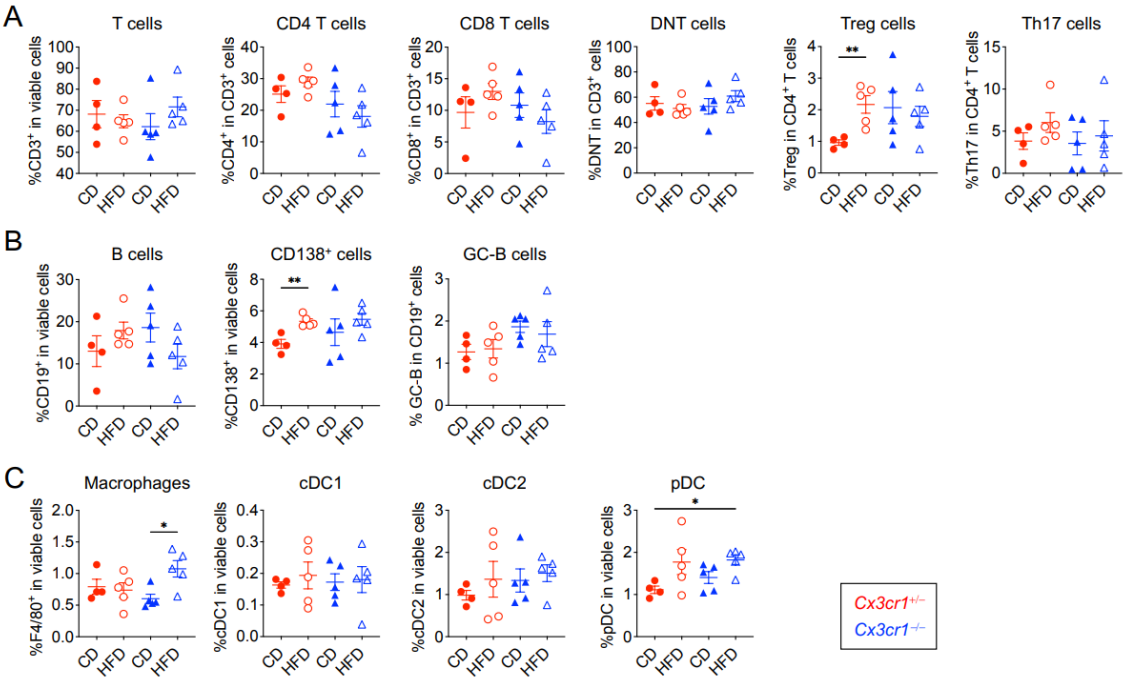

Figure S5. FACS analysis of splenocytes. (**A**) T cell subsets. (**B**) B cell subsets. (**C**) Myeloid cells.

Supplemental Figure 6

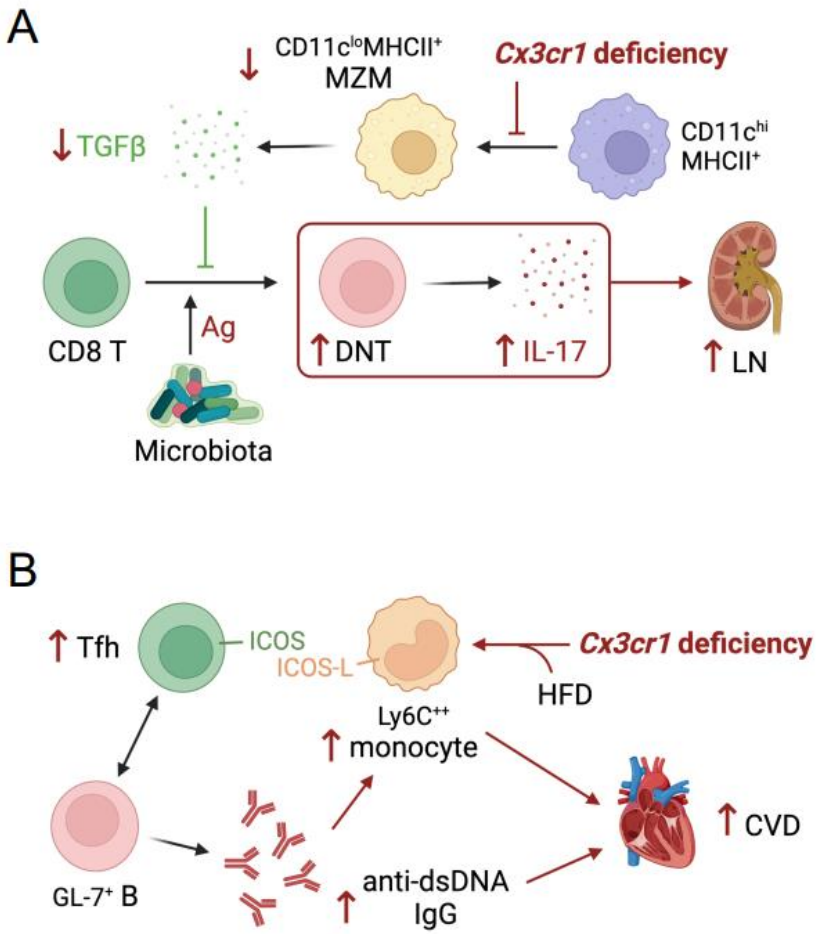

Figure S6. Working models for the pathogenesis of lupus nephritis (LN; panel **A**) and lupus-associated cardiovascular disease (CVD; panel **B**) in *Cx3cr1*$^{-/-}$ MRL/lpr mice. MZM, marginal zone macrophages; DNT, double-negative T cells; Ag, antigen; HFD, high-fat diet.

CHAPTER 5

Discussion and Future Directions

Many autoimmune diseases have been associated with a disrupted gut microbiota. It is important to understand how microbial dysbiosis occurs, and whether it is from early on or during disease progression. Environmental factors can incline the commensal bacteria into opportunistic pathogens; in contrast, a right proportion of beneficial commensal bacteria can help to ameliorate the course of autoimmune disease. Importantly, the gut microbiota has a big impact on educating our immune system. Not only the presence of gut bacteria, but also their metabolism, can trigger an immune cascade. Understanding how the gut microbiota acts on our immune system can answer many of our questions regarding autoimmune disease. Moreover, certain bacteria and their metabolites may improve the outcome of autoimmune disease and/or ameliorate the secondary effects of the current treatments. The aim of this dissertation is to suggest new approaches and provide some mechanistic insight into a promising field that is also growing.

In chapter 1, we went in depth of what we know so far about the gut microbiota and its metabolism. Gut microbiota has a broad spectrum of bioactive compounds that have the capacity to modulate the host molecular pathways. In addition, little is known about how commensal bacteria modulate host metabolism in a healthy state and even less in autoimmune disease. Short-chain fatty acids (SCFAs), tryptophan metabolites, lipids and polyamines can have significant effects on our body, such as anti-inflammatory properties. Their benefits, especially when there is an impaired intestinal epithelium or a disrupted microbiota, restore the imbalance and bring hope to the field. These metabolites

by themselves or in conjunction with current treatments could help ameliorate symptoms in autoimmune diseases. Our current limitations are that most of the mechanistic pathways remain unclear, and the lack of understanding of how metabolites from both sides, namely the host and the gut microbiota, interact to exert beneficial results. In that sense, it important to not only study what metabolites are being produced under certain conditions, but also study how the host interacts with theses metabolites and reacts to them. The next few chapters would try to expand our limited knowledge on the interactions of environment, gut microbiota, and host immune system in the context of the autoimmune disease systemic lupus erythematosus (SLE).

In chapter 2, we first studied the environmental conditions for our animal model MRL/*lpr*. MRL/*lpr* mice have been extensively used as a lupus mouse model. These mice have multiple SLE susceptibility loci enabling them to spontaneously develop autoimmune disease resembling that of SLE patients. When comparing MRL/*lpr* mice from a vendor to those housed in our facility for years, we observed the same phenotypic drift (attenuation of glomerulonephritis) for both colonies that suggests a significant change in environmental factors at both facilities. We found differential expression of microRNAs in the spleen that may be associated with phenotypic changes as well as fluctuations of the gut microbiota composition. This study was important to confirm that our animal model was still suitable for our following projects. However, it would be beneficial to characterize, in future investigations, specific SLE-associated microRNAs for their mechanisms in gene regulation that could explain some of the phenotypic changes. In addition, our understanding of how the environment impacts lupus is still limited, and characterization of more lupus mouse models would be required to establish

commonalities among the models for better translation to the human disease. Moreover, even though we did not see big differences between facilities with regard to the gut microbiota at the end of the experiment, a complete mapping of the gut microbiome and its metabolome may be able to help us understand how MRL/*lpr* mice at both facilities developed the same phenotypic loss (attenuated glomerulonephritis). Additionally, it would have been interesting to compare genomes from JAX 2015 to JAX 2018, and decipher if a genetic drift had occurred at their facility. We need to take into consideration the possibility that we accidentally introduced JAX mice into our mouse colony and through generations of breeding, the potential genetic drift was picked up by our In-house mice, ending with the same genome as JAX 2018. One potential experiment to resolve this is to cross foster the offspring of both facilities to an MRL/*lpr* strain that has not lost the phenotype. If the loss of phenotype was due to a big environmental event, changing the breeders should bring back the aggravated renal disease. This experiment, together with the characterization of commensal bacteria and their metabolites, will help us understand how microbial changes drive disease progression.

In chapter 3, we investigated, following previously published results (Mu et al., 2027), how the use of 5 different strains of probiotics (*Lactobacillus* species (spp.), *L. reuteri, L. oris, L. johnsonii, L. gasseri* and *L. rhamnosus*) could reverse the leaky gut present in lupus mice and SLE patients to attenuate lupus symptoms, including splenomegaly and lymphadenopathy. Since we already knew that gut microbiota was a cause of disease, we proceeded to investigating whether individual probiotic would work, or a cooperation among different probiotics are necessary. Our results showed that the probiotic strains individually could not recapitulate the same result; instead, they acted in

synergy. Interestingly, MRS broth media and the *Lactobacillus* spp. culture supernatant, containing secreted metabolites, exerted similar effects as mixed Lactobacilli in attenuating splenomegaly and lymphadenopathy. These three treatments (mixed bacteria, MRS broth, and culture supernatant) most likely helped the proliferation of commensal bacteria that are yet to be discovered as immune regulatory. Some of these bacteria may be SCFA producers, which not only inhibit pathogenic bacteria but also help reverse the leaky gut and correct imbalanced microbiota. Additionally, when comparing gut microbiota changes among groups, we observed that *Lactobacillales* were significantly higher following the mixed bacteria treatment, and that this change preceded the change of disease, suggesting that the increase of *Lactobacilliales* is the reason for disease attenuation. We also characterized the CX_3CR1 pathway that when the gene is missing, we did not observe the same beneficial results seen with the MRS broth. It is likely that the CX_3CR1 receptor is important for antigen presentation in the proximal lymph nodes that triggers a regulatory immune response. Moreover, upon characterization of the cell populations in the spleen and mesenteric lymph nodes, we noticed an increase in type 1 regulatory T (Tr1) cells, which are IL-10 producers promoting an anti-inflammatory environment, and an increase of T effector memory (T_{EM}) cells as well as a decrease of T central memory (T_{CM}) cells, the latter of which is known to promote a persistent inflammatory state. Furthermore, double-negative T (DNT) cells, characteristic in SLE, were suppressed by the *Lactobacillus* treatment, leading to less inflammatory cytokines produced by DNT cells, thus slowing the progression of SLE. Although we observed encouraging results, one must be careful extrapolating these results. First of all, these studies were only done in MRL/*lpr* mice. Secondly, even though we uncovered the

phenotypic loss in chapter 2 and corroborated on why we could not replicate the results regarding kidney disease (lupus nephritis), additional steps need to be considered. Thirdly, *Lactobacillus* spp. were beneficial together, but the mechanism has not been explored yet. To elucidate how this synergistic action works, I would like to propose the following experiments: 1) Study the culture supernatant to identify the metabolites responsible, then determine the effect of these metabolites, singly or in combination, on gut barrier functions and disease attenuation; 2) Analyze and identify translocated bacteria in distal organs due to the leaky gut; and 3) Consider the formation of biofilms that act like a protective layer for intestinal epithelial cells, and visualize the interaction and localization of *Lactobacillus* spp. with fluorescence *in situ* hybridization (FISH). With these experiments we hope to better understand which metabolites are modulators of the immune system and/or the gut microbiota itself, what mechanistic pathways are involved, and how one may target them to restore the imbalanced immune response.

In chapter 4, we generated and characterized a *Cx3cr1*-deficient MRL/*lpr* lupus-prone mouse which exhibits an exacerbated glomerulonephritis compared to its wildtype counterpart, as well as an increase of atherosclerotic inflammation following a high fat diet. Lupus nephritis and lupus-associated cardiovascular disease are two main causes of morbidity and mortality in SLE patients. We found that the treatment with the 5 different strains of Lactobacilli abrogated the lupus nephritis induced by *Cx3cr1* deficiency. We hypothesize that the lack of tolerogenic antigen presentation caused by *Cx3cr1* deficiency exacerbated lupus progression. The lack of the receptor may allow certain stimulatory antigens to activate DNT cells, which in turn trigger B cells to produce autoantibodies that subsequently infiltrate the kidneys and exacerbate lupus nephritis. Once we balanced

the gut microbiota with the *Lactobacillus* strains, the frequency of DNT cells decreased. Interestingly, we observed significant losses of $CD11c^{high}MHC\text{-}II^{+}$ and $CD11c^{low}MHC\text{-}II^{+}$ marginal zone macrophages (MZMs) in *Cx3cr1*$^{-/-}$ MRL/*lpr* that were recovered by *Lactobacillus* treatment. MZMs are known to be able to induce tolerance and are involved in inhibiting the generation of DNT cells through producing TGFβ. The removal of TGFβ-producing MZM leads to the conversion of $CD8^{+}$ T cells to IL-17-producing DNT cells, thereby exacerbating SLE. The *Cx3cr1* deletion is also correlated with cardiovascular complications. We hypothesize that the gene deletion coupled with a high-fat diet promote $Ly6C^{high}$ monocytes, which expand T follicular helper (Tfh) cells that in turn induce more autoantibody-producing B cells. The autoantibodies, forming immune complexes with autoantigens, are deposited in the heart, thereby promoting SLE-associated cardiovascular disease. Therefore, feeding *Cx3cr1*$^{-/-}$ MRL/*lpr* mice with a high-fat diet, we observed a significantly larger atherosclerotic plaque size, significantly more activated $Ly6C^{high}$ monocytes displaying ICOS-L, which subsequently promote the germinal center reaction to increase circulatory autoantibodies, thus aggravating cardiovascular disease. As little is known on the relationship between SLE-associated cardiovascular disease and the CX_3CR1 signaling pathway, this study can help us understand one of the mechanisms by which aggravated heart disease develops in some SLE patients. In addition, crosstalk between the gut microbiota and distal organs such as the kidney is not well understood, and we are proposing a pathway that splenic MZM cells can help to make this connection. Furthermore, it is likely that gut-resident *Cx3cr1*$^{-/-}$ cells are educated by the gut microbiota and can travel to distal organs such as the heart and kidneys to trigger an inflammatory response leading to exacerbation of both diseases.

Additionally, it is interesting that a high-fat diet is required for the promotion of the germinal center reaction through the action of proinflammatory Ly6C^{high}, ICOS-L-expressing monocytes. Following upon these data, I propose to establish the importance of $CX_3CR1^{+/+}$ antigen presenting cells by adoptively transferring them from wild-type MRL/*lpr* into *Cx3cr1*-deficient MRL/*lpr* mice. We would expect an improvement of both diseases, and that CX_3CR1-expressing antigen presenting cells can balance the proinflammatory response triggered by the absence of the CX_3CR1 receptor. I also propose to study the changes of the gut microbiota upon administration of a high-fiber-diet, as gut microbiota through secreting certain metabolites could be the bridge between the expansion of Ly6C^{high} monocytes and exacerbated cardiovascular disease.

In summary, the goal of this dissertation is to better understand and characterize how probiotics, in particular *Lactobacillus* spp., offer their beneficial effects to educate an immune system that is self-reactive. Ultimately, I hope that we will be able to translate these advances to human trials, for probiotics to be used as potential therapies, by themselves or in conjunction with currently medications, to treat SLE while eliminating the secondary effects of immunosuppressants.